Titre: Title:	Development of a critically evaluated thermodynamic database for magnesium alloys
Auteur: Author:	Adarsh Shukla
Date:	2008
Type:	Mémoire ou thèse / Dissertation or Thesis
Référence: Citation:	Shukla, A. (2008). Development of a critically evaluated thermodynamic database for magnesium alloys [Mémoire de maîtrise, École Polytechnique de Montréal]. PolyPublie. https://publications.polymtl.ca/8368/

Document en libre accès dans PolyPublie
Open Access document in PolyPublie

URL de PolyPublie: PolyPublie URL:	https://publications.polymtl.ca/8368/
Directeurs de recherche: Advisors:	Arthur Pelton
Programme: Program:	Non spécifié

UNIVERSITÉ DE MONTRÉAL

DEVELOPMENT OF A CRITICALLY EVALUATED THERMODYNAMIC
DATABASE FOR MAGNESIUM ALLOYS

ADARSH SHUKLA
DÉPARTEMENT DE GÉNIE CHIMIQUE
ÉCOLE POLYTECHNIQUE DE MONTRÉAL

MÉMOIRE PRÉSENTÉ EN VUE DE L'OBTENTION
DU DIPLÔME DE MAÎTRISE ÈS SCIENCES APPLIQUÉES
(GÉNIE MÉTALLURGIQUE)
MAI 2008

UNIVERSITÉ DE MONTRÉAL

ÉCOLE POLYTECHNIQUE DE MONTRÉAL

Ce mémoire intitulé :

DEVELOPMENT OF A CRITICALLY EVALUATED THERMODYNAMIC
DATABASE FOR MAGNESIUM ALLOYS

présenté par : SHUKLA Adarsh

en vue de l'obtention du diplôme de : Maîtrise ès sciences appliquées

a été dûment acceptée par le jury d'examen constitué de :

M. CHARTRAND Patrice, Ph.D., président

M. PELTON Arthur D., Ph.D., membre et directeur de recherche

M. SPENCER Philip, Ph.D., membre

Acknowledgements

I would like to express my gratitude towards my mentor Dr. Arthur D. Pelton, without whom this work was not at all possible. His guidance and support provided the impetus for successful completion of this work.

I would like to thank Dr. Youn-Bae Kang, for his continual helpful advice and collaboration in my study. I enjoyed all discussions with him during my study.

I am also grateful to Drs. P. Chartrand and P. Spencer for their critical review and constructive comments.

I am indebted to Dr. James Sangster for his assistance in the literature survey. I thank Zhenya and Katherine for their assistance. I am greateful to Christian for the French translation. I am also thankful to all the members of the CRCT, who directly or indirectly helped me during my study.

I also express my gratitude towards Dr. S. Srikanth whose encouragement during my studies in India helped me to develop an interest for the higher education.

Résume

Bien que les alliages de magnésium aient depuis longtemps des applications commerciales importantes (industrie automobile, etc.), il reste encore beaucoup à apprendre sur leurs propriétés de base. Un intérêt accru pour les alliages courroyés légers (incluant les tôles et les tubes) est apparu récemment, s'accompagnant d'efforts pour développer une meilleure compréhension des nouveaux alliages de magnésium, tels les alliages avec Ce et Y comme éléments d'addition. Ces alliages ainsi que d'autres sont considérés comme des candidats potentiels très sérieux pour le développement d'alliages de magnésium ayant une meilleure ductilité ou pouvant être mis en forme à température ambiante.

Les propriétés des alliages de fonderie ou des alliages courroyés dépendent en premier lieu des phases présentes et de leurs constituants microstructuraux (eutectiques, précipités, solutions solides, etc.). Dans un alliage constitué de plusieurs éléments, les relations de phases sont très complexes. Pour pouvoir étudier et comprendre de manière efficace ces relations de phases complexes, il est très utile de développer des banques de données thermodynamiques (contenant des paramètres de modèles) donnant les propriétés thermodynamiques de toutes les phases en fonction de la température et de la composition. En utilisant des logiciels de minimisation de l'énergie de Gibbs tel que FactSage™, les industries de l'automobile et de l'aéronautique ainsi que leurs fournisseurs pourront avoir accès aux banques de données pour calculer les quantités et

compositions de toutes les phases en présence à toute température et à toute composition d'alliages multicomposants, pour suivre l'évolution d'un refroidissement à l'équilibre ou hors équilibre, pour calculer les effets thermiques correspondants, etc.

De telles banques de données thermodynamiques sont obtenues par évaluation critique, modélisation et optimisation. Lors d'une optimisation thermodynamique, des paramètres de modèles ajustables sont calculés en utilisant simultanément toutes les données thermodynamiques et tous les équilibres de phases disponibles, de façon à obtenir un ensemble d'équations de modèles dépendant de la température et de la composition. Des données thermodynamiques telles que les activités peuvent faciliter l'évaluation des diagrammes de phases, et des informations sur des équilibres de phases permettent de déduire certaines propriétés thermodynamiques. Ainsi, il est souvent possible de résoudre des désaccords entre les données expérimentales disponibles. L'ensemble des propriétés thermodynamiques et des diagrammes de phases peuvent être calculés à partir des équations des modèles, et des interpolations et extrapolations peuvent être réalisées d'une manière thermodynamiquement correcte. Les données expérimentales sont de ce fait rendues cohérentes entre elles et cohérentes avec les principes thermodynamiques, conduisant à l'obtention d'un petit jeu de paramètres de modèles idéal pour le stockage informatique.

Ce travail consiste en l'évaluation critique et en l'optimisation des systèmes Si-Zn, Ce-Si, Y-Si, Mn-Si, Al-Mn, Mg-Si-Zn, Mg-Ce-Si, Mg-Y-Si, Mg-Mn-Si et Mg-Al-Mn. Il fait

partie d'un projet de recherche plus vaste réalisé au *Centre de Recherche en Calcul Thermochimique* de l'Ecole Polytechnique de Montréal, et consistant à développer une banque de données thermodynamiques pour des alliages de Mg avec 25 éléments d'alliage potentiels.

Tous les systèmes binaires ont été évalués de façon critique et optimisés à partir des équilibres de phases et des données thermodynamiques disponibles. Les paramètres des modèles obtenus ont été utilisés pour représenter les énergies de Gibbs de toutes les phases en fonction de la température et de la composition. Les paramètres binaires optimisés ont été combinés à d'autres paramètres binaires préalablement optimisés (au CRCT de l'Ecole Polytechnique de Montréal) pour évaluer les propriétés thermodynamiques des solutions ternaires Mg-Si-Zn, Mg-Ce-Si, Mg-Y-Si, Mg-Mn-Si et Mg-Al-Mn. Les diagrammes de phases ternaires correspondants ont été calculés et ont été comparés aux données expérimentales disponibles. Des modèles géométriques appropriés ont été utilisés pour ces calculs. En général, les données expérimentales ternaires disponibles ont été bien reproduites à l'aide des paramètres binaires seulement. Les diagrammes de phases prédits seront utiles pour la planification d'expériences lors de l'étude approfondie des systèmes ternaires correspondants.

La phase liquide, optimisée dans ce travail pour les systèmes binaires, présente de l'ordre à courte distance mis en évidence par la forme en « V » très prononcée des courbes d'enthalpies de mélange. Les optimisations précédentes de ces systèmes avaient été

réalisées en utilisant un modèle de type Bragg-Williams (mélange aléatoire) pour la phase

liquide. L'utilisation d'un modèle de type Bragg-Williams pour les liquides avec une

forte tendance à l'ordre à courte distance conduit généralement à des résultats peu

satisfaisants une faible prédictibilité des propriétés ternaires à partir des paramètres des

systèmes binaires. Dans la cadre de ce travail, le modèle quasichimique modifié qui est

capable de prendre en compte l'ordre à courte distance a été utilisé. De plus, les

optimisations et évaluations actuelles prennent en compte des données expérimentales qui

n'avaient pas été considérées dans les travaux précédents

ABSTRACT

Although magnesium-based materials have a long history of important commercial applications, including automotive, there remains much to be learned about the basic properties of the metal and its alloys. With the recent renewed interest in lightweight wrought materials, including both sheet and tube applications, there has been an increased focus on developing a better understanding of novel magnesium alloys, including those that incorporate additions of elements such as Si, Ce, Y, Mn, Zn, and Al. These alloy systems, along with other potential candidates, are being actively pursued as possible routes to develop magnesium materials with improved ductility, or even practical room temperature formability.

The properties of cast or wrought material depend first and foremost upon the phases and microstructural constituents (eutectics, precipitates, solid solutions, etc.) which are present. In an alloy with several alloying elements, the phase relationships are very complex. In order to investigate and understand these complex phase relationships effectively, it is very useful do develop thermodynamic databases containing model parameters giving the thermodynamic properties of all phases as functions of temperature and composition. Using Gibbs free energy minimization software such as FactSage^{TM}, the automotive and aeronautical industries and their suppliers will be able to access the databases to calculate the amounts and compositions of all phases at equilibrium at any

temperature and composition in multicomponent alloys, to follow the course of equilibrium or non-equilibrium cooling, to calculate corresponding heat effects, *etc.*

Such thermodynamic databases are prepared by critical evaluation, modeling, and optimization. In a thermodynamic "optimization" adjustable model parameters are calculated using, simultaneously, all available thermodynamic and phase-equilibrium data in order to obtain one set of model equations as functions of temperature and composition. Thermodynamic data, such as activities, can aid in the evaluation of the phase diagrams, and information on phase equilibria can be used to deduce thermodynamic properties. Thus, it is frequently possible to resolve discrepancies in the available data. From the model equations, all of the thermodynamic properties and phase diagrams can be back-calculated, and interpolations and extrapolations can be made in a thermodynamically correct manner. The data are thereby rendered self-consistent and consistent with thermodynamic principles, and the available data are distilled into a small set of model parameters, ideal for computer storage.

As part of a broader research project being conducted at the *Centre de Recherche en Calcul Thermochimique* (CRCT) at Ecole Polytechnique, Montreal to develop a comprehensive thermodynamic database for Mg-alloys with 25 potential alloying elements, the present work deals with the critical evaluation and optimization of the Si-Zn, Ce-Si, Y-Si, Mn-Si, Al-Mn, Mg-Si-Zn, Mg-Ce-Si, Mg-Y-Si, Mg-Mn-Si and Mg-Al-Mn systems.

All the binary systems have been critically evaluated and optimized based upon available phase-equilibrium and thermodynamic data. The model parameters obtained as a result of simultaneous optimization have been used to represent the Gibbs energies of all phases as functions of temperature and composition. Optimized binary model parameters were combined with those of previously optimized (at the CRCT, Ecole Polytechnique) binary systems to estimate the thermodynamic properties of ternary solutions in the Mg-Si-Zn, Mg-Ce-Si, Mg-Y-Si, Mg-Mn-Si and Mg-Al-Mn systems. Proper "geometric" models were used for these estimations. Ternary phase diagram were calculated and compared with experimental data where available. Usually, the available ternary data were well reproduced with only the binary model parameters. These phase diagrams predictions will be helpful in future planning of experiments for the detailed study of these ternary systems.

The liquid phase of the binary systems optimized in the present work exhibit considerable short-range ordering as evidenced by the very negative "V-shaped" enthalpy of mixing curves. Previous optimizations of these systems were based upon a Bragg-Williams random-mixing model for the liquid phase. The use of the Bragg-Williams model in liquids with a high degree of short-range ordering often results in unsatisfactory results and in poor predictions of ternary properties from binary model parameters. In the present work, the Modified Quasichemical Model which is capable of taking short-range ordering into account has been used. Furthermore, the present optimizations and evaluations take into account experimental data which were not considered in the previous optimizations.

Condensé en français

Bien que les alliages de magnésium aient depuis longtemps des applications commerciales importantes (industrie automobile, etc.), il reste encore beaucoup à apprendre sur leurs propriétés de base. Un intérêt accru pour les alliages courroyés légers (incluant les tôles et les tubes) est apparu récemment, s'accompagnant d'efforts pour développer une meilleure compréhension des nouveaux alliages de magnésium, tels les alliages avec Ce et Y comme éléments d'addition. Ces alliages ainsi que d'autres sont considérés comme des candidats potentiels très sérieux pour le développement d'alliages de magnésium ayant une meilleure ductilité ou pouvant être mis en forme à température ambiante.

Les propriétés des alliages de fonderie ou des alliages courroyés dépendent en premier lieu des phases présentes et de leurs constituants microstructuraux (eutectiques, précipités, solutions solides, etc.). Dans un alliage constitué de plusieurs éléments, les relations de phases sont très complexes. Pour pouvoir étudier et comprendre de manière efficace ces relations de phases complexes, il est très utile de développer des banques de données thermodynamiques (contenant des paramètres de modèles) donnant les propriétés thermodynamiques de toutes les phases en fonction de la température et de la composition. En utilisant des logiciels de minimisation de l'énergie de Gibbs tel que FactSage^{TM}, les industries de l'automobile et de l'aéronautique ainsi que leurs fournisseurs pourront avoir accès aux banques de données pour calculer les quantités et

compositions de toutes les phases en présence à toute température et à toute composition d'alliages multicomposants, pour suivre l'évolution d'un refroidissement à l'équilibre ou hors équilibre, pour calculer les effets thermiques correspondants, etc.

De telles banques de données thermodynamiques sont obtenues par évaluation critique, modélisation et optimisation. Lors d'une optimisation thermodynamique, des paramètres de modèles ajustables sont calculés en utilisant simultanément toutes les données thermodynamiques et tous les équilibres de phases disponibles, de façon à obtenir un ensemble d'équations de modèles dépendant de la température et de la composition. Des données thermodynamiques telles que les activités peuvent faciliter l'évaluation des diagrammes de phases, et des informations sur des équilibres de phases permettent de déduire certaines propriétés thermodynamiques. Ainsi, il est souvent possible de résoudre des désaccords entre les données expérimentales disponibles. L'ensemble des propriétés thermodynamiques et des diagrammes de phases peuvent être calculés à partir des équations des modèles, et des interpolations et extrapolations peuvent être réalisées d'une manière thermodynamiquement correcte. Les données expérimentales sont de ce fait rendues cohérentes entre elles et cohérentes avec les principes thermodynamiques, conduisant à l'obtention d'un petit jeu de paramètres de modèles idéal pour le stockage informatique.

Ce travail consiste en l'évaluation critique et en l'optimisation des systèmes Si-Zn, Ce-Si, Y-Si, Mn-Si, Al-Mn, Mg-Si-Zn, Mg-Ce-Si, Mg-Y-Si, Mg-Mn-Si et Mg-Al-Mn. Il fait

partie d'un projet de recherche plus vaste réalisé au *Centre de Recherche en Calcul Thermochimique* de l'Ecole Polytechnique de Montréal, et consistant à développer une banque de données thermodynamiques pour des alliages de Mg avec 25 éléments d'alliage potentiels.

Les terres rares tels que Ce et Y augmentent la stabilité à haute température des alliages de Mg ; Mn améliore la résistance à la corrosion de ces alliages ; Al et Zn augmentent leurs propriétés mécaniques par solution ou par précipitation (durcissement structural). Si est souvent ajouté aux alliages de Mg. Tous ces éléments sont considérés comme des éléments d'alliage potentiels pour le développement de nouveaux alliages de Mg, et présentent de ce fait un intérêt.

Tous les systèmes binaires ont été évalués de façon critique et optimisés à partir des équilibres de phases et des données thermodynamiques disponibles. Les paramètres des modèles obtenus ont été utilisés pour représenter les énergies de Gibbs de toutes les phases en fonction de la température et de la composition. Les paramètres binaires optimisés ont été combinés à d'autres paramètres binaires préalablement optimisés (au CRCT de l'Ecole Polytechnique de Montréal) pour évaluer les propriétés thermodynamiques des solutions ternaires Mg-Si-Zn, Mg-Ce-Si, Mg-Y-Si, Mg-Mn-Si et Mg-Al-Mn. Les diagrammes de phases ternaires correspondants ont été calculés et ont été comparés aux données expérimentales disponibles. Des modèles géométriques appropriés ont été utilisés pour ces calculs. En général, les données expérimentales

ternaires disponibles ont été bien reproduites à l'aide des paramètres binaires seulement. Les diagrammes de phases prédits seront utiles pour la planification d'expériences lors de l'étude approfondie des systèmes ternaires correspondants.

Le Modèle Quasichimique Modifié (MQM) développé au *Centre de Recherche en Calcul Thermochimique* de l'Ecole Polytechnique de Montréal a été utilisé pour modéliser les alliages liquides. Ce modèle peut prendre en compte l'existence d'un ordre à courte distance dans une phase liquide. Cette dernière constitue technologiquement l'une des phases les plus importantes. Une bonne représentation de l'énergie de Gibbs de la phase liquide est primordiale lors de la préparation d'une banque de données pour des alliages multicomposants. Le MQM a déjà été utilisé avec succès pour modéliser des alliages liquides mais aussi des laitiers, des mattes et des sels fondus. La phase liquide des systèmes binaires optimisés dans ce travail présente un ordre à courte distance très important ; ce qui est mis en évidence par la forme en V très marquée des courbes d'enthalpie de mélange. Dans les optimisations précédentes de ces systèmes, la phase liquide avait été modélisée à l'aide d'un modèle de distribution aléatoire (Bragg-Williams). L'utilisation d'un tel modèle pour des liquides fortement ordonnés conduit généralement à des résultats insatisfaisants et à de mauvaises prédictions pour les propriétés ternaires à partir des paramètres binaires. Dans ce travail, nous avons utilisé le Modèle Quasichimique Modifié prenant en compte l'ordre à courte distance. De plus, nous avons considéré des données expérimentales non prises en compte dans les optimisations précédentes.

Nos différents résultats nous ont permis d'écrire trois articles, soumis et publiés dans des journaux scientifiques. Ces articles sont présentés dans les chapitres 3, 4 et 5. Le premier article (chapitre 3), soumis à *International Journal of Materials Research*, présente les optimisations thermodynamiques des systèmes Mg-Si-Ce et Mg-Si-Y. Le deuxième article (chapitre 4), soumis à *Calphad*, décrit les optimisations thermodynamiques des systèmes Mg-Si-Zn et Mg-Si-Mn. Finalement, le troisième article (chapitre 5), soumis à *Journal of Phase Equilibria and Diffusion*, correspond à l'optimisation thermodynamique du système Mg-Al-Mn.

La prise en compte de données récentes pour les équilibres de phases et les propriétés thermodynamiques des systèmes binaires, et l'utilisation du MQM pour la phase liquide ont permis d'obtenir des résultats plus satisfaisants que ceux des optimisations précédentes. De plus, l'entropie de mélange de la phase liquide et les entropies de formation des phases intermétalliques obtenues sont physiquement raisonnables.

Les optimisations précédentes étaient basées sur un modèle de distribution aléatoire (Bragg-Williams) pour la phase liquide. Dans les régions de composition diluées, les propriétés partielles résultantes déviaient souvent des données expérimentales, particulièrement dans le cas des enthalpies de mélange partielles. Les propriétés partielles obtenues dans ce travail sont plus « lisses » et plus proches des données expérimentales.

Une meilleure optimisation des propriétés partielles dans les solutions liquides diluées jouera un rôle majeur pour développer de nouveaux alliages de magnésium.

L'estimation des propriétés d'une phase ternaire à partir des paramètres binaires optimisés dépend de ces derniers et des techniques d'interpolation utilisées. Les paramètres binaires optimisés devraient, en principe, donner une estimation satisfaisante des propriétés ternaires. Dans ce travail, un très petit paramètre d'interaction ternaire a été utilisé pour reproduire les données expérimentales disponibles pour le système Mg-Al-Mn alors que l'optimisation précédente, basée sur un modèle de distribution aléatoire (Bragg-Williams) pour la phase liquide, nécessitait un paramètre ternaire élevé. A toute fin pratique, les données ternaires pour le système Mg-Al-Mn situées au-dessous de 760°C peuvent être reproduites sans l'ajout de paramètre ternaire. Dans ce travail, une meilleure estimation des propriétés ternaires a pu être obtenue grâce à l'utilisation du MQM et de la méthode d'interpolation asymétrique (avec Al comme composé asymétrique).

Un liquidus plat (voire une lacune de miscibilité liquide-liquide) est observé dans la section A_xB_y-C d'un système ternaire A-B-C lorsque le liquide binaire A-B est fortement ordonné tandis que les deux autres liquides binaires (B-C et A-C) sont proches de l'idéalité. Suite à l'ordre à courte distance, les atomes A et B s'associent, excluant les atomes C et conduisant ainsi à des déviations positives le long du joint A_xB_y-C. Dans ce travail, des lacunes de miscibilité liquide-liquide ont été calculées dans les sections

Mg-CeSi et Mg-YSi des systèmes ternaires Mg-Ce-Si et Mg-Y-Si. Dans ces systèmes ternaires, les liquides binaires Ce-Si et Y-Si présentent de fortes déviations négatives (par rapport à l'idéalité) comparativement aux deux autres sous-systèmes binaires. Dans le cas du système ternaire Mg-Mn-Si, le liquide binaire Mn-Si est moins ordonné que les liquides binaires Ce-Si et Y-Si ; un liquidus plat a été obtenu dans la section Mg-MnSi. Si un modèle de distribution aléatoire (Bragg-Williams) était utilisé pour modéliser ces différents systèmes ternaires, il surestimerait les déviations positives et pourrait ainsi prédire une lacune de miscibilité liquide-liquide alors que celle-ci n'existe pas. Un modèle d'associés ne prédirait aucune déviation positive puisqu'un tel modèle suppose un mélange aléatoire d'associés A_xB_y et d'atomes C le long du joint A_xB_y-C. Il s'avère donc que le MQM est le modèle le plus approprié pour prédire les propriétés thermodynamiques des liquides ternaires à partir des paramètres binaires.

L'extension dans un système ternaire d'une lacune de miscibilité liquide-liquide binaire dépend du modèle utilisé. Le MQM prédit une extension plus petite que celles relatives au modèle de distribution aléatoire (Bragg-Williams) et au modèle d'associés. Néanmoins, dans le cas du MQM, l'extension prédite dans le système ternaire dépend des nombres de coordination utilisés pour modéliser la phase liquide. Les extensions de la lacune de miscibilité binaire Mg-Mn calculées dans les systèmes ternaires Mg-Mn-Si et Mg-Al-Mn sont petites comparées aux extensions qui seraient obtenues à partir d'un mélange de distribution aléatoire. La température critique de la lacune de miscibilité liquide-liquide binaire Mg-Mn obtenue dans ce travail avec le MQM est environ

1500-2000 °C plus basse que les températures critiques des optimisations précédentes réalisées avec un modèle de distribution aléatoire. Il en résulte des extensions calculées dans les systèmes ternaires Mg-Mn-Si et Mg-Mn-Al de plus petite taille.

Les différents systèmes optimisés dans ce travail permettront le calcul de diagrammes de phases multicomposants et de diagrammes de fractions de phases, ainsi que le suivi de la solidification d'alliages liquides. A l'aide de ces calculs, des alliages potentiellement intéressants et des systèmes aux propriétés indésirables pourront être aisément identifiés. Le nombre d'expériences requises s'en trouvera diminué. La connaissance des phases précipitées et de leurs quantités respectives expliquera l'évolution de la microstructure des alliages et sera ainsi utile pour expliquer les propriétés mécaniques de ces derniers. Les résultats obtenus dans ce travail sont meilleurs que ceux des optimisations précédentes ; ils permettront donc de mieux répondre aux problèmes inhérents à l'évolution du magnésium comme matériau de construction léger.

En résumé, l'utilisation du Modèle Quasichimique Modifié (MQM) pour la phase liquide a permis de prendre en compte l'existence d'un ordre à courte distance. Ce modèle permet de mieux reproduire les données expérimentales comparativement à un modèle de distribution aléatoire (Bragg-Williams). Il permet également une meilleure représentation des propriétés partielles d'éléments en solution diluée dans le magnésium (les activités de ces solutés ont une grande importance pratique.). L'utilisation du MQM conduit généralement à une meilleure estimation des propriétés thermodynamiques des alliages

liquides ternaires et d'ordre supérieur. Ces estimations d'équilibres de phases faciliteront

l'élaboration de nouveaux alliages de magnésium.

TABLE OF CONTENTS

LIST OF FIGURES

LIST OF TABLES

LIST OF SYMBOLS

C_p	Molar heat capacity (J/mol·K)
G^0_i	Standard Gibbs energy of i
G^m	Gibbs energy of solution
G^E	Excess Gibbs energy in solution
g^E	Molar excess Gibbs energy in solution
g^0_i	Molar Gibbs energy of i
Δg_{ij}	Gibbs energy change for the formation of two moles of i-j pairs
H^0_i	Standard enthalpy of i
ΔH	Molar enthalpy of mixing
ΔH_T	enthalpy of formation of the compound from elements
n_{ij}	Number of moles of i-j bonds in one mole of solution
q^{ij}_{AB}	Excess interaction parameter between A and B
S^0_i	Standard entropy of component i
ΔS_T	entropy of formation of the compound from elements
ΔS^{conf}	Molar configurational entropy of solution
$S^{non-conf}$	Molar non-configurational entropy of solution
n_i	Number of moles of component i
T	Absolute temperature (K)
$wt.\ \%$	Weight percent
y_i	Site fraction of component i
Y_i	Coordination-equivalent fractions
X_i	Mole fraction of component i in solution
X_{ij}	Pair fraction of i-j pairs
Z_i	Coordination number of i
Z^i_{ii}	The values of Z_i when all the nearest neighbors of an i are i's
Z^i_{ij}	The values of Z_i when all the nearest neighbors of an i are j's

Chapter 1: Introduction

There is an increasing interest in light-weight construction since the automobile industry's commitment to achieve a 25 % reduction in average fuel consumption. In the drive to reduce exhaust emissions, an important step is to reduce the weight of the automobile. Magnesium, with its high strength to weight ratio, is one of several potential materials in light-weight construction, and it must compete with several other materials in this area. But still, magnesium has high potential as a substitute for conventional materials. Magnesium alloyed with other materials can have a high specific Young's modulus and a high specific strength for use in light-weight constructions.

Magnesium alloys have two major disadvantages for use in automotive applications; they have low high-temperature strength and relatively poor corrosion resistance. Alloying can improve the general corrosion behavior. Similarly, use of proper alloying material can drastically improve the high-temperature strength of magnesium. The new high-temperature resistant alloys are under further development and testing. A few alloys are already on the market. These alloys contain mostly aluminum for good castablility and strontium, calcium and rare earth elements for high-temperature stability. Several rare-earth elements act as grain refiners in magnesium alloys and form the basis of creep-resistant alloys. For automotive applications, the development of new casting alloys with good creep resistance and low cost is important. In this respect, Mg-Al-Rare Earth, Mg-Al-Ca, Mg-Al-Sr, Mg-Al-Si alloys and quaternary combinations of these are very new

systems having immense potential. Automotive applications also require good ductility for many components. Shock absorption during a car accident is a very crucial issue. One direction for alloy development will be to optimize the energy absorption of the material.

In short, magnesium when alloyed with proper materials can show drastically improved behavior and can be used in light-weight construction, especially in automobile, space and aeronautical engineering. These alloys systems are being actively pursued as possible routes to develop magnesium materials with improved behavior. The properties of cast or wrought materials derived from a specific alloy system depend first and foremost upon the phases and microstructural constituents (eutectics, precipitates, solid solutions, etc.) that are present. With the help of computational thermochemistry, not only the computation of multi-component phase diagrams, but also tracking of alloys during heat treatment or solidification is possible. The calculation of the amount and composition of the phases precipitated helps in understanding the microstructural evolution of alloys. In an alloy with several alloying elements, the phase relationships are very complex. In order to effectively investigate and understand these complex phase relationships, it will be very useful to develop a database containing model parameters, giving the thermodynamic properties of all the involved phases as functions of temperature and composition. Such a thermodynamic database will provide a clear guideline for selection of these alloys and will help to avoid unproductive long-term experiments with alloys having less potential for commercial purposes. Using these databases with Gibbs energy minimizing software like FactSage^{TM} (FactSage 2008), one will be able to calculate the

amounts and compositions of all phases at equilibrium at any temperature and composition in multicomponent alloys, to follow the course of equilibrium or nonequilibrium (Scheil-Gulliver) cooling, to calculate corresponding heat effects, *etc.*

Such thermodynamic databases are prepared by critical evaluation, modeling, and optimization. In a thermodynamic ''optimization'' adjustable model parameters are calculated using, simultaneously, all available thermodynamic and phase-equilibrium data in order to obtain one set of model equations as functions of temperature and composition. Thermodynamic data, such as activities, can aid in the evaluation of the phase diagrams, and information on phase equilibria can be used to deduce thermodynamic properties. Thus, it is frequently possible to resolve discrepancies in the available data. From the model equations, all of the thermodynamic properties and phase diagrams can be back-calculated, and interpolations and extrapolations can be made in a thermodynamically correct manner. The data are thereby rendered self-consistent and consistent with thermodynamic principles, and the available data are distilled into a small set of model parameters, ideal for computer storage

As part of a broader research project to develop a thermodynamic database for Mg-alloys with 25 potential alloying elements, the present work deals with the critical evaluation and optimization of the Si-Zn, Ce-Si, Y-Si, Mn-Si, Al-Mn, Mg-Si-Zn, Mg-Ce-Si, Mg-Y-Si, Mg-Mn-Si and Mg-Al-Mn systems.

Rare earth elements like Ce and Y increase the high-temperature stability of Mg-alloys. Mn is known to improve the corrosion resistance of Mg-alloys. Al and Zn increase the mechanical properties of Mg-alloys by solution and precipitation hardening. Si is often added as an alloying element to Mg-alloys. All these elements are considered as potential alloying elements for development of novel Mg-alloys and are of interest.

In the present work, first the binary systems Si-Zn, Ce-Si, Y-Si, Mn-Si and Al-Mn have been critically evaluated. (All other binary sub-systems have been critically evaluated and optimized previously.) All available thermodynamic and phase diagram data for these systems were collected and critically assessed for their reliability. The Gibbs energies of all phases were represented by appropriate model equations. The parameters of these models were obtained by an optimization procedure using the FactSage™ (FactSage 2008) software. These binary parameters were then used along with the models to predict the thermodynamic properties and phase diagrams of the ternary systems. All available data on the ternary systems (Mg with each of the above binary systems) were collected. The predictions for the ternary systems were compared with the available ternary data, and the models were refined through the inclusion of ternary parameters, where required, for those systems where sufficient data were available.

The Modified Quasichemical Model (MQM) (Pelton, Degterov, Eriksson, Robelin and Dessureault, 2000) developed at the *Centre de Recherche en Calcul Thermochimique* at

Ecole Polytechnique, Montreal was used to model the liquid alloys. This model is capable of taking into account ordering or clustering in the liquid phase. The liquid phase is technologically one of the most important phases appearing in every system. The adequate representation of its Gibbs energy plays a decisive role in database preparation for multicomponent alloys. This model has been satisfactorily used by its developers and others to model not only liquid alloys but also slags, mattes and salts.

In addition to the development of new models to represent the Gibbs energies of phases and the development of thermodynamic databases to describe the behavior of solutions, the *Centre de Recherche en Calcul Thermochimique* (CRCT) at Ecole Polytechnique, Montreal has developed the software FactSage^{TM} (FactSage 2008). FactSage^{TM} is the fusion of the FACT-Win/F*A*C*T and ChemSage/SOLGASMIX (Eriksson and Hack, 1990) thermochemcial packages that were founded 25 years ago. The FactSage package runs on a PC operating under Microsoft Windows and consists of a series of information, database, calculation and manipulation modules that enable one to access and manipulate databases for pure substances and solutions. With the various modules one can perform a wide variety of thermochemical calculations like calculations and plotting of binary and ternary phase diagrams, *etc.*

Chapter 2: Literature review

In this chapter a general review of the literature on the topic of evaluation and optimization of phase diagrams is given. In this literature survey, the doctoral thesis by Jung (Jung, 2003) on a similar work on database preparation for oxides was of immense help. The literature on specific systems optimized in this are not reviewed in this chapter as they are presented in Chapters 4, 5 and 6 which are in the form of articles submitted to journals.

2.1 CALPHAD

Calphad is an acronym for the CALculation of PHAse Diagrams. It is better described as "The Computer Coupling of Phase Diagrams and Thermochemistry".

Kattner (Kattner, 1997) described phase diagrams as "visual representations of the equilibrium state of a material as a function of temperature, pressure and concentrations of the constituent components." They are, therefore, frequently hailed as basic blueprints or roadmaps for alloy design, development, processing and basic understanding. Pelton and Schmalzried (Pelton and Schmalzried, 1973) defined a phase diagram as "the geometrical representation of the loci of the thermodynamic parameters when equilibrium among phases under a specified set of conditions is established". Phase diagrams provide vital inputs required for addressing many technological problems involving multi-component, multi-phase equilibria. Be it to select the proper eutectic composition for a

casting alloy, or to check the solubility of elements in a metal for a forged alloy, or to know the possible precipitates from a primary phase to help in age-hardening mechanisms, phase diagrams have long been helpful in alloy designing. However, many phase diagrams of ternary systems are poorly known, and very few phase diagrams of system of four or more components have been studied experimentally.

The correlation between thermodynamics and phase equilibria was established more than a century ago by J.W. Gibbs. Later, J. J. van Laar (van Laar, 1908) published his mathematical synthesis of hypothetical binary systems. With the advance of computing technology, construction of multicomponent thermodynamic databases began in the late 1960's. Kattner (Kattner, 1997) has summarized some early examples, between 1908 and 1970, of mathematical calculations of phase diagrams. In 1970 Kaufman and Bernstein (Kaufman and Bernstein, 1970) summarized the general features of the calculation of phase diagrams and also presented listings of computer programs. In 1973 Larry Kaufman organized the first project meeting of the international CALPHAD group.

Under the CALPHAD technique, all types of thermodynamic information such as phase diagrams, enthalpy of mixing in a phase, activities *etc.* are critically evaluated and optimized simultaneously, using proper thermodynamic models, in order to construct multicomponent databases. The thermodynamic models required to represent the thermochemistry of phases have also been developed. A model capable of closely reflecting the thermochemical properties of a phase with a minimum number of

adjustable parameters should be chosen. Also, these models should be based on a good physical microscopic picture of a solution to obtain better predictions in multicomponent systems using these models from lower-order optimized parameters.

Normally a software package capable of performing multivariable optimizations is used in the optimization process. All the input data are back-calculated from the single set of model parameters obtained from the optimization. The databases containing model parameters for lower-order (binary and ternary) systems are used to predict the thermodynamic properties in multicomponent systems. There are various techniques (Chapter 2.5) to extrapolate the Gibbs energy from binary systems into higher-order systems. In case, these predictions are not able to reproduce the available data in the higher-order system within the experimental error limits, then higher-order interaction parameters is included to reproduce the available data.

Recently, new approaches to thermodynamic modeling have been conducted with the advent of computing technologies. First-principles calculations can be cited in this area. A first-principles calculation starts from quantum mechanics to examine the fundamental properties of materials such as which structure is stable at a certain temperature and pressure. First-principles calculations are extensively used in conjunction with the "Cluster Variation Method" (CVM) which was introduced in the 1950's by Kikuchi (Kikuchi, 1951) who introduced this method to treat order-disorder phenomena in solid

phases. Although these calculations are computationally very intensive, enormous progress in recent years in the area of computing techniques have made them easier.

Nevertheless, these techniques are still in their nascent stages and cannot be satisfactorily applied to complex systems. The phase diagrams predicted by these techniques are generally approximately correct but currently still lack sufficient accuracy for practical applications. In conclusion, the development of thermodynamic databases for applications in complex industrial processes can be done by the CALPHAD technique, although first-principles calculations can often provide reasonable estimations of certain properties, particularly enthalpies of stoichiometric solids, when experimental data are lacking.

Schmid-Fetzer and Grobner (Schmid-Fetzer and Grobner, 2001) reported on the development of Mg-alloys by the CALPHAD technique. They summarized the current status of the CALPHAD technique with the following highlights:

1. Predictive capability allows extrapolation of thermodynamic descriptions and phase equilibria into higher-order systems from the assessed lower-order systems.

2. Identification of key experiments in multicomponent systems to provide maximum information with the minimal possible number of experiments.

3. Calculation of stable phase equilibria and also of metastable phase equilibria by suspending the stable phase in cases where the stable phase does not form under specific conditions for kinetic reasons.

4. The driving forces for all the phase transformations are available.

5. Calculation of local phase equilibria in materials processing software like solidification simulation or reactor modeling.

6. The reading of multicomponent phase diagrams is drastically simplified with the help of phase diagrams through the CALPHAD technique. For example, for any given alloy the amounts and compositions of the phases at a given temperature can be readily calculated and plotted; such information is cumbersome to extract from a ternary phase diagram and virtually impossible to represent in a phase diagram of a multicomponent system.

2.2 Thermodynamic modeling

Thermodynamic models are required to adequately represent the thermodynamic properties of materials. Complex solutions require sophisticated and refined models for the proper representation of their thermochemical properties. A good model should be able to represent the thermodynamic properties with just a small numbers of adjustable parameters. For this, the model should be based on the structure of the solution to adequately represent the configurational entropy of the solution. Also these models have high predictive capability in higher-order systems. Hence, models should be developed which can describe the configurational entropy of the solutions without the addition of large arbitrary model parameters.

General Equations:

The standard Gibbs energy of a pure component *i* is written as:

$$G^0_i = H^0_i - TS^0_i \tag{2.1}$$

where G^0_i, H^0_i, and S^0_i are respectively the standard Gibbs energy, enthalpy and entropy of *i*, and *T* is the absolute temperature.

When two components A and B are mixed then the energy of the solution depends upon the interaction between the A and B atoms or molecules. The Gibbs energy of a solution in which there is no interaction between A and B is an ideal solution for which:

$$G^m = g^0_A n_A + g^0_B n_B - T\Delta S^{conf} \tag{2.2}$$

where G^m is the molar Gibbs energy of the solution, g^0_i is the molar Gibbs energy of component i, and ΔS^{conf} is configurational entropy obtained by randomly mixing n_A moles of A and n_B mole of B on the same sublattice:

$$\Delta S^{conf} = -R\ (n_A\ ln\ X_A + n_B\ ln\ X_B) \tag{2.3}$$

Practically however, all solutions do have interactions among the atoms mixing to form a solution. Such interactions can be called g^E, the molar excess Gibbs energy of the solution. In this case the energy of the solution is given by:

$$G^m = g^0_A n_A + g^0_B n_B - T\Delta S^{conf} + (n_A + n_B)\ g^E \tag{2.4}$$

g^E is often expanded as a polynomial in the mole fractions as:

$$g^E = \Sigma\ q^{ij}_{AB}\ X^i_A X^j_B \tag{2.5}$$

where the excess interaction parameters q^{ij}_{AB} (= a +bT +cT^2 + ...) may be temperature dependent.

In many cases, the thermodynamic properties of a binary solution can be described by using the expression in Eq. 2.5. Although it is satisfactory in binary systems not showing large deviations from ideality, problems arise when such an expression is used to predict the thermodynamic properties of higher-order systems from the model parameters of the lower-order sub-systems. In this case, large arbitrary parameters are often needed in these higher-order systems to reproduce the available data. Even sometimes in a binary system

also a large number of interaction parameters are needed in this simple polynomial based model in order to adequately represent all the thermodynamic properties of the system.

The liquid phase is of utmost commercial importance as the metals crystallize from the liquid alloy. To adequately represent the thermodynamic properties of the liquid phase, Pelton and co-workers (Pelton, Degterov, Eriksson, Robelin and Dessureault, 2000) and Pelton and Chartrand (Pelton and Chartrand 2001) developed the Modified Quasichemical Model (MQM). They modified the classical quasichemical model by improving the configurational entropy term of the model. Other modifications were also made to make it more flexible and practical for real and complicated systems.

The MQM developed by Pelton *et al.* (Pelton, Degterov, Eriksson, Robelin and Dessureault, 2000) has been applied not only to metallic alloys but to liquid slags, sulphides, and salts. In fact, the utility of the MQM over a simple polynomial or random-mixing model can be better realized with these solutions which show more ordering than metallic solutions, and where the configurational entropy terms become more important. Simple models can not take this ordering into account.

2.3 Modified Quasichemical Model (MQM)

In the present work the MQM was used to model the liquid alloys in the binary and ternary systems. Recently, the model has been described in detail by Pelton and co-workers (Pelton, Degterov, Eriksson, Robelin and Dessureault, 2000). A brief summary of this model is presented here.

In the MQM in the pair approximation, the following pair exchange reaction between atoms A and B on neighboring lattice sites is considered:

$$(A - A) + (B - B) = 2(A - B); \qquad \Delta g_{AB} \tag{2.6}$$

where $(i - j)$ represents a first-nearest-neighbor pair. The non-configurational Gibbs energy change for the formation of two moles of $(A - B)$ pairs is Δg_{AB}.

Let n_A and n_B be the number of moles of A and B, n_{ij} be the number of moles of $(i - j)$ pairs, and Z_A and Z_B be the coordination numbers of A and B. The pair fractions, mole fractions, and "coordination-equivalent" fractions are defined respectively as:

$$X_{ij} = n_{ij} / (n_{AA} + n_{BB} + n_{AB}) \tag{2.7}$$

$$X_A = n_A / (n_A + n_B) = 1 - X_B \tag{2.8}$$

$$Y_A = Z_A n_A / (Z_A n_A + Z_B n_B) = Z_A X_A / (Z_A X_A + Z_B X_B) = 1 - Y_B \tag{2.9}$$

The following equations may be written:

$$Z_A X_A = 2n_{AA} + n_{AB} \tag{2.10}$$

$$Z_B X_B = 2n_{BB} + n_{AB} \tag{2.11}$$

The Gibbs energy of the solution is given by:

$$G^m = \left(n_A g_A^\circ + n_B g_B^\circ\right) - T\Delta S^{config} + \left(n_{AB}/2\right)\Delta g_{AB} \qquad (2.12)$$

$$= \left(n_A g_A^\circ + n_B g_B^\circ\right) - T\Delta S^{config} + g^E \qquad (2.13)$$

where g_A° and g_B° are the molar Gibbs energies of the pure components and ΔS^{config} is

the configurational entropy of mixing given by randomly distributing the $(A-A)$,

$(B-B)$ and $(A-B)$ pairs in the one-dimensional Ising approximation:

$$\Delta S^{config} = -R\left(n_A \ln X_A + n_B \ln X_B\right)$$
$$- R\left[n_{AA} \ln\left(X_{AA}/Y_A^2\right) + n_{BB} \ln\left(X_{BB}/Y_B^2\right) + n_{AB} \ln\left(X_{AB}/2Y_A Y_B\right)\right] \qquad (2.14)$$

Δg_{AB} is expanded in terms of the pair fractions:

$$\Delta g_{AB} = \Delta g_{AB}^\circ + \sum_{i\geq 1} g_{AB}^{i0} X_{AA}^i + \sum_{j\geq 1} g_{AB}^{0j} X_{BB}^j \qquad (2.15)$$

where Δg_{AB}°, g_{AB}^{i0} and g_{AB}^{0j} are the parameters of the model which may be functions of

temperature.

The equilibrium pair distribution is calculated by setting

$$\left(\partial G/\partial n_{AB}\right)_{n_A, n_B} = 0 \qquad (2.16)$$

(It should be noted that in the FactSage software pair fractions are calculated by Equilib

module using the Gibbs energy minimization algorithm widely known as SOLGASMIX).

This gives the "equilibrium constant" for the "quasichemical reaction" of (Eq. 1):

$$\frac{X_{AB}^2}{X_{AA}X_{BB}} = 4\exp\left(-\frac{\Delta g_{AB}}{RT}\right) \tag{2.17}$$

As Δg_{AB} becomes progressively more negative, the reaction (Eq. 1) is shifted progressively to the right, and the calculated enthalpy and configurational entropy of mixing assume, respectively, the negative "V" and "m" shapes characteristic of SRO.

The composition of maximum SRO is determined by the ratio of the coordination numbers Z_B/Z_A, as given by the following equations:

$$\frac{1}{Z_A} = \frac{1}{Z_{AA}^A}\left(\frac{2n_{AA}}{2n_{AA}+n_{AB}}\right) + \frac{1}{Z_{AB}^A}\left(\frac{n_{AB}}{2n_{AA}+n_{AB}}\right) \tag{2.18}$$

$$\frac{1}{Z_B} = \frac{1}{Z_{BB}^B}\left(\frac{2n_{BB}}{2n_{BB}+n_{AB}}\right) + \frac{1}{Z_{BA}^B}\left(\frac{n_{AB}}{2n_{BB}+n_{AB}}\right) \tag{2.19}$$

where Z_{AA}^A and Z_{AB}^A are the values of Z_A respectively when all the nearest neighbors of an A are A's, and when all nearest neighbors of an A are B's, and where Z_{BB}^B and Z_{BA}^B are defined similarly. (Note that Z_{AB}^A and Z_{BA}^B represent the same quantity and can be used interchangeably.)

Although the model is sensitive to the ratio of the coordination numbers, it is less sensitive to their absolute values. The use of the one-dimensional Ising model in Eq. 2.14 introduces a mathematical approximation into the model which we have found, by

experience, can be partially compensated by selecting values of Z_B and Z_A which are smaller than the actual values.

Recently, Saulov (Saulov, 2007) pointed out some issues which may provide a useful note of caution in the use of the MQM. Pelton and Chartrand (Pelton and Chartrand, 2007) replied on these issues that they rarely cause any problem in real systems. Saulov's issue on the stability calculations of the Gibbs energy of a solution phase by the MQM is due to the use of improbable and physically unlikely values of the quasichemical parameter Δg_{AB}. Saulov's suggestions on the use of coordination number as a function of mole fraction and the use of splines for the Gibbs energy of the quasichemical reaction are not of any particular advantages and their usage result in mathematically cumbersome expansions. Use of splines may be useful for binary systems, but then a simple general equation for multicomponent systems could not be written.

2.4 Thermodynamic modeling of solids

Solid phases appear in phase diagrams as stoichiometric compounds, terminal solid solutions or stoichiometric compounds with ranges of homogeneity. Sometimes some compounds have such a large homogeneity range that they are called solutions with specific names.

The Gibbs energy function for any stoichiometric phase A_xB_y per mole of atoms is represented as:

$$g^{A_xB_y}(T) = \frac{x}{x+y} \; g_A^0 + \frac{y}{x+y} \; g_B^0 + \Delta H_T - T\Delta S_T \tag{2.20}$$

where ΔH_T and ΔS_T are the enthalpy and entropy of formation of the compound from the states i and j of elements A and B respectively.

The terminal solid solutions appearing in a binary system are usually treated with a random-mixing single-sublattice model. As the name suggests, this model assumes the random mixing of the atoms, one randomly replacing the other by substitution on lattice sites. The Gibbs energy of such a solution in which atoms A and B replace each other on lattice sites is given as:

$$G^m = (x \; g_A^0 + x_B \; g_B^0) + RT[x_A \ln x_A + x_B \ln x_B] + g^E \tag{2.21}$$

The phases with two or more sublattices exhibiting ranges of homogeneity are modeled using sublattice models. The sublattice model with random-mixing on each sublattice in it's the most general form is called as Compound Energy Formalism (CEF). This formalism was advanced by Hillert who has given a detailed description (Hillert, 2000). In the CEF, the Gibbs energy per mole of solution in the compound (A, B)$_P$ (D,E)$_Q$ is given by;

$$G = y_A y_D G_{A:D} + y_A y_E G_{A:E} + y_B y_D G_{B:D} + y_B^a y_E^b G_{B:E} + PRT\left(y_A \ln y_A + y_B \ln y_B\right) +$$
$$QRT\left(y_D \ln y_D + y_E \ln y_E\right) + \left(\sum_{k=D,E} y_A y_B y_k L_{AB:k} + \sum_{k=A,B} y_k y_D y_E L_{k:DE} \right)$$

In the CEF the atoms are assumed to mix randomly on each sublattice. The interactions between the atoms on different sublattices are taken into account by the Gibbs energy of end members $G_{i:j}$, and interactions among the atoms on the same sublattice is taken into account by excess terms (the last term in the above equation). The Gibbs energy of end members $G_{i:j}$ and excess parameters $L_{ij:k}$ are the model parameters.

2.5 Extension to a ternary system from binary systems

To estimate the excess Gibbs energy of a ternary solution from optimized binary model parameters, several "geometric" models have been proposed. Pelton (Pelton, 2001) presented a detailed description of these models. Some of these models are illustrated in Figure 2.1 (reproduced from (Pelton, 2001)). In all of these models the excess Gibbs energy (g^E in Eq. 2.13) at any composition p can be estimated from the binary interaction parameters or the excess Gibbs energies of the binary sub-systems at points a, b and c. This excess Gibbs energy when the solution is modeled using the MQM is estimated as:

$$g^E = X_{12}\Delta g_{12}/2 + X_{13}\Delta g_{13}/2 + X_{31}\Delta g_{23}/2 + \text{(ternary terms)} \qquad (2.22)$$

where Δg_{ij} is the Gibbs energy change for the reaction:

$$i\text{-}i + j\text{-}j = 2(i\text{-}j) \qquad (2.23)$$

If ternary data are available, they can be used to estimate the ternary interactions. However, these terms should not be large, otherwise doubt is cast upon the predictive ability of the model. These ternary terms are identically zero in the three binary sub-systems.

The Kohler and Muggianu models in Figure 2.1 are "symmetric" models, whereas the Kohler/Toop and Muggianu/Toop models in Figure 2.1 are "asymmetric" models inasmuch as one component is singled out. An asymmetric model is more physically reasonable than a symmetric model if component 2 and 3 are chemically similar while component 1 is chemically different. When g^E is large and Δg_{ij} depends strongly upon

composition, a symmetric model and an asymmetric model will give very different results. Pelton (Pelton, 2001) showed that improper use of these models can lead to thermodynamically inconsistent and unjustifiable results.

Pelton and Chartrand (Pelton and Chartrand, 2001) presented a detailed description of the estimation of the excess Gibbs energies in a ternary solution from binary model parameters when the MQM is used to model the liquid phase. If the data for the three binary subsystems of a ternary system have been optimized and the parameters are in the form of Eq. 2.15, when a symmetric Kohler-type approximation is chosen for the 1-2 subsystem, then Δg_{12} can be written:

$$\Delta g_{12} = \Delta g_{12}^0 + \sum_{1 \le (i+j)} g_{12}^{ij} \left(\frac{X_{11}}{X_{11} + X_{12} + X_{22}} \right)^i \left(\frac{X_{22}}{X_{11} + X_{12} + X_{22}} \right)^j \qquad (2.21)$$

If a Toop-type approximation is chosen, then Δg_{12} can be written:

$$\Delta g_{12} = \Delta g_{12}^0 + \sum_{1 \le (i+j)} g_{12}^{ij} X_{11}^i \left(X_{22} + X_{23} + X_{33} \right)^j \qquad (2.22)$$

The form of these expressions was chosen because in the limit of a very small degree of short-range ordering they reduce to the well-known Kohler and Kohler-Toop approximations with the Bragg-Williams random-mixing model.

The FactSage^{TM} thermodynamic software (FactSage, 2008) allows users to use any of these "geometric models" to increase the flexibility and the ability to estimate the Gibbs energy of ternary or multicomponent solutions from the optimized lower-order parameters.
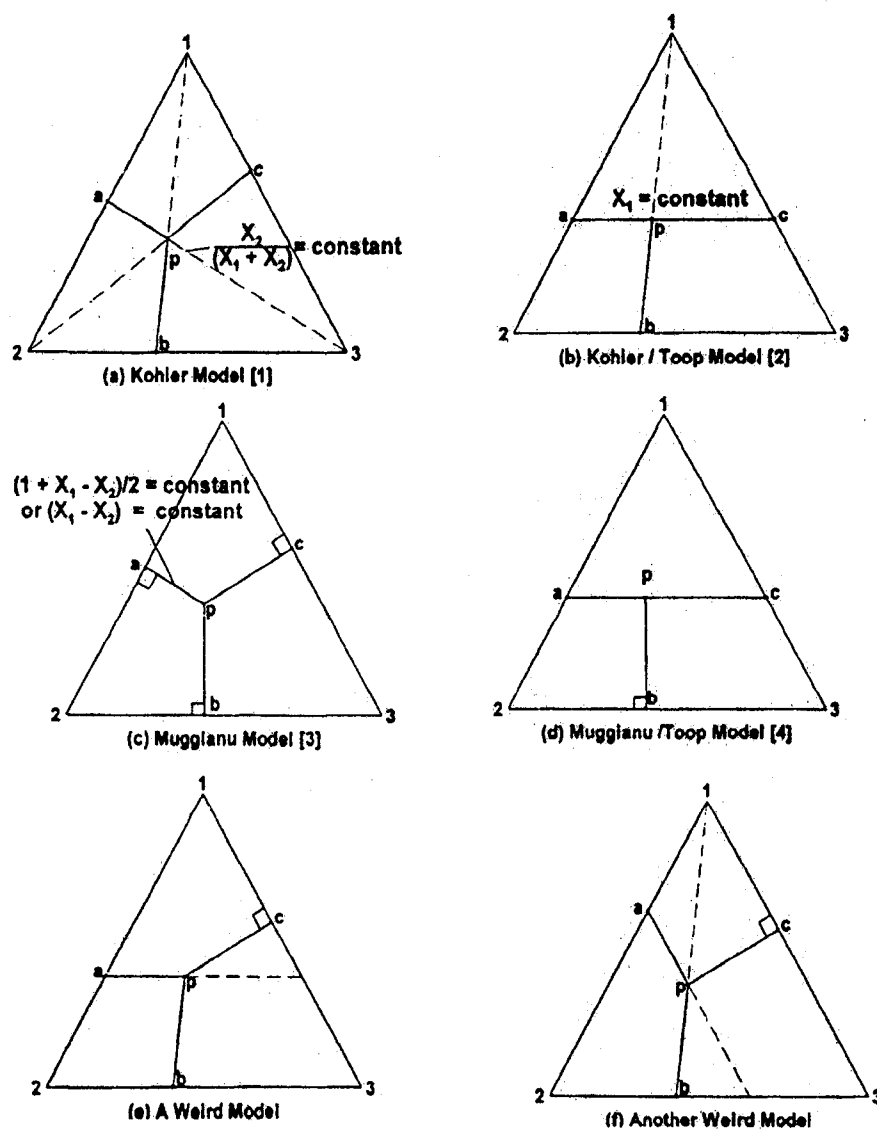
Figure 2.1 Some geometric models for estimating ternary thermodynamic properties from the optimized binary data (reproduced from Pelton, 2001).

2.6 Predictions using only binary parameters

The choice of a model must be based not only on how well it reproduces data in binary systems, but also on how well it predicts and represents properties of ternary solutions. Pelton and Kang (Pelton and Kang, 2007) showed how the MQM generally predicts better the property of ternary solutions from the optimized model parameters than does the random-mixing model.

In a ternary system A-B-C in which the binary solution A-B exhibits a strong tendency to short-range ordering, while the B-C and C-A binary solutions are closer to ideality, positive deviations from ideal mixing behavior will be observed, centered along the A_xB_y-C join where A_xB_y is the binary composition of maximum short-range ordering . If the ordering in the A-B system is sufficiently large, then a miscibility gap is observed along the join. Such positive deviations are expected because the addition of C atoms breaks the energetically favored A-B pairs, and consequently the solution tends to maximize the number of A-B pairs by separating into A_xB_y-rich and C-rich solutions.

A Bragg-Williams model overestimates the positive deviations observed in such ternary systems. In fact, it may predict a miscibility gap when there is none. An associate model, in which the short-range ordering in the A-B binary solution is modeled as being due to A_xB_y molecules or associates, will not at all predict such deviations. The associate model simply predicts that, along the A_xB_y-C join, the solution is an ideal mixture of A_xB_y

associates and C atoms. The MQM, with proper choice of coordination numbers, predicts better such positive deviations along the A_xB_y-C join.

Pelton and Kang (Pelton and Kang, 2007) also showed that usually the MQM better predicts extensions of binary miscibility gaps into a ternary system. A miscibility gap in a binary liquid phase modeled using the MQM is much flatter with a comparatively lower consolute temperature than is obtained by a random-mixing model. As a result, the MQM predicts a smaller extension of a binary miscibility gap into a ternary system.

Chapter 3: Approach to the work and presentation of articles

As part of a broader research project to develop a thermodynamic database for Mg-alloys with 25 potential alloying elements, the objective of the present work was to prepare a critically evaluated thermodynamic database for Mg-alloys, five binary systems: Si-Zn, Ce-Si, Y-Si, Mn-Si and Al-Mn, and five ternary systems: Mg-Si-Zn, Mg-Ce-Si, Mg-Y-Si, Mg-Mn-Si and Mg-Al-Mn, were critically evaluated and optimized. No optimizations taking short-range ordering in the liquid phase in these systems have been reported before.

Rare earth elements like Ce and Y increase the high-temperature stability of Mg-alloys. Mn is known to improve the corrosion resistance of Mg-alloys. Al and Zn increase the mechanical properties of Mg-alloys by solution and precipitation hardening. Si is often added as an alloying element to Mg-alloys. All these elements are considered as potential alloying elements for development of novel Mg-alloys and are of interest.

All the calculations and optimizations in the present work were perfomed with the FactSage^{TM} thermochemical software. The various steps followed in the present work which collectively come under the CALPHAD approach were:

\# *The binary systems to be optimized during the present work were identified.*

Collection of data in the literature for the system:

All the data in the literature on the thermodynamic properties of the chosen systems were collected. These data were phase diagram data, thermodynamic properties like enthalpy of mixing in a solution phase or enthalpy of formation for compounds, activity of constituents in a solution, *etc.* Sometimes data other than thermodynamic properties, such as magnetism or electrical conductivity, which can be helpful in evaluation of a system, were also collected. When enough data were not available in a lower-order binary system, data from a ternary system were used to deduce some necessary conclusions.

Selection of the appropriate thermodynamic model:

As stated in Chapter 2.2, an adequate model representing the Gibbs energy functions for a phase is required. This is very important since a good physical model based on the structure of the phase increases the accuracy of predictions of solution properties in multicomponent systems. In the present work, the Modified Quasichemical Model (MQM) capable of taking into account ordering or clustering in the liquid alloy was chosen. In the present work, solid phases appeared in the form of stoichiometric and terminal solid solutions which were modeled using Eqs. 2.20 and 2.21 respectively.

Critical evaluation of collected experimental data:

The experimental data by different authors were often found to differ from each other by more than the stated experimental error limits. Sometimes data were not thermodynamically consistent with each other. Therefore, all the available experimental

data were evaluated on the basis of experimental techniques and thermodynamic consistency. When the accuracy of the experimental data was difficult to evaluate from the description of the experimental technique, their consistency or inconsistency was discernible during the simultaneous optimization of the data.

Optimization of model parameters for the system:

After evaluation of the experimental data, optimization was performed on the basis of selected reliable data to obtain the values of the model parameters. In this stage, optimization software, the OptiSage module in FactSage^{TM}, was quite useful.

OptiSage is an optimizer module which generates a consistent set of model parameters from a given set of experimental data which in turn are used to represent the Gibbs energies of phases. In simple words, OptiSage gives model parameters which can reproduce the input data. While using OptiSage to get the best fit, the researcher has to use his own judgment on the selection of parameters, such as which should be fixed or altered and if additional parameters have to be introduced. The convergence of the results in OptiSage depends upon the starting values given to the model parameters and the error limits set for the input data. Sometimes several steps are required to obtain the model parameters which can satisfactorily reproduce the input data. Also in some cases, it is easier and faster to obtain starting values from OptiSage, which can roughly reproduce the data, and then refine the fitting by the trial and error method. In the present work, the optimized parameters were obtained with the help of OptiSage or sometimes with both OptiSage and the trial and error method.

 # Back-calculation of all thermodynamic data and phase diagrams: Once satisfactory model parameters were obtained, all the thermodynamic data and experimental data were back-calculated for comparison with the optimized values.

 # Evaluation of ternary systems:

The presently obtained model parameters for the binary systems were combined with previously optimized binary parameters of the other binary sub-systems to estimate the Gibbs energies of solutions in the ternary systems using the techniques given in Chapter 2.5. With the help of these Gibbs energies, evaluations and predictions were made for the ternary systems.

The various results obtained in the present work following the above steps were prepared as three articles which have been submitted to journals. These articles are presented in Chapters 3, 4 and 5.

The first article in Chapter 3 contains the thermodynamic optimizations of the Ce-Si, Y-Si, Mg-Ce-Si and Mg-Y-Si systems. This article has been submitted to the *International Journal of Materials Research.* This article contains the literature review and thermodynamic optimizations of these systems. Polythermal liquidus projections were also predicted and calculated for the ternary systems.

The second article in Chapter 4 contains the thermodynamic optimizations of the Si-Zn, Mn-Si, Mg-Si-Zn and Mg-Mn-Si systems. This article has been submitted to the *Calphad* Journal. This article contains the literature review and thermodynamic optimizations of these systems. Polythermal liquidus projections were also predicted and calculated for the ternary systems.

The third article in Chapter 5 contains the thermodynamic optimizations of the Al-Mn and Mg-Al-Mn systems. This article has been submitted to the *Journal of Phase Equilibria and Diffusion*. This article contains the literature review and thermodynamic optimizations of these systems. There are many ternary data available for the Mg-Al-Mn system compared to the other ternary systems stated above. All these ternary data have been satisfactorily reproduced after their critical evaluation. Polythermal projections for this ternary system were also predicted and calculated.

Chapter 4:   Article 1

Adarsh Shukla, Youn-Bae Kang and Arthur D. Pelton

Centre de Recherche en Calcul Thermochimique, Département de Génie Chimique,

Ecole Polytechnique, Montréal, Québec, Canada

Thermodynamic assessment of the Ce-Si, Y-Si, Mg-Ce-Si and Mg-Y-Si systems.

The binary Ce-Si and Y-Si systems have been critically evaluated based upon available phase equilibrium and thermodynamic data, and optimized model parameters have been obtained giving the Gibbs energies of all phases as functions of temperature and composition. The liquid solution has been modeled with the Modified Quasichemical Model (MQM) to account for the short-range-ordering. The results have been combined with those of our previous optimizations of the Mg-Si, Mg-Ce and Mg-Y systems to predict the phase diagrams of the Mg-Ce-Si and Mg-Y-Si systems. The predictions have been compared with available data.

4.1 **Introduction**

Although magnesium-based materials have a long history of important commercial applications, including automotive, there remains much to be learned about the basic properties of the metal and its alloys. With the recent renewed interest in lightweight wrought materials, including both sheet and tube applications, there has been an increased focus on developing a better understanding of novel magnesium alloys, including those that incorporate additions of such elements as Ce and Y. These alloy systems, along with other potential candidates, are being actively pursued as possible routes to develop magnesium materials with improved ductility, or even practical room temperature formability. Silicon is often added to Mg as an alloying element. Hence, the Mg-Ce-Si and Mg-Y-Si systems are of interest.

The properties of cast or wrought material depend first and foremost upon the phases and microstructural constituents (eutectics, precipitates, solid solutions, etc.) which are present. In an alloy with several alloying elements, the phase relationships are very complex. In order to investigate and understand these complex phase relationships effectively, it is very useful do develop thermodynamic databases containing model parameters giving the thermodynamic properties of all phases as functions of temperature and composition. Using Gibbs free energy minimization software such as FactSage [1, 2], the automotive and aeronautical industries and their suppliers will be able to access the databases to calculate the amounts and compositions of all phases at equilibrium at

any temperature and composition in multicomponent alloys, to follow the course of equilibrium or non-equilibrium cooling, to calculate corresponding heat effects, *etc.*

Such thermodynamic databases are prepared by critical evaluation, modeling, and optimization. In a thermodynamic "optimization," adjustable model parameters are calculated using, simultaneously, all available thermodynamic and phase-equilibrium data in order to obtain one set of model equations as functions of temperature and composition. Thermodynamic data, such as activities, can aid in the evaluation of the phase diagrams, and information on phase equilibria can be used to deduce thermodynamic properties. Thus, it is frequently possible to resolve discrepancies in the available data. From the model equations, all of the thermodynamic properties and phase diagrams can be back-calculated, and interpolations and extrapolations can be made in a thermodynamically correct manner. The data are thereby rendered self-consistent and consistent with thermodynamic principles, and the available data are distilled into a small set of model parameters, ideal for computer storage.

As part of a broader research project to develop a thermodynamic database for Mg alloys with 25 potential alloying elements, the present study reports on evaluations and optimizations of the Ce-Si, Y-Si, Mg-Ce-Si and Mg-Y-Si systems. A recent work by Bulanova et al. [3] reports phase equilibria for the Ce-Si system, but no thermodynamic optimization of the system based upon these phase diagram data has yet been reported. Previous optimizations [4-6] of the Ce-Si and Y-Si systems were based upon a Bragg-

Williams (BW) random-mixing model for the liquid phase. However, the liquid phase in these binary systems are expected to exhibit considerable short-range-ordering (SRO) as evidenced by the very negative "V-shaped" enthalpy of mixing curves. In the present work the Modified Quasichemcial Model (MQM) has been used to account for the SRO. As has been shown by the present authors [7], the use of the Bragg-Williams model in liquids with a high degree of SRO generally results in unsatisfactory results and in poor predictions of ternary properties from binary model parameters. Furthermore, recent thermodynamic data [8] for solid phases in the Y-Si system were not considered in the previous optimizations. Hence the Ce-Si and Y-Si systems have been re-optimized.

The binary model parameters have then been combined with those from our previous optimizations of the Mg-Ce [9], Mg-Y [9] and Mg-Si [10] systems in order to predict the thermodynamic properties and phase equilibria of the Mg-Ce-Si and Mg-Y-Si ternary systems. The experimental data available for the ternary systems are very sparse; wherever available they have been compared with the present predictions.

4.2 Modified Quashichemical Model (MQM)

The Modified Quasichemical Model (MQM) in the pair approximation [11] was used to model the liquid alloys. Previous optimizations of the Mg-Ce [9], Mg-Y [9] and Mg-Si [10] systems have also used the MQM to model the liquid phase. This model, which takes SRO into account, has been used extensively for molten salts [12-14], slags [15]

and sulfides [16-18]. All details of the model and notation have been described previously [11] and only a brief summary is given here.

In the MQM in the pair approximation, the following pair exchange reaction between atoms A and B on neighboring lattice sites is considered:

$$(A-A)+(B-B)=2(A-B); \qquad \Delta g_{AB} \tag{1}$$

where $(i-j)$ represents a first-nearest-neighbor pair. The non-configurational Gibbs energy change for the formation of two moles of $(A-B)$ pairs is Δg_{AB}.

Let n_A and n_B be the number of moles of A and B, n_{ij} be the number of moles of $(i-j)$ pairs, and Z_A and Z_B be the coordination numbers of A and B. The pair fractions, mole fractions, and "coordination-equivalent" fractions are defined respectively as:

$$X_{ij} = n_{ij}/(n_{AA} + n_{BB} + n_{AB}) \tag{2}$$

$$X_A = n_A/(n_A + n_B) = 1 - X_B \tag{3}$$

$$Y_A = Z_A n_A/(Z_A n_A + Z_B n_B) = Z_A X_A/(Z_A X_A + Z_B X_B) = 1 - Y_B \tag{4}$$

The following equations may be written:

$$Z_A X_A = 2n_{AA} + n_{AB} \tag{5}$$

$$Z_B X_B = 2n_{BB} + n_{AB} \tag{6}$$

The Gibbs energy of the solution is given by:

$$G = (n_A g_A^\circ + n_B g_B^\circ) - T\Delta S^{\text{config}} + (n_{AB}/2)\Delta g_{AB} \tag{7}$$

where g_A° and g_B° are the molar Gibbs energies of the pure components and $\Delta S^{\mathrm{config}}$ is the configurational entropy of mixing given by randomly distributing the $(A-A)$, $(B-B)$ and $(A-B)$ pairs in the one-dimensional Ising approximation [11]:

$$
\Delta S^{\mathrm{config}} = -\mathrm{R}\left(n_A \ln X_A + n_B \ln X_B\right)
$$
$$
- \mathrm{R}\left[n_{AA}\ln\left(X_{AA}/Y_A^2\right) + n_{BB}\ln\left(X_{BB}/Y_B^2\right) + n_{AB}\ln\left(X_{AB}/2Y_A Y_B\right)\right]
$$

(8)

Δg_{AB} is expanded in terms of the pair fractions:

$$
\Delta g_{AB} = \Delta g_{AB}^\circ + \sum_{i\geq 1} g_{AB}^{i0} X_{AA}^i + \sum_{j\geq 1} g_{AB}^{0j} X_{BB}^j
$$

(9)

where Δg_{AB}°, g_{AB}^{i0} and g_{AB}^{0j} are the parameters of the model which may be functions of temperature.

The equilibrium pair distribution is calculated by setting

$$
\left(\partial G / \partial n_{AB}\right)_{n_A, n_B} = 0
$$

(10)

This gives the "equilibrium constant" for the "quasichemical reaction" of (Eq. 1):

$$
\frac{X_{AB}^2}{X_{AA} X_{BB}} = 4\exp\left(-\frac{\Delta g_{AB}}{\mathrm{R}T}\right)
$$

(11)

As Δg_{AB} becomes progressively more negative, the reaction (Eq. 1) is shifted progressively to the right, and the calculated enthalpy and configurational entropy of mixing assume, respectively, the negative "V" and "m" shapes characteristic of SRO.

The composition of maximum SRO is determined by the ratio of the coordination numbers Z_B/Z_A, as given by the following equations [11]:

$$\frac{1}{Z_A} = \frac{1}{Z_{AA}^A}\left(\frac{2n_{AA}}{2n_{AA}+n_{AB}}\right) + \frac{1}{Z_{AB}^A}\left(\frac{n_{AB}}{2n_{AA}+n_{AB}}\right) \tag{12}$$

$$\frac{1}{Z_B} = \frac{1}{Z_{BB}^B}\left(\frac{2n_{BB}}{2n_{BB}+n_{AB}}\right) + \frac{1}{Z_{BA}^B}\left(\frac{n_{AB}}{2n_{BB}+n_{AB}}\right) \tag{13}$$

where Z_{AA}^A and Z_{AB}^A are the values of Z_A respectively when all the nearest neighbors of an A are A's, and when all nearest neighbors of an A are B's, and where Z_{BB}^B and Z_{BA}^B are defined similarly. (Note that Z_{AB}^A and Z_{BA}^B represent the same quantity and can be used interchangeably.) In order to set the composition of maximum SRO at $X_{Si} = 0.5$ (corresponding to the compositions CeSi and YSi) in the binary systems, we set the $Z_{ij}^i/Z_{ij}^j = 1$ so that the compositions of maximum SRO occur at the equimolar composition in both binary systems. Although the model is sensitive to the ratio of the coordination numbers, it is less sensitive to their absolute values. The use of the one-dimensional Ising model in Eq. 8 introduces a mathematical approximation into the model which we have found, by experience, can be partially compensated by selecting values of Z_B and Z_A which are smaller than the actual values. The value of the coordination numbers selected in the present study are listed in Tab. 4.1.

The liquid phase shows maximum SRO in the Mg-Ce system at the composition $X_{Mg} = 3/4$ (CeMg$_3$) [9], in the Mg-Y system at $X_{Mg} = 2/3$ [9], and in the Mg-Si system at the equimolar composition [10].

From the MQM model parameters for the binary liquid phases, the thermodynamic properties of a ternary liquid phase may be estimated as discussed previously [19]. If ternary experimental data are available, additional ternary model parameters may be added if required.

4.3 Binary Systems

All calculations and optimizations in the present study were performed with the FactSage thermochemical software [1, 2].

The optimized model parameters of all phases obtained in the present study are listed in Tab. 4.1. The crystallographic data [20] of all phases in the Ce-Si and Y-Si systems are listed in Tab. 4.2. The Gibbs energies of all stable and metastable phases of pure Ce, Y and Si were taken from Dinsdale [21].

4.3.1 The Ce-Si system

The calculated optimized phase diagram of the Ce-Si system is compared with experimental data in Fig. 4.1. The optimized enthalpies of formation of the solid alloys and partial enthalpies of mixing in the liquid phase are compared with experimental data and previous optimization in Figs. 4.2 and 4.3 respectively. The calculated entropy of mixing in the liquid phase is compared with the ideal mixing curve and the previous optimizations in Fig. 4.4.

A complete literature review of the Ce-Si system up to 1989 was reported by Munitz et al. [22]. Benesovsky et al. [23] investigated the system by metallograpy and melting point studies. The most recent investigation of the system is by Bulanova et al. who used DTA, XRD and metallographic techniques. Grobner et al. [4] performed a thermodynamic optimization of the system but did not refer to the paper by Bulanova and co-workers. Bulanova et al. [3], by XRD, identified six intermetallic phases: Ce_5Si_3, Ce_3Si_2, Ce_5Si_4, $CeSi$, $CeSi_{2-a1}$ and $CeSi_{2-a2}$. These authors reported that the compounds $CeSi_{2-a1}$ and $CeSi_{2-a2}$ have small homogeneity ranges, but their results did not permit the single-phase composition limits to be determined quantitatively. These compounds have been given various designations [3, 22]. Following Muntiz et al. [22] and Grobner et al. [4], we have modeled them as the stoichiometric compounds Ce_3Si_5 and $CeSi_2$. Other intermetallic compounds were also modeled as stoichiometric in the absence of evidence of appreciable homogeneity ranges.

The different structures of Ce and Si (Tab. 4.2) and the large difference in their atomic radii (0.185 nm and 0.110 nm respectively) [24] mitigate against any appreciable mutual terminal solid solubility. Hence, none was assumed.

The standard enthalpies of formation at 25 ^{0}C of CeSi, $CeSi_2$ and Ce_5Si_3 were measured by Meschel and Kleppa [25, 26] using direct synthesis calorimetry. These data are well reproduced by the present optimization as can be seen in Fig. 4.2. These authors also reported heat contents ($H_T - H_{298K}$) of CeSi and $CeSi_2$ at 1200 ^{0}C and of Ce_5Si_3 at 1000

^{0}C. Their results are shown in Tab. 4.3. As shown in Tab. 4.1, the Neumann-Kopp (NK) approximation was used for the heat capacities of CeSi and CeSi$_2$. This reproduced the measured heat contents very well as shown in Tab. 4.3. However for Ce$_5$Si$_3$ it was necessary to increase the heat capacity slightly by 1.250 J·mol-atoms^{-1}·K^{-1} above the value given by the NK approximation in order to reproduce the measured heat content, as shown in Tab. 4.3. For the compounds Ce$_3$Si$_2$ and Ce$_5$Si$_4$, the heat capacities predicted by the NK approximation were then increased by 1.600 and 0.778 J·mol-atoms^{-1}·K^{-1} respectively in order that the estimated heat capacities of these compounds vary linearly with atomic fraction between those of Ce$_5$Si$_3$ and CeSi.

It should be noted that the optimized entropies of formation of the intermetallic compounds from the elements at 25 ^{0}C are all very small as is generally expected for such compounds. That is, the optimized entropies are physically reasonable.

Ryss et al. [27], at 1650 ^{0}C, and Sudavtsova et al. [28], at 1617 ^{0}C, measured partial enthalpies of mixing in the liquid phase by high-temperature isothermal calorimetry. Ryss et al. [27] reported only smoothed curves. The present optimized curves are compared to these data in Fig. 4.3 where good agreement can be seen, keeping in mind that the data of Ryss et al. [27] are from smoothed curves.

The shape of the partial enthalpy curves in Fig. 4.3, which are very negative with points of inflection and a point of intersection near the equimolar composition, are strongly

indicative of a high degree of SRO about this composition. An entropy of mixing with a strong minimum near the equimolar composition as in Fig. 4.4 is thus expected. These shapes of the enthalpy and entropy of mixing curves are well reproduced by the MQM.

4.3.2 The Y-Si system

The optimized phase diagram of the Y-Si system is compared with the experimental data in Fig. 4.5. Calculated thermodynamic properties are shown and compared with experimental data and previous optimizations in Figs. 4.6 to 4.10.

Lundin [29] first investigated the system by XRD and metallographic methods. Gschneidner [30] mentioned that the mutual terminal solid solubilities of silicon and yttrium are less than 0.01 wt. % but did not specify the source. Ran et al. [6] performed a thermodynamic optimization of the system based upon the phase diagram data of Lundin [29], modeling the liquid with a Bragg-Williams random-mixing model. Later, Button and McColm [31] investigated the system by thermal analysis, metallography, XRD and hardness measurements. They suggested 0.8 at. % solubility of silicon in solid yttrium by studying the microstructure of the eutectic. Button and McColm [31], by X-Ray powder diffraction, reported Y_5Si_3, Y_5Si_4, YSi and Y_3Si_5 as equilibrium phases. There is controversy in the literature regarding the existence of a stable phase YSi_2. Gschneidner [30] cites references claiming that this phase is not stable, whereas Gokhale and Abbaschian [32] cite references claiming that it is stable. In the optimization of COST 507 [5] and Ran et al. [6] YSi_2 was included as a stable phase. In view of the fact that the

most recent XRD study [31] does not report YSi_2 as a stable phase, it is not included in the present optimization.

Perri et al. [33] reported an allotropic transformation of Y_3Si_5 at 450 ^0C; the low-temperature form is orthorhombic and the high temperature form is hexagonal. No other information regarding this transformation could be found. In the present optimization the Gibb energy of this transformation was taken to be zero.

No evidence of appreciable homogeneity ranges for the intermediate compounds could be found in the literature. Hence all the intermediate phases have been modeled as stiochiometric compounds.

The different structures of Y and Si (Tab. 4.2) and the large difference in their atomic radii (0.180 nm and 0.110 nm respectively) [24] mitigate against any appreciable mutual terminal solid solubility. Hence, none was assumed.

Polotskaya et al. [8] reported Gibbs energies of formation of the silicides by EMF measurements at 577 ^0C as shown in Fig. 4.6. The standard enthalpy of formation of Y_5Si_3 as reported by Topor and Kleppa [34] who used solvent drop calorimetry is reproduced well by the present optimization as can be seen in Fig. 4.7. To reproduce simultaneously the Gibbs energy of formation of Y_5Si_3 reported by Polotskaya et al. [8] and the enthalpy of formation reported by Topor and Kleppa [34] would require the

assumption of an improbably large entropy of formation. As shown in Fig. 4.7, more weight was given to the direct calorimetric measurement of Topor and Kleppa [34] than to the enthalpies of Polotskaya et al. [8] which were obtained from the temperature dependence of their EMF measurements.

As in the Ce-Si system, the optimized entropies of formation of the intermetallic compounds in the Y-Si system from the elements at 25 ^{0}C are all very small as is generally expected for such compounds. That is, the optimized entropies are physically reasonable.

Ryss et al. [35] and Esin et al. [36] measured partial enthalpies of mixing in the liquid phase at 1597 ^{0}C and 1607 ^{0}C respectively using high-temperature isothermal calorimetry as shown in Fig. 4.8. Stukalo et al. [37] measured the integral enthalpy of mixing in the liquid at 1780 ^{0}C by the same method, as shown in Fig. 4.9. The shape of the partial enthalpy curves in Fig. 4.8, which are very negative with points of inflection near the equimolar composition, and the corresponding "V-shaped" enthalpy of mixing curve in Fig. 4.9 with a sharp minimum at the equimolar composition, are indicative of a high degree of SRO about this composition, and are well reproduced by the MQM. The SRO also results in an entropy of mixing curve with a strong minimum near the equimolar composition as seen in Fig. 4.10.

4.4 Ternary Systems

4.4.1 The Mg-Ce-Si system

The phase diagrams of the Mg-Ce and Mg-Si systems from previous optimizations [9, 10] are shown in Figs. 4.11 and 4.12 respectively. These optimizations were combined with the present optimization of the Ce-Si system in order to predict the thermodynamic properties and phase diagram of the Mg-Ce-Si system. The resultant calculated polythermal projection of the liquidus surface is shown in Fig. 4.13. No measurements of the liquidus have been reported.

Mutual solubilites between binary compounds have been assumed to be negligible, there being no experimental data available. Although Mg_2Ce and Mg_2Si have similar stoichiometries, they have different structures, as is also the case for CeSi and MgCe (Tab. 4.2). Furthermore, the atomic radii of Si, Ce and Mg are quite different (0.111, 0.185 and 0.150 nm respectively) [24]. All these factors mitigate against appreciable mutual solubility of the compounds.

The thermodynamic properties of the ternary liquid phase were calculated by the MQM from the binary model parameters. No additional ternary parameters were included. The "asymmetric approximation" [19, 38] with Mg as "asymmetric component" was used since the Ce-Si liquid phase exhibits very negative deviations from ideal solution behavior whereas the Mg-Si and Mg-Ce liquid phases are much closer to ideality.

Zmii and Gladyshevkii [39] investigated the system using XRD in the region from 0 to 33 at. % Ce and reported a partial section at 400 ^{0}C. They reported the presence of three ternary compounds: $CeMg_2Si_2$, $CeMgSi$ and $CeMg_3Si$ in this region. In another work [40] they reported the crystal structure of the compound $CeMg_2Si_2$. Recently, Dhar et al. [41] confirmed the presence of the compound $CeMg_2Si_2$ by XRD but did not observe the other two compounds. They also reported the presence of an additional compound, Ce_2MgSi. In the absence of any other data concerning the ternary compounds, it was assumed that they are not stable at liquidus temperatures and they were not included in the present calculations.

The calculated liquid-liquid immiscibility region seen in Fig. 4.13 is expected [7]. The very strong negative deviation from ideal mixing behavior in the binary liquid Ce-Si phase indicates that Ce and Si atoms have a strong tendency to remain paired and not to mix with Mg. It may be noted that the use of a Bragg-Williams random-mixing model rather than the MQM for the liquid phase would result in an even larger calculated immiscibility gap as has been discussed by the present authors [7].

4.4.2 The Mg-Y-Si system

The phase diagrams of the Mg-Si and Mg-Y systems from previous optimizations [9, 10] are shown in Figs. 4.12 and 4.14 respectively. These optimizations were combined with the present optimization of the Y-Si system in order to predict the thermodynamic

properties and phase diagram of the Mg-Y-Si system. The resultant calculated polythermal projection of the liquidus surface is shown in Fig. 4.15.

As in the Mg-Ce-Si system, and for the same reasons, mutual solubilities between binary compounds have been assumed to be negligible, there being no experimental data available. Although Mg_2Y and Mg_2Si have similar stoichiometries, they have different structures, as is also the case for YSi and MgY (Tab. 4.2). Furthermore, the atomic radii of Si, Y and Mg are quite different (0.111, 0.180 and 0.150 nm respectively) [24].

The thermodynamic properties of the ternary liquid phase were calculated by the MQM from the binary model parameters. No additional ternary parameters were included. The "asymmetric approximation" [19, 38] with Mg as "asymmetric component" was used since the Y-Si liquid phase exhibits very negative deviations from ideal solution behavior whereas the Mg-Si and Mg-Ce liquid phases are much closer to ideality. In the absence of any evidence of ternary compounds, none were assumed.

Drits et al. [42] reported the only investigation of the system. By metallographic and thermal cooling methods, they reported phase equilibria in the section from Mg -13 wt. % Y to Mg- 4 wt. % Si. The calculated section is compared with the measurements in Fig. 4.16. Drits et al. also reported an isopleth at constant wt. % Y = 15 for Si contents up to 4 wt. %. This isopleth is compared with the present calculations in Fig. 4.17. The same authors also reported the equilibrium phases present in Mg-rich alloys at 400 ^{0}C.

Comparison with the present calculations is shown in Fig. 4.18 where it is assumed that the "X" phase reported by Drits et al. [42] was YSi. Although the agreement between the calculated phase equilibria and the data points in Figs. 4.16 and 4.17 is not good, it is clear from these figures that the results of Drits et al. [42] are not consistent with the optimized binary Mg-Y phase diagram [9] which is based upon numerous and more recent experimental data.

As in the case of the Mg-Ce-Si system, and for the same reasons, a small calculated liquid-liquid immiscibility region is seen in Fig. 4.15.

4.5 Conclusions

Gibbs energy functions for all phases in the Ce-Si and Y-Si systems have been obtained. All available thermodynamic and phase equilibrium data have been critically evaluated in order to obtain one set of optimized model parameters of the Gibbs energies of all phases which can reproduce the experimental data within experimental error limits. Evaluations and tentative calculated phase diagrams of the ternary systems Mg-Ce-Si and Mg-Y-Si have been given.

The use of the Modified Quasichemical Model for the liquid phase has permitted short-range ordering to be taken into account. Use of this model results in a better fitting of the data for the liquid phase than is the case when a Bragg-Williams random-mixing model is used. This results in a better representation of the partial properties of the solutes in dilute

solution in magnesium, the activities of solutes in dilute solution being of much practical importance. As shown by the present authors [7], the use of the MQM generally also results in better estimations of the properties of ternary and higher-order liquid alloys from binary model parameters. These estimations of phase equilibria will aid in the design of novel magnesium alloys.

4.6 Acknowledgements

4.7 References

[1] C. W. Bale, P. Chartrand, S. A. Degterov, G. Eriksson, K. Hack, R. Ben Mahfoud, J. Melançon, A.D. Pelton, S. Petersen: Calphad 26 (2002) 189.

[2] C. W. Bale, A. D. Pelton, W. Thompson: Factsage thermochemical software and databases, http:// www.crct.polymtl.ca (2008).

[3] M.V. Bulanova, P.N. Zheltov, K.A. Meleshevich, P.A. Saltykov, G. Effenberg: J. Alloys Comp. 345 (2002) 110.

[4] J. Grobner, D. Mirkovic, R. Schmid-Fetzer: Met. and Mat. Trans. A 35 (2004) 3359.

[5] H.L. Lukas: COST 507 – Thermochemical Databases for Light Metal Alloys, Vol. 2 I. Ansara, A.T. Dinsdale, M.H. Rand (eds), (1998) 274.

[6] Q. Ran, H. L. Lukas, G. Effenberg, G. Petzow: Z. Metallkd. 80 (1989) 402.

[7] A. D. Pelton, Y.-B. Kang: Int. J. Mat. Res. 10 (2007) 905.

[8] R. I. Polotskaya, V. R. Sidorko: Powder Metall. Met. Ceram. 36 (1997) 315.

[9] Y.-B. Kang, A. D. Pelton, P. Chartrand, P. Spencer, C. D. Fuerst: J. Phase Equilib. Diffus. 28 (2007) 342.

[10] J. P. Harvey: Masters Thesis, Ecole Polytechnique, Montreal (2006).

[11] A. D. Pelton, S. A. Degterov, G. Eriksson, C. Robelin, Y. Dessureault: Metall. Mater. Trans. B. 31 (2000) 651.

[12] P. Chartrand, A.D. Pelton: Metall. Mater. Trans. A. 32 (2001) 1361.

[13] P. Chartrand, A.D. Pelton: Metall. Mater. Trans. A. 32 (2001) 1385.

[14] P. Chartrand, A.D. Pelton: Metall. Mater. Trans. A. 32 (2001) 1417.

[15] S. A. Decterov, I.-H. Jung, E. Jak, Y.-B. Kang, P. Hayes and A.D. Pelton: Proc. VII International Conference on Molten Slags, Fluxes and Salts, C. Pistorius, Ed., The South African Institute of Mining and Metallurgy, Johannesburg, South Africa, 2004, p 839-850

[16] P. Waldner, A. D. Pelton: Z. Metallkunde 95 (2004) 672.

[17] P. Waldner, A. D. Pelton: Metall. Mater. Trans. B 35 (2004) 897.

[18] P. Waldner, A. D. Pelton: J. Phase Equilib. 26 (2005) 23.

[19] A. D. Pelton, P. Chartrand: Metall. Mater. Trans. A. 32 (2001) 1355.

[20] T. B. Massalski, P.R. Subramanian, H. Okamoto, L. Kacprazak, (Eds.): Binary Alloy Phase Diagram, 2nd edition, ASM International, Materials Park, Ohio, 1990.

[21] A. T. Dinsdale: Calphad 15 (1991) 317 plus updates (private communication) http:// www.sgte.org (2000).

[22] A. Munitz, A.B. Gokhale, G.Y. Abbaschian: Bull. Alloy Phase Dia. 1 (1989) 73.

[23] F. Benesovsky, H. Nowotny, W. Rieger, H. Rassaerts: Monatsh. Chem. 97 (1966) 221.

[24] http:// www.webelements.com (reference as stated in the site; C. Slater: J. Chem. Phys. 39 (1964) 3199).

[25] S.V. Meschel, O.J. Kleppa: J. Alloys Comp. 220 (1995) 88.

[26] S.V. Meschel, O.J. Kleppa: J. Alloys Comp. 243 (1996) 186.

[27] G. M. Ryss, Yu. O. Esin, A. I. Stroganov, P.V.Gel'd: Zh. Fiz. Khim. 51 (1977) 232.

[28] V. S. Sudavtsova, Yu. G. Gorobets, G. I. Batalin: Rasplavy 2 (1988) 79.

[29] C. E. Lundin Jr.: Rare Earth, NY, John Wiley Sons (1961) 264.

[30] K. A. Gschneidner: Rare Earth Alloys, D. Van Nostrand, NY (1961) 276.

[31] T. W. Button, I. J. McColm, J. M. Ward: J. Less-Common Met. 159 (1990) 205.

[32] A. B. Gokhale, G. J. Abbaschian: Bull. Alloy Phase Dia. 7 (1986) 485.

[33] J. A. Perri, E. Banks, B Post: J. Phys. Chem. 63 (1959) 2073.

[34] L. Topor, O. J. Kleppa: J. Less-Common Metals. 167 (1990) 91.

[35] G. M. Ryss, Yu. O. Esin, M. S. Petrushevskii, A. I. Stroganov P. V. Geld: Russ. Metall. 6 (1979) 67.

[36] Yu. O. Esin, M. G. Valeshev, P. V. Geld, L. M. Tushkova: Russ. Metall. 1 (1976) 19.

[37] V. A. Stukalo, G. I. Batalin, N. Ya. Neschbimenko, V. P. Kurach: Ukr. Khim. Zh. 46 (1980) 98.

[38] A. D. Pelton, Calphad, 25 (2001) 319.

[39] O. F. Zmii, E. I. Gladyshveskii: Visnki L'viv. un-tu. Ser. Khim. 15 (1974) 24.

[40] O. F. Zmii , E. I. Gladyshevskii: Kristallografiya 15 (1971) 817.

[41] S. K. Dhar, P. Manfrinetti, A.Palenzona: J. Alloys Comp. 252 (1997) 24.

[42] M. E. Drits, M. E. Padezhnova T. V. Dobatkina: Redk. Metally V Tsvet. Splavakh, (1975) 5.

Table 4.1. Optimized model parameters of binary phases in the Ce-Si and Y-Si systems.

Liquid:

Co-ordination numbers:

Ce-Si $\quad Z_{SiSi}^{Si} = Z_{CeCe}^{Ce} = Z_{SiCe}^{Si} = Z_{CeSi}^{Ce} = 6$

Y-Si $\quad Z_{SiSi}^{Si} = Z_{YY}^{Y} = Z_{SiY}^{Si} = Z_{YSi}^{Y} = 6$

Optimized values of Δg_{AB} (Eq 1), in Joules

$\Delta g_{\text{Ce-Si}}$: $\quad$ (-57265 + 3.347 T) + (-9599 + 9.205 T) X_{CeCe} + (-23053) X_{SiSi}

$\Delta g_{\text{Y-Si}}$: $\quad$ (-56484) + (-10878) X_{YY} + (- 2.092 T) X_{SiSi}

Stoichiometric compounds :

Compounds	ΔH^{0}_{298} * (J· mol-atoms^{-1})	S^{0}_{298} ** (J· mol-atoms^{-1}· K^{-1})	ΔS^{0}_{298} * (J· mol-atoms^{-1}· K^{-1})	Cp (J· mol-atoms^{-1}· K^{-1})
$\frac{1}{8}$Ce$_5$Si$_3$	-57225	50.300	- 0.163	0.625 C$_p$(Ce, FCC) + 0.375 C$_p$ (Si, Dia.)+ 1.250
$\frac{1}{5}$Ce$_3$Si$_2$	-60900	48.280	- 0.916	0.600 C$_p$ (Ce, FCC) + 0.400 C$_p$ (Si, Dia.) + 1.600
$\frac{1}{9}$Ce$_5$Si$_4$	-65656	46.833	- 0.113	0.555 C$_p$ (Ce, FCC) + 0.444 C$_p$ (Si, Dia.) + 0.778
$\frac{1}{2}$CeSi	-70500	44.500	0.368	0.500 C$_p$ (Ce, FCC) + 0.500 C$_p$ (Si, Dia.)
$\frac{1}{8}$Ce$_3$Si$_5$	-68104	39.750	1.948	0.375 C$_p$(Ce, FCC) + 0.625 C$_p$ (Si, Dia.)
$\frac{1}{3}$CeSi$_2$	-62733	38.000	2.308	0.333 C$_p$ (Ce, FCC) + 0.667 C$_p$ (Si, Dia.)
$\frac{1}{8}$Y$_5$Si$_3$	-69025	37.125	2.079	0.625 C$_p$(Y, HCP) + 0.375 C$_p$ (Si, Dia.) – 0.750
$\frac{1}{9}$Y$_5$Si$_4$	-82889	30.778	-2.464	0.555 C$_p$(Y, HCP) + 0.444 C$_p$ (Si, Dia.)
$\frac{1}{2}$YSi	-91670	26.350	-5.449	0.500 C$_p$(Y, HCP) + 0.500 C$_p$ (Si, Dia.)
$\frac{1}{8}$Y$_3$Si$_5$	-67250	30.500	1.948	0.375 C$_p$ (Y, HCP) + 0.625 C$_p$ (Si, Dia.)

* Enthalpy and entropy of formation from the elements at 298.15 K
** Absolute Third-Law entropy at 298.15 K

Table 4.2. Crystallographic data [20] of all phases considered in the present optimization in the Ce-Si, Y-Si, Mg-Ce-Si, Mg-Ce-Si and Mg-Y-Si systems.

Phase	Strukturbe-richt	Prototype	Pearson symbol	Space group	Comments
Liquid	-	-	-	-	
FCC	$A1$	Cu	$cF4$	$Fm\bar{3}m$	Ce is stable phase.
BCC	$A2$	W	$cI2$	$Im\bar{3}m$	Ce, Y are stable phases.
HCP	$A3$	Mg	$hP2$	$P6_3/mmc$	Mg, Y are stable phases.
DHCP	$A3'$	α-La	$hP4$	$P6_3/mmc$	Ce is stable phase.
Si (Dia.)	$A4$	C(Dia.)	$cF8$	$Fd\bar{3}m$	
$Mg_{24}Y_5$	$A12$	α-Mn	$cI58$	$I\bar{4}3m$	
Laves-C14	$C14$	$MgZn_2$	$hP12$	$P6_3/mmc$	Mg_2Y is stable phase.
Laves-C15	$C15$	Cu_2Mg	$cF24$	$Fd\bar{3}m$	$CeMg_2$, is stable phase.
BCC-B2	$B2$	CsCl	$cP2$	$Pm3m$	MgY, CeMg are stable phases.
$CeMg_3$	$D0_3$	$BiFe_3$	$cF16$	$Fm\bar{3}m$	
$CeMg_{12}$	$D2_b$	$Mn_{12}Th$	$tI26$	$I4/mmm$	
Ce_5Mg_{41}	-	Ce_5Mg_{41}	$tI92$	$I4/m$	
Ce_2Mg_{17}	-	$Ni_{17}Th_2$	$hP38$	$P6_3/mmc$	
Mg_2Si	$C1$	CaF_2	$cF12$	$Fm\bar{3}m$	
Ce_5Si_3	$D8_m$	$Si_3W_5{}^{**}$	$tI32$	$I4/mcm$	
Ce_3Si_2	$D5_a$	Si_2U_3	$tP10$	$P4/mbm$	
Ce_5Si_4	-	Si_4Zr_5	$(a)^*$	-	
CeSi	$B27$	FeB	$oP8$	$Pnma$	
Ce_3Si_5	-	$GdSi_2$	$(b)^*$	$Imma$	
$CeSi_2$	C_c	$ThSi_2$	$tI12$	$I4_1/amd$	
Y_5Si_3	$D8_8$	Mn_5Si_3	$hP16$	$P6_3/mcm$	
Y_5Si_4		Sm_5Ge_4	$oP36$	-	
YSi	B_f	CrB	$oC8$	$Cmcm$	
Y_3Si_5	C_c	$ThSi_2$ distorted	$tI12$	$I4_1/amd$	Low temperature form
Y_3Si_5	-	-	-	-	High temperature form

(a)* Tetragonal   (b)* Orthorhombic

Table 4.3. Reported heat contents of compounds in the Ce-Si system compared with the present calculations.

Compound	Experimental $H_T - H_{298K}$ (kJ·mol-atoms^{-1})	$H_T - H_{298K}$ calculated from Neumann-Kopp approximation (kJ·mol-atoms^{-1} ·K^{-1})	$H_T - H_{298K}$ Calculated (kJ·mol-atoms^{-1}·K^{-1})
Ce$_5$Si$_3$	31.3 ± 0.4 (1000 ^{0}C) [25]	29.85	31.07
CeSi	35.2 ± 2.2 (1200 ^{0}C) [26]	35.47	35.47 *
CeSi$_2$	33.5 ± 1.3 (1200 ^{0}C) [26]	33.61	33.61 *

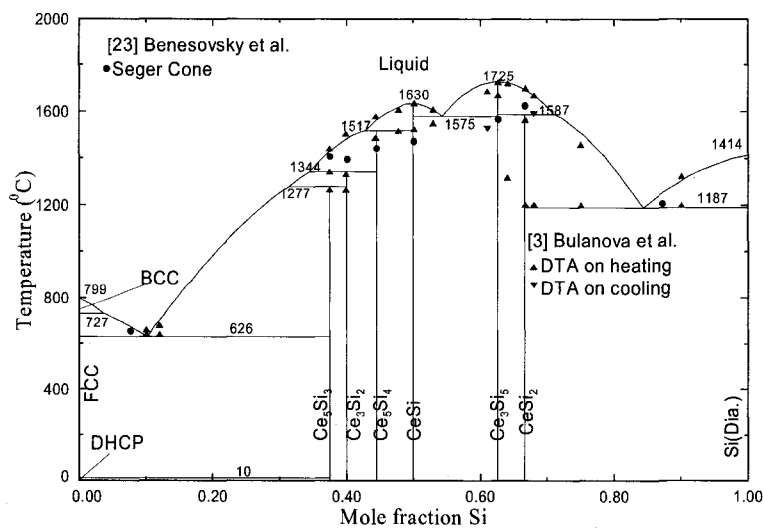* No alteration to the Neumann-Kopp heat capacity was required.

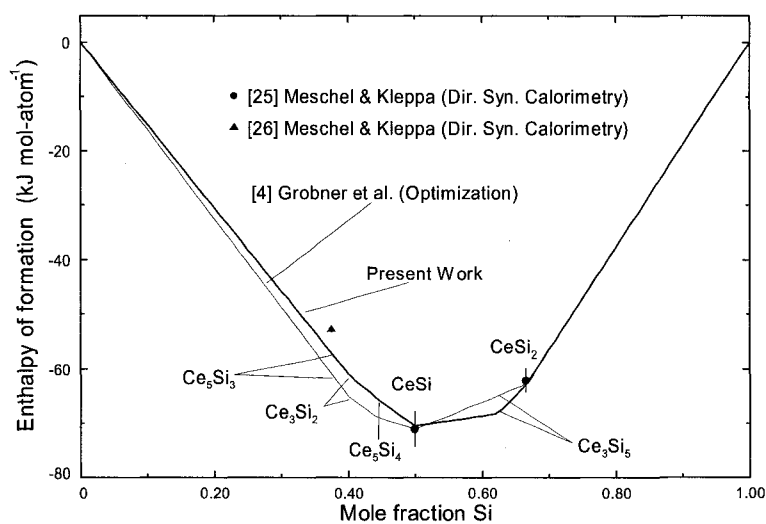Fig. 4.1. Optimized phase diagram of the Ce-Si system.

Fig. 4.2. Standard enthalpy of formation at 25 ^{0}C of intermetallic compounds
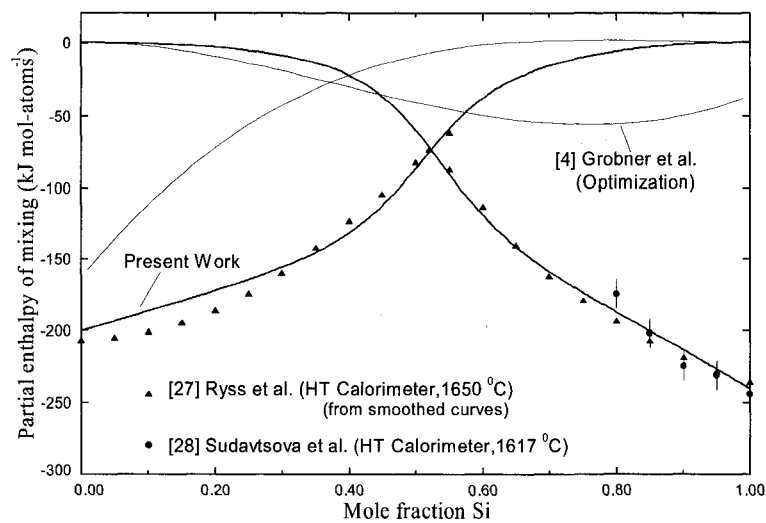
in the Ce-Si system.

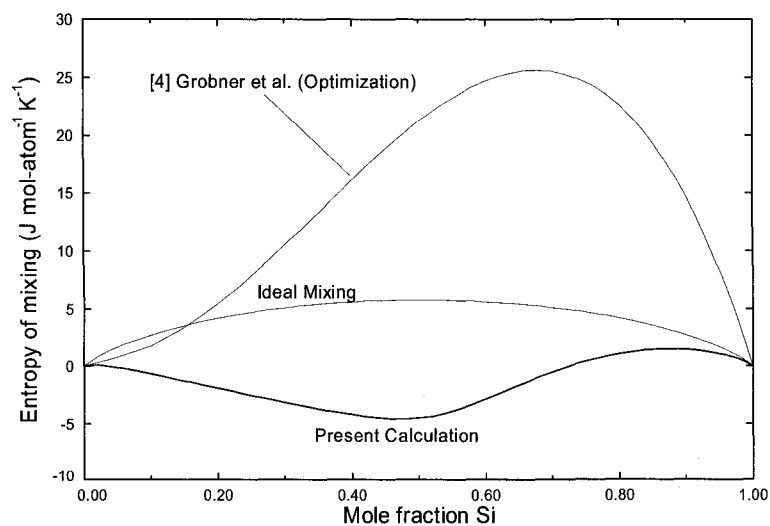Fig. 4.3. Partial enthalpies of mixing in liquid Ce-Si solutions at 1650 ^{0}C.

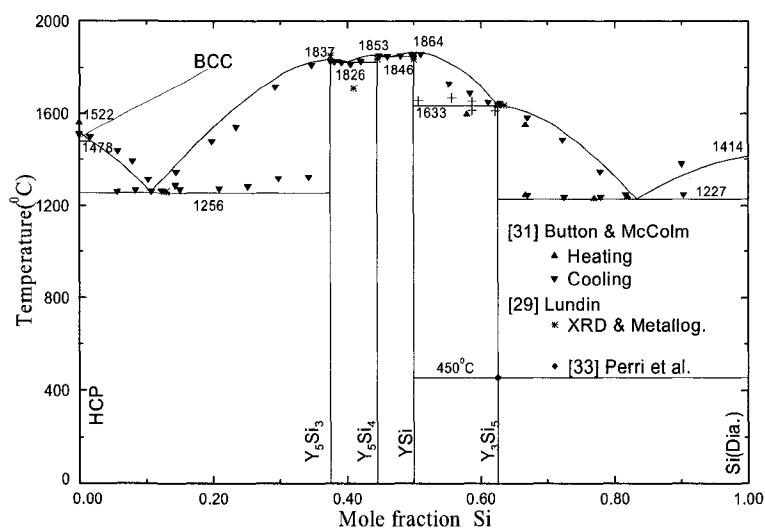Fig. 4.4. Calculated entropy of mixing in liquid Ce-Si solutions at 1650 ^{0}C.

Fig. 4.5. Optimized phase diagram of the Y-Si system.
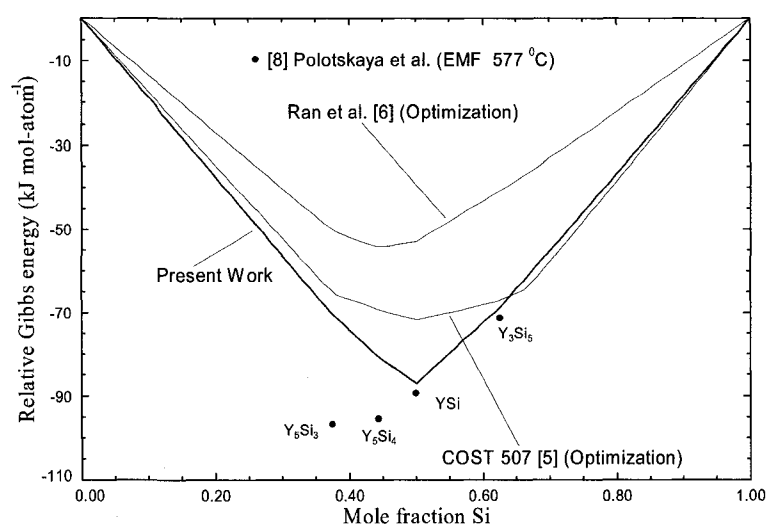
Fig. 4.6. Calculated Gibbs energy of formation from the elements of intermetallic compounds in the Y-Si system at 577 ^{0}C.
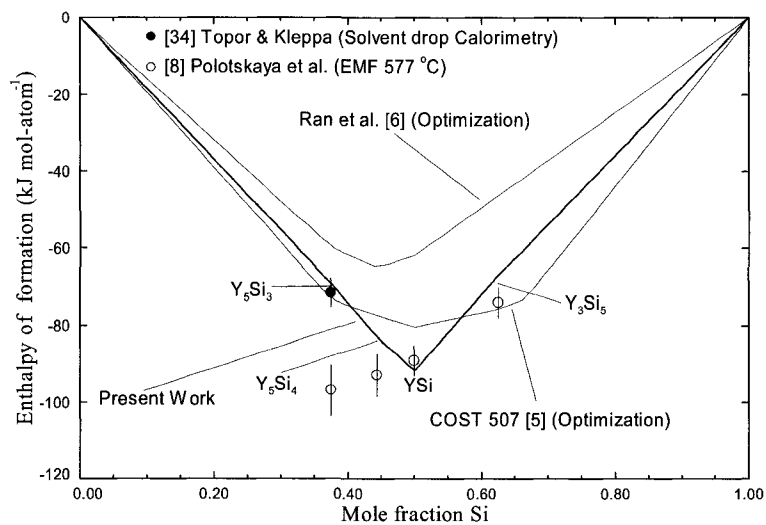
Fig. 4.7. Standard enthalpy of formation of intermetallic compounds in the Y-Si system.
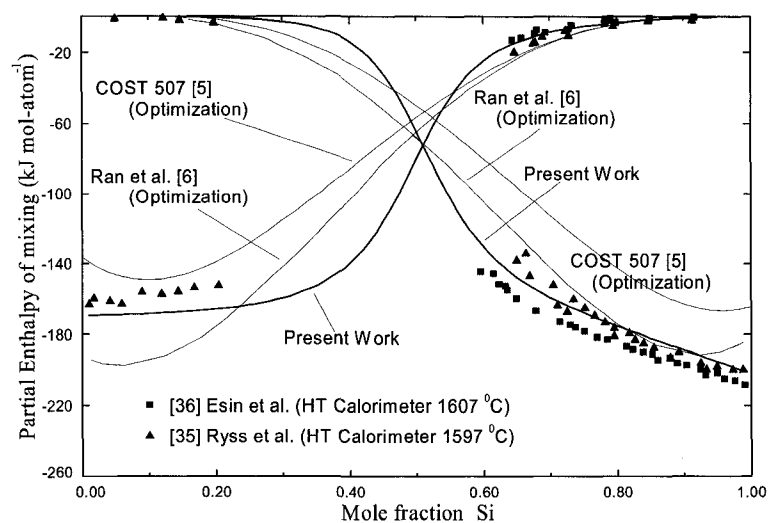
Fig. 4.8. Partial enthalpies of mixing in liquid Y-Si solutions at 1600 ^{0}C.
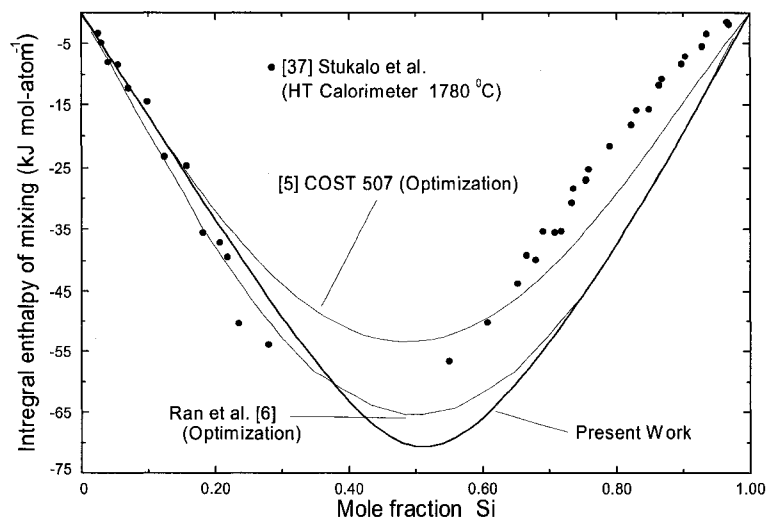
Fig. 4.9. Integral enthalpy of mixing in liquid Y-Si solutions at 1780 ^{0}C.
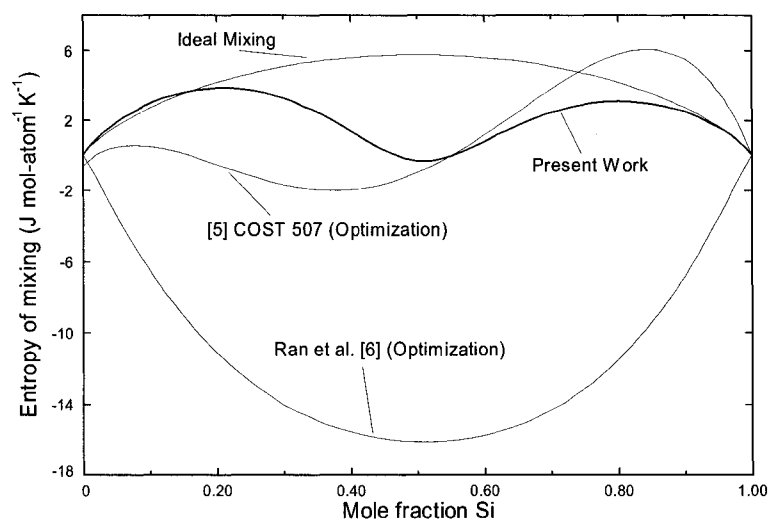
Fig. 4.10. Calculated entropy of mixing in liquid Y-Si solutions at 1600 ^{0}C.
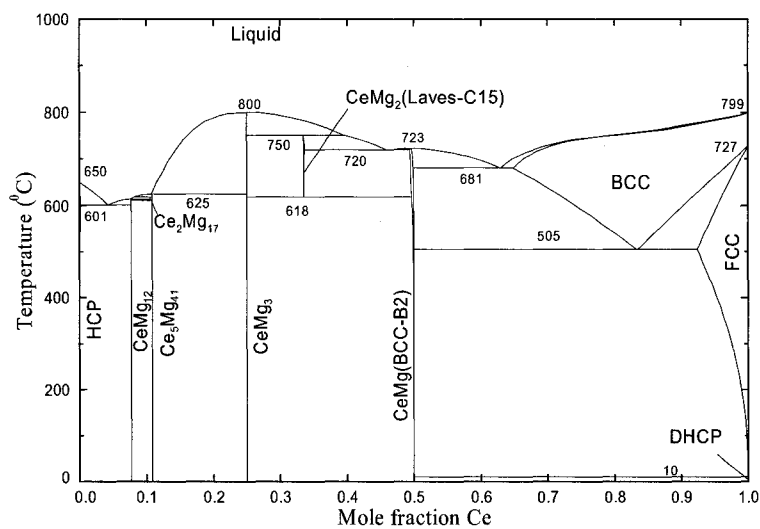
Fig. 4.11. Previously optimized phase diagram of the Mg-Ce system [9].
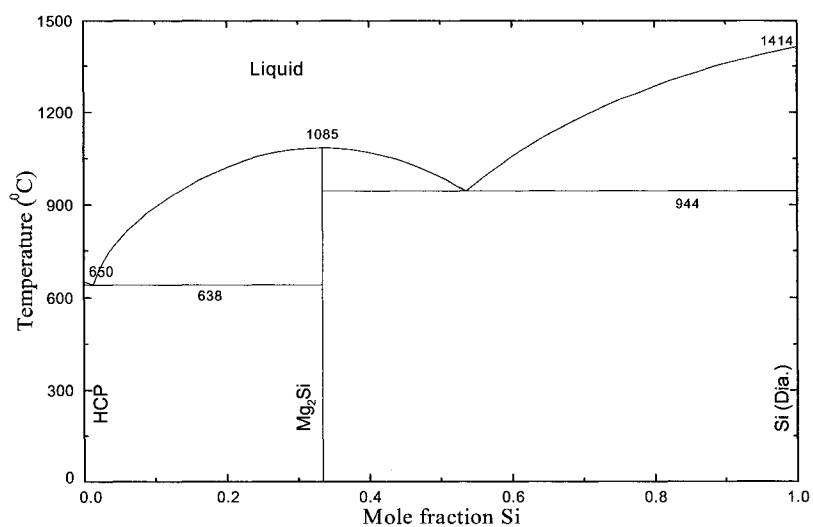
Fig. 4.12. Previously optimized phase diagram of the Mg-Si system [10].
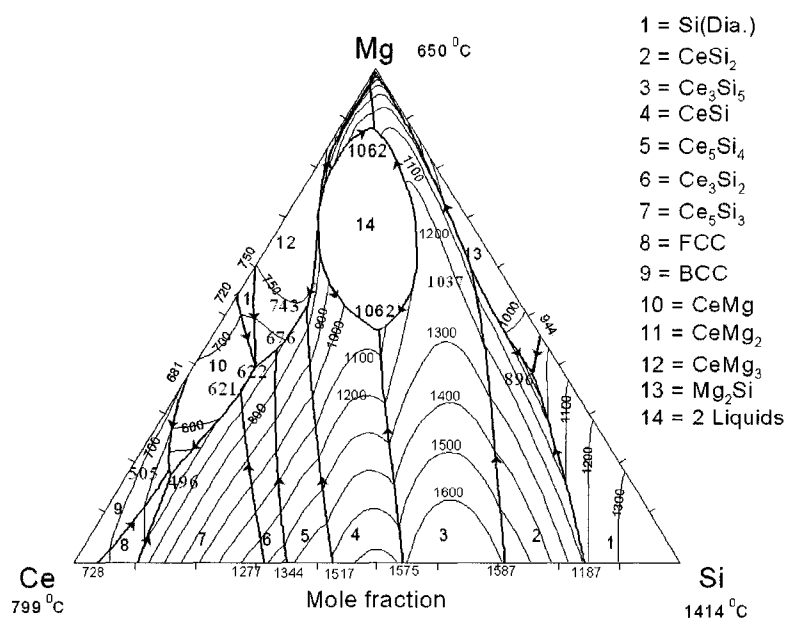
Fig. 4.13. Predicted polythermal projection of the Mg-Ce-Si ternary system. Calculated temperatures of invariants points are shown (^{0}C).
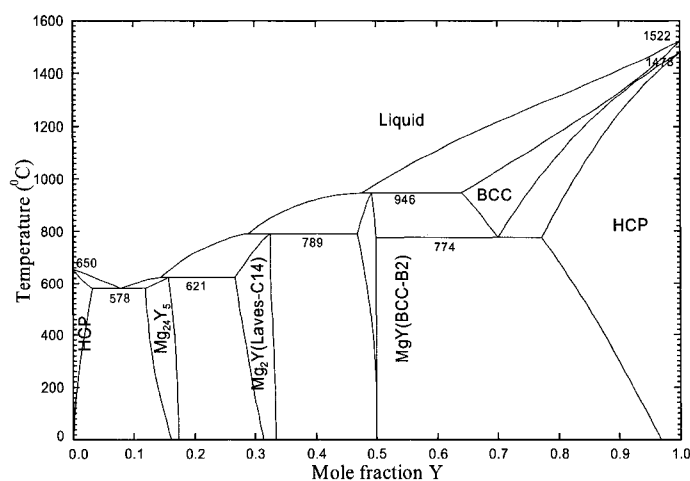
Fig. 4.14. Previously optimized phase diagram of the Mg-Y system [9].
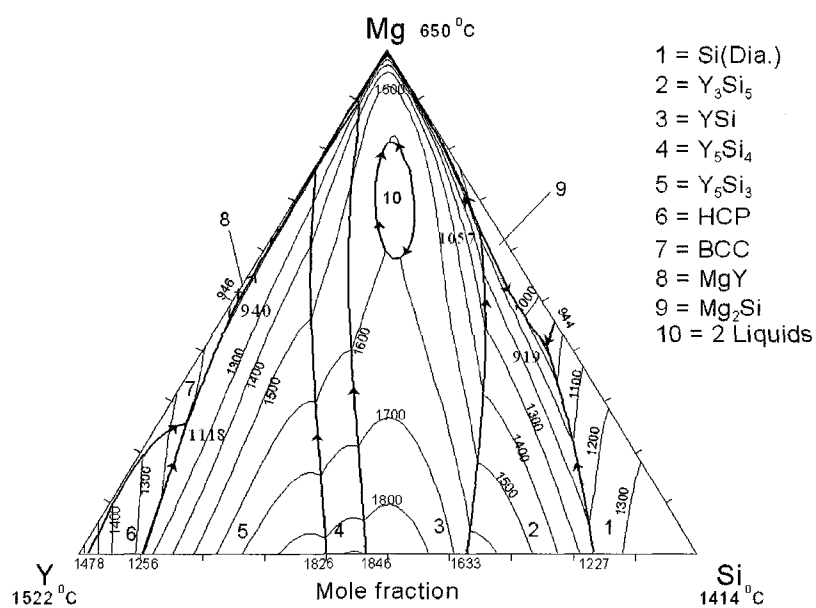
Fig. 4.15. Predicted polythermal projection for the Mg-Y-Si system. Calculated temperatures of invariants points are shown (^{0}C).
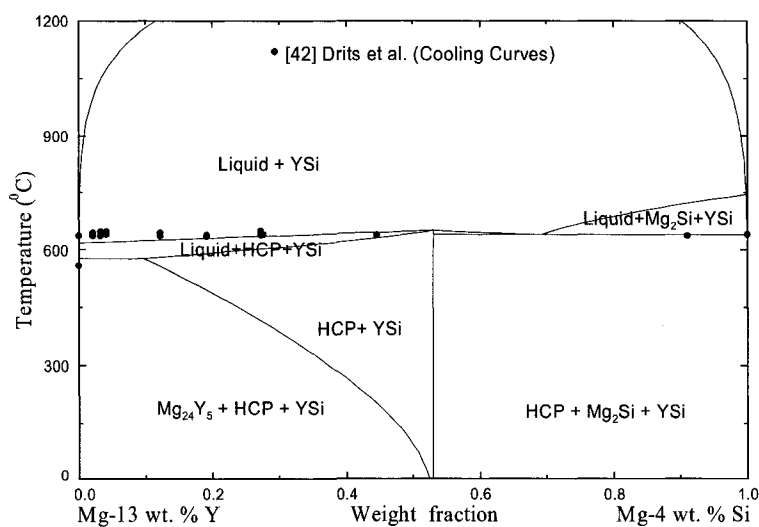
Fig. 4.16. Calculated section of the Mg-Y-Si phase diagram from Mg-13 wt. % Y to Mg-4 wt. % Si.
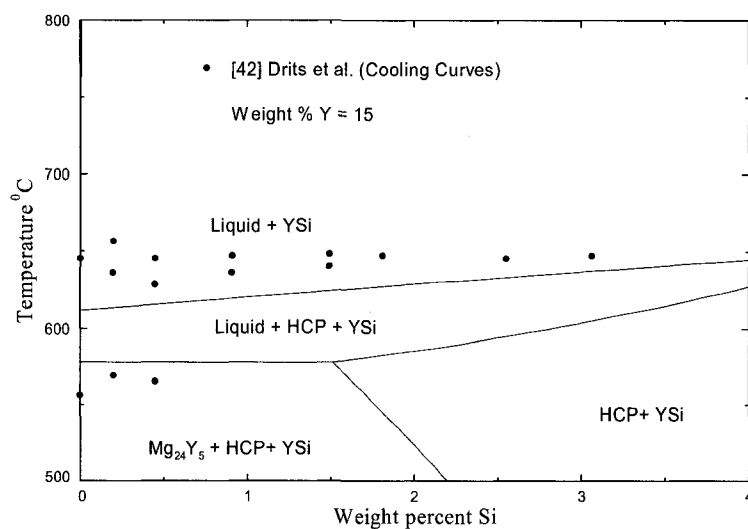
Fig. 4.17. Calculated isoplethal section of the Mg-Y-Si phase diagram at 15 wt. % of Y.
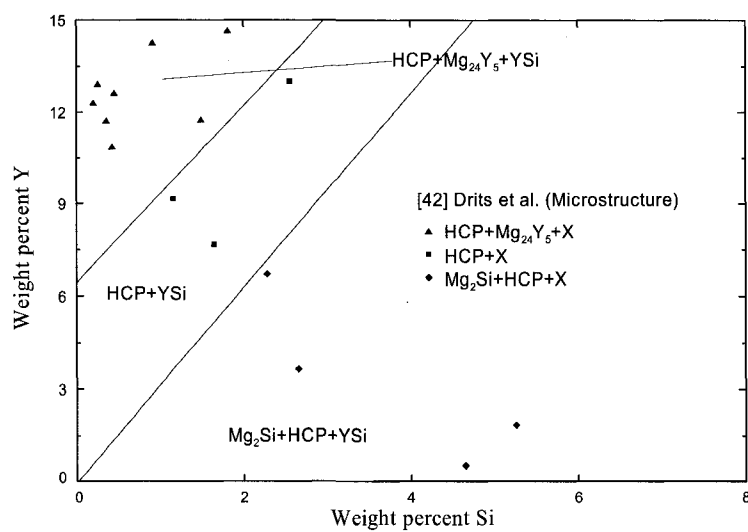
Fig. 4.18. Calculated isothermal section at 400 ^{0}C of the Mg-Y-Si phase diagram.

Chapter 5: Article 2

Adarsh Shukla, Youn-Bae Kang and Arthur D. Pelton

Centre de Recherche en Calcul Thermochimique, Département de Génie Chimique,

Ecole Polytechnique, Montréal, Québec, Canada

Thermodynamic assessment of the Si-Zn, Mn-Si, Mg-Si-Zn and Mg-Mn-Si systems.

The binary Si-Zn and Mn-Si systems have been critically evaluated based upon available phase equilibrium and thermodynamic data, and optimized model parameters have been obtained giving the Gibbs energies of all phases as functions of temperature and composition. The liquid solution has been modeled with the Modified Quasichemical Model (MQM) to account for the short-range-ordering. The results have been combined with those of our previous optimizations of the Mg-Si, Mg-Zn and Mg-Mn systems to predict the phase diagrams of the Mg-Si-Zn and Mg-Mn-Si systems. The predictions have been compared with available data.

5.1 Introduction

Although magnesium-based materials have a long history of important commercial applications, including automotive, there remains much to be learned about the basic properties of the metal and its alloys. With the recent renewed interest in lightweight wrought materials, including both sheet and tube applications, there has been an increased focus on developing a better understanding of novel magnesium alloys, including those that incorporate additions of such elements as Si, Mn and Zn. These alloy systems, along with other potential candidates, are being actively pursued as possible routes to develop magnesium materials with improved ductility, or even practical room temperature formability.

The properties of cast or wrought material depend first and foremost upon the phases and microstructural constituents (eutectics, precipitates, solid solutions, etc.) which are present. In an alloy with several alloying elements, the phase relationships are very complex. In order to effectively investigate and understand these complex phase relationships, it is very useful to develop thermodynamic databases containing model parameters giving the thermodynamic properties of all phases as functions of temperature and composition. Using Gibbs free energy minimization software such as FactSage [1, 2], the automotive and aeronautical industries and their suppliers will be able to access the databases to calculate the amounts and compositions of all phases at equilibrium at any temperature and composition in multicomponent alloys, to follow the course of equilibrium or non-equilibrium cooling, to calculate corresponding heat effects, *etc.*

As part of a broader research project to develop a thermodynamic database for Mg alloys with 25 potential alloying metals, the present study reports on the evaluation and optimization of the Si-Zn, Mn-Si, Mg-Si-Zn and Mg-Mn-Si systems.

Previous optimizations of the Mn-Si system in the framework of COST 507 [3] and by Chevalier *et al.* [4] were based upon a Bragg-Williams (BW) random-mixing model for the liquid phase. The liquid in this binary system is expected to exhibit considerable short-range-ordering (SRO) as evidenced by the very negative enthalpy of mixing curve. As has been shown by the present authors [5], the use of a BW model in liquids with a high degree of SRO generally results in unstatisfactory results and in poor predictions of ternary properties from binary model parameters. In the present work, the Modified Quasichemcial Model (MQM) has been used to account for the SRO in the liquids. As well, there are vapor pressure measurements [6, 7] of Mn-Si alloys and measurement of the enthalpy of formation [8] of compounds which were not taken into account in previous optimizations. Hence the Si-Zn and Mn-Si systems have been re-optimized in the present study.

The binary model parameters have then been combined with those from our previous optimizations of the Mg-Zn [9], Mg-Mn [10] and Mg-Si [11] systems in order to predict thermodynamic properties and phase equilibria in the Mg-Si-Zn and Mg-Y-Si ternary systems.

5.2 Modified Quasichemical Model (MQM)

The Modified Quasichemical Model (MQM) in the pair approximation [12] was used to model the liquid alloys. A description of the MQM and its associated notation is given by Pelton *et al.* [12]. The same notation is used in the present paper. The composition of maximum SRO is determined by the ratio of the coordination numbers Z_{ij}^i / Z_{ij}^j. The values of the coordination numbers selected in the present study are listed in Table 5.1. All the binary subsystems of the Mg-Si-Zn and Mg-Mn-Si systems exhibit SRO near the equimolar composition; hence $Z_{ij}^i = Z_{ij}^j$ in all cases.

From the MQM model parameters of the binary liquid phases, the thermodynamic properties of a ternary liquid phase may be estimated as discussed previously [13]. If ternary experimental data are available, additional ternary model parameters may be added.

5.3 Binary Systems

All calculations and optimizations in the present study were performed with the FactSage thermochemical software [1, 2].

The optimized model parameters of all phases obtained in the present study are listed in Table 5.1. The crystallographic data [14] of all phases in the Si-Zn and Mn-Si systems are listed in Table 5.2. The Gibbs energies of all stable and metastable condensed phases

of the elements were taken from Dinsdale [15], while the Gibbs energies of the gaseous elements were taken from the JANAF Tables [16].

5.3.1 The Si-Zn System

The optimized phase diagram of the system is shown in Fig. 5.1. It may be noted that no temperature dependent terms were required in the optimized parameters (Table 5.1) of the liquid Si-Zn solution. This system was optimized by Jacobs and Spencer [17] who used a BW random-mixing model for the liquid phase. The present calculated eutectic temperature and composition are 419.2 ^{0}C and $X_{Zn} = 0.999$.

The only data available are the coordinates of the liquidus. No thermodynamic property data were found. Girault [18], Thurmond and Kowalchik [19] and Moissan and Siemens [20] determined the liquidus in the range 0.85 to 5.3 at. % Zn by a gravimetric method. John *et al.* [21] and Schneider and Krumnacker [22] measured the liquidus by DTA in the range from 1 to 55 at. % Zn. The solid solubility of Zn in Si was determined by diffusion investigations in the temperature ranges from 820 to 1076 ^{0}C [23], 1040 to 1200 ^{0}C [24] and 900 to 1360 ^{0}C [25]. All these investigations reported negligible solubility of Zn in Si. In the absence of data for the solubility of Si in solid Zn, negligible solubility was assumed.

5.3.2   The Mn-Si system

The optimized phase diagram of the Mn-Si system is shown in Fig. 5.2 and is compared with the experimental data in Figs. 5.3 and 5.4. Various calculated thermodynamic properties of the system are compared with experimental data and previous optimizations in Figs. 5.5 to 5.13.

A complete literature review of the Mn-Si system up to 1990 was reported by Gokhale and Abbaschian [26]. COST 507 [3] and Chevalier et al. [4] performed thermodynamic optimizations of the system, using a BW random-mixing model for the liquid phase. Chakraborti and Lukas [27] optimized the phase diagram data without taking account of any thermodynamic data. Kanibolotskii and Lesnyak [28] fitted the thermodynamic properties of the system to polynomial equations, but performed no optimization.

The optimized Mn-rich side of the phase diagram ($X \leq 0.5$) is compared with the experimental data in Fig. 5.3. Gokhale and Abbaschian [26] reported speculative phase boundaries between the FCC, BCC and liquid phases upon which the calculations in Fig. 5.3 were based.

Wieser and Forgeng [29] reported phase equilibria in the region from 2 to 24 at. % Si by metallography and XRD. These authors reported a phase ε with a homogeneity range from 12 to 15 at. % Si and a phase ξ with a homogeneity range from 16 to 18 at. % Si (Mn_6Si and Mn_9Si_2 respectively in Fig. 5.3). Kuz'ma and Gladyshevskii [30] and Gupta

[31] confirmed the existence of the ϵ and ξ phases respectively by XRD. Later, Gokhale and Abbaschian [26] referred to these compounds as **R** and υ and suggested their approximate stoichiometries as Mn_6Si and Mn_9Si_2 respectively.

Boren [32] from XRD, and Vogel and Bedarff [33] from thermal and metallography, reported the existence of Mn_3Si. Later, Letun *et al.* [34] reported an allotropic transformation of this phase at 677 ^0C. The Gibbs energy change of this transformation was assumed to be zero in the present work. The congruently melting compounds Mn_5Si_3 and $MnSi$ were first reported by Doerinckel [35] from thermal and metallographic analysis, and later by Vogel and Bedarff [33] who used the same technique.

The optimized silicon-rich side of the phase diagram is compared with the experimental data in Fig. 5.4. Different authors [32, 36-40] disagree on the exact designation, the width of the single-phase region (0.3 to 0.5 at. % Si), and the structure of the highest silicide, $Mn_{11}Si_{19}$. Gokhale and Abbaschian [26] preferred the designation $MnSi_{1.75-x}$ with a homogeneity width of 0.4 at. % Si. Morkhovets *et al.* [41], from microstructural and thermal analysis, reported this compound as $MnSi_{1.72}$. Following Chakraborti and Lukas [26] and Chevalier *et al.* [4], this phase is modeled in the present study as stoichiometric $Mn_{11}Si_{19}$.

There are no data on the solubility of Mn in solid Si. The slope of the liquidus curve [42] at $X_{Si} = 1.0$ is consistent with the limiting van't Hoff equation when the solid solubility is

negligible. Hence, negligible solubility was assumed. All intermediate compounds have been modeled as stoichiometric, there being no data to the contrary except for Mn_6Si and Mn_9Si_2. For these compounds, it proved impossible to reproduce simultaneously all the data points of Wieser and Forgeng [29] for the boundaries of the single-phase regions of these phases and of the CUB phase with reasonable thermodynamic parameters. Since there are no corroborating data from other authors in this region of the phase diagram, it was decided to treat these phases as stoichiometric.

Zaitsev *et al.* [6, 43] reported vapor pressure measurements in two-phase regions using high-temperature mass spectrometry. The data from their first paper [6] are in good agreement with the present calculations as can be seen in Fig. 5.5. The data from their second paper [43] were presented only in the form of a small ambiguous figure.

In a different work, Zaitsev *et al.* [7] reported vapor pressure measurements of monatomic Si and Mn over liquid alloys by Knudsen effusion/mass spectrometry. The data for Mn vapor pressures are well reproduced as seen in Fig. 5.5a. The calculated vapor pressure of monatomic Si is shown in Fig. 5.6. The composition dependence of the data in Fig. 5.6 is well reproduced by the model, while the calculated curves and measured points differ by a nearly constant value. In view of the expanded vertical scale of Fig. 5.6, and the very low vapor pressure of Si, this difference is within the experimental error limits. Since the authors [7] did not report measurements of the vapor

pressure of pure liquid Si, one cannot check for consistency with the data for the vapor

pressure of pure Si [16] used in the present calculations.

Tanaka [44] by a transportation method at 1400 ^{0}C, and Ahmad and Pratt [45] by a

torsion-effusion technique, measured Mn partial pressures over liquid alloys. The present

calculations are compared with these vapor pressure data in Fig. 5.5. At high Si contents,

these data are inconsistent with the vapor pressure data of Zaitsev *et al.* [7] in Fig. 5.5a.

The data of Tanaka [44] in Fig. 5.5c are inconsistent with the vapor pressure data of

Zaitsev *et al.* [6, 7] in Fig. 5.5a and with the vapor pressure of pure liquid Mn given by

JANAF [16].

Batalin and Sudavtsova [46] performed EMF measurements in the range 1247-1427 ^{0}C to

report the partial excess Gibbs energy of Mn in the liquid phase at 1400 ^{0}C. These Gibbs

energies are compared with the present calculations in Fig. 5.7. These data are

inconsistent with the Mn vapor pressure data [6, 7] in Fig. 5.5. Previous optimizations [3,

4] did not take into account the vapor pressure data. In the present work, more weight

was given to the vapor pressure data [6, 7] than to the EMF measurements.

Zaitsev *et al.* [47] derived standard enthalpies of formation of intermediate compounds

from vapor pressure measurements using high-temperature mass spectroscopy. Their

vapor pressure data points were presented only in the form an ambiguous figure. Meschel

and Kleppa [8] measured the standard enthalpies of formation of Mn_5Si_3 and $MnSi$ by

direct synthesis calorimetery. Zaitsev *et al.* [47] also cite data from other sources [48-52]. All these data are shown on Fig. 5.8. In the present work, the greatest weight was given to the results of Meschel and Kleppa [8].

It should be noted that the optimized entropies of formation of the intermetallic compounds from the elements at 25 ^{0}C (Table 5.1) are all very small as is generally expected for such compounds. That is, the optimized entropies are physically reasonable.

Gel'd *et al.* [53] and Esin *et al.* [54] measured partial enthalpies of mixing in Mn-Si melts at 1500 ^{0}C by high-temperature isothermal calorimetry. It is unclear in the article of Esin *et al.* [54] whether all their data points are experimental or if some points were obtained by integration of the Gibbs-Duhem equation. These data are compared with the present and previous optimizations in Fig. 5.9. Batalin *et al.* [55] at 1450 ^{0}C, and Gorbunov *et al.* [56] at 1500 ^{0}C, measured the integral enthalpy of mixing in liquid solutions by high-temperature isothermal calorimetry. These data are well reproduced by the present optimization as seen in Fig. 5.10.

The shape of the partial enthalpy curves in Fig. 5.9, which are very negative with points of inflection and a point of intersection near the equimolar composition, are strongly indicative of a high degree of SRO about this composition. An entropy of mixing with a strong minimum near the equimolar composition as in Fig. 5.11 is thus expected. These shapes of the enthalpy and entropy of mixing curves are well reproduced by the MQM.

5.4 Ternary Systems

5.4.1 The Mg-Si-Zn system

The phase diagrams of the Mg-Zn and Mg-Si systems from previous optimizations [9, 11] are shown in Figs. 5.12 and 5.13 respectively. Spencer [9] obtained the optimized phase diagram in Fig. 5.12 using the MQM for the liquid solution, and taking model parameters for the solid phases from the optimization of Liang *et al.* [57]. His optimized model parameters for the liquid phase are reported in Table 5.1. These previous optimizations were combined with the present optimization of the Si-Zn system in order to predict the thermodynamic properties and phase diagram of the Mg-Si-Zn system.

Mutual solubilites between binary compounds were assumed to be negligible, there being no experimental data available. All the intermetallic compounds have different crystal structures (Table 5.2) and different stoichiometries. These factors mitigate against there being appreciable mutual solubility of the compounds. In the absence of any evidence for ternary compounds, none were assumed.

The thermodynamic properties of the ternary liquid phase were calculated by the MQM from the binary model parameters. The "symmetric approximation" [13, 58] was used. No additional ternary parameters were included. The resultant calculated polythermal projection of the liquidus surface is shown in Fig. 5.14.

Bollenrath [59], using cooling curves, reported a partial section along the Mg_2Si-$MgZn_2$

join. These data are compared with the calculated section in Fig. 5.15. When the

"asymmetric approximation" [13, 58] was used with Si and Mg as "asymmetric

component", the calculated liquidus deviated by over 50^0 from the measurements [59].

Hence the "symmetric approximation" was preferred.

5.4.2 The Mg-Mn-Si system

The phase diagrams of the Mg-Mn and Mg-Si systems from previous optimizations [11,

13] are shown in Figs. 5.16 and 5.13 respectively. These optimizations were combined

with the present optimization of the Mn-Si system in order to predict the thermodynamic

properties and phase diagram of the Mg-Mn-Si system. The resultant calculated

polythermal projection of the liquidus surface is shown in Fig. 5.17. No measurements of

the liquidus have been reported.

As in the Mg-Si-Zn system, and for the same reasons, no mutual solubilities between

binary compounds were assumed. In the absence of any evidence for ternary compounds,

none were assumed.

The thermodynamic properties of the ternary liquid phase were calculated by the MQM

from the binary model parameters. No additional ternary parameters were included. The

"asymmetric approximation" [13, 58] with Si as "asymmetric component" was used since

the Mg-Mn liquid phase exhibit positive deviations from ideal solution behavior whereas the Mg-Si and Mn-Si liquid phases exhibit considerable negative deviations.

The Mg-Mn binary system exhibits a large liquid miscibility gap (Fig. 5.16). With the addition of Si, this miscibility gap extends into the ternary system. As shown by the present authors [5], the use of the MQM generally results in better predictions of ternary miscibility gaps then when a BW random-mixing model is used. It should be noted that the consolute temperature of the binary miscibility gap calculated in our previous optimization of the Mg-Mn system [10], in which the liquid phase was modeled by the MQM, is approximately 2000^0 lower than the calculated consulate temperatures in earlier optimizations [60, 61] in which the BW random-mixing model was used. This results in a much smaller extension of the calculated miscibility gap into the ternary system in the present optimization.

In Fig. 5.17 the liquidus surface approximately along the Mg-MnSi join is very flat. This is a result of the high degree of SRO in the Mn-Si binary liquid phase which results in a tendency for Mn and Si atoms to cluster and exclude Mg. As shown by the present authors [5] such liquidus surfaces are generally predicted better by the MQM than by BW or "associate" models.

5.5 Conclusions

Gibbs energy functions for all the phases in the binary Si-Zn and Mn-Si systems have been obtained. All available thermodynamic and phase equilibrium data have been critically evaluated in order to obtain one set of optimized model parameters of the Gibbs energies of all phases which can reproduce the experimental data within experimental error limits. Evaluations and tentative phase diagrams for the ternary systems Mg-Si-Zn and Mg-Mn-Si have been given.

The use of the Modified Quasichemical Model for the liquid phase has permitted short-range ordering to be taken into account. Use of this model results in a better fitting of the data for the liquid phase than is the case when a Bragg-Williams random-mixing model is used. This results in a better representation of the partial properties of the solutes in dilute solution in magnesium, the activities of solutes in dilute solution being of much practical importance. As shown by the present authors [5], the use of the MQM generally also results in better estimations of the properties of ternary and higher-order liquid alloys from binary model parameters. These estimations of phase equilibria will aid in the design of novel magnesium alloys.

5.6 Acknowledgements

5.7 References

[1] C. W. Bale, P. Chartrand, S.A. Degterov, G. Eriksson, K. Hack, R. Ben Mahfoud, J. Melançon, A.D. Pelton, S. Petersen: Calphad 26 (2002) 189.

[2] C.W.Bale, A.D. Pelton, W. Thompson, Factsage thermochemical software and databases, http:// www.crct.polymtl.ca (2008).

[3] J. Tibbals, COST 507 – Thermochemical Databases for Light Metal Alloys, I. Ansara, A.T. Dinsdale, M.H. Rand (eds.), 2 (1998) 236.

[4] P. -Y. Chevalier, E. Fischer, A. Rivet, Calphad 19 (1995) 57.

[5] A. D. Pelton, Y.-B. Kang, Int. J. Mat. Res. 10 (2007) 905.

[6] A. I. Zaitsev, M. A. Zemchenko, B. M. Mogutnov, Russ. Metall. 1 (1990) 208.

[7] A. I. Zaitsev, M. A. Zemchenko, B. M. Mogutnov, Rasplavy 3 (1989) 86.

[8] S. V. Meschel, O. J. Kleppa, J. Alloys Compd. 267 (1998) 128.

[9] P. Spencer, in "Database and Software for Mg Alloy Design" (report to GM Canada by A. D. Pelton, P. Spencer, P. Chartrand, C. Bale, G. Eriksson, C. Aliravci, A. Shukla), Ecole Polytechnique, Montreal, June 2007.

[10] Y.-B. Kang, A. D.Pelton, P. Chartrand, P. Spencer, C. D. Fuerst, J. Phase Equilib. Diffus. 28 (2007) 342.

[11] J. P. Harvey, Masters Thesis, Ecole Polytechnique, Montreal (2006).

[12] A. D. Pelton, S.A. Degterov, G. Eriksson, C. Robelin and Y. Dessureault, Metall. Mater. Trans. B. 31 (2000) 651.

[13] A. D. Pelton, P. Chartrand: Metall. Mater. Trans. A. 32 (2001) 1355.

[14] T. B. Massalski, P.R. Subramanian, H. Okamoto, L. Kacprazak (Eds.), Binary Alloy Phase Diagram, 2nd edition, ASM International, Materials Park, Ohio, 1990.

[15] A. T. Dinsdale, Calphad, 15 (1991) 317 plus updates (private communication), http:// www.sgte.org (2000).

[16] D. R. Stull, H. Prophet, JANAF Thermochemical Tables, U.S. Department of Commerce, Washington (1985).

[17] M. H. G. Jacobs, P. J. Spencer, Calphad 20 (1996) 307.

[18] B. Girault, C. R. Acad. Sci. Paris B 284 (1977) 1.

[19] C.D. Thurmond , M. Kowalchik, Bell Syst. Tech. J. 39 (1960) 39.

[20] H. Moissan, F. Siemens, C. R. Acad. Sci. Paris 138 (1904) 657.

[21] M. John, K. Hein, Cryst. Res. Technol. 14 (1979) 841.

[22] M. Schneidner, M. Krumnacker, Neue Hutte 17 (1972) 519.

[23] M. M. Blouke, N. Holonyak, B. G. Streetman, J. Phys. Chem. Solids 31 (1970) 173.

[24] R. O. Carlson, Phys. Rev. 108 (1957) 1390.

[25] C. S. Fuller, F. J. Morin, Phys. Rev. 105 (1957) 379.

[26] A. B. Gokhale, R. Abbaschian, Bull. Alloy Phase Diagrams 11 (1990) 468.

[27] N. Chakraborti, H.L. Lukas, Calphad 13 (1989) 293.

[28] D. S. Kanibolotskii, V.V. Lesnyak, Russ. Metall. 3 (2006) 199.

[29] P. F. Wieser, W. D. Forgeng, Trans. Metall. Soc. AIME 230 (1964) 1675.

[30] Yu. B. Kuz'ma, E.I. Gladyshveskii, Russ. J. Inorg. Chem. 9 (1964) 373.

[31] K. P. Gupta, Trans. Metall. Soc. AIME 230 (1964) 253.

[32] B. Boren, Ark. Kem., Miner.Geol. 11 (1933) 1.

[33] R. Vogel, H. Bedarff, Arch. Eisenhuttenwes 7 (1933) 423.

[34] S. M. Letun, P.V. Geld, N. N. Serebrennikov, Russ. Metall. 6 (1965) 97.

[35] F. Doerinckel, Z. Anorg. Chem. 50 (1906) 117.

[36] V. A. Korshunov, F. A. Sidorenko, P. V. Geld, K. N. Davydov, Fiz. Met. Metalloved. 12 (1961) 277.

[37] Y. Fujino, D. Shinoda, S. Asanabe, Y. Sasaki, Jpn. J. Appl. Phys. 3 (1961) 431.

[38] L. D. Dudkin, E. A. Kuznetsova, Dokl. Akad. Nauk SSSR, 141 (1961)94.

[39] L. D. Dudkin, E. S. Kuznetsova, Poroshk. Metall. 12 (1962) 20.

[40] N. Kh. Abrikosov, L. D. Ivanova, V. G. Muravev, Neorg. Mater. 8 (1972) 1194.

[41] M. A. Morkhovets, E. I. Elagina, N. Kh. Abrikosov, Inorg. Mater. 2 (1966) 561.

[42] T. Mager , E.Wachtel, Z. Metallkd. 61 (1970) 853.

[43] A. I. Zaitsev, M.A.Zemchenko, B.M. Mogutnov, Russ. Metall. 2 (1990) 188.

[44] A. Tanaka, J. Jpn. Inst. Met. 41 (1977) 601.

[45] N. Ahmad, J. N. Pratt, Met. Trans. A 9 (1978) 1857.

[46] G. I. Batalin, V. S. Sudavtsova, Sov. Prog. Chem. 40 (1974) 88.

[47] A. I. Zaitsev, M. A. Zemchenko, B. M. Mogutnov, Russ. J. Phys. Chem. 63 (1989) 806.

[48] H. Nowotny, J Tomiska, L Erdelyi, A Neckel, Monatsh. Chem., 108 (1977) 7.

[49] V.N. Eremenko, G.M. Lukashenko and V.R. Sidorko, Poroshkovaya Metallurgiya, 74 (1969) 2.

[50] P. V. Gel'd, F. A. Sidorenko, Izd. Metallurgiya, Moscow (1972) 582.

[51] V. G. Muradov, Russ. J. Phys. Chem. 48 (1974) 1274.

[52] Yu. Gertman and P.V. Gel'd, Izd. Akad. Nauk SSSR, Moscow (1961).

[53] P. V. Gel'd, M.S.Petrushevskii, Yu. O. Esin, Yu. V. Gorbunov, Doklady Akademii Nauk SSSR 217 (1974) 1114.

[54] Yu. O. Esin, Yu.Gorbunov, M. S. Petrushevskii, P. V. Gel'd, Chernaya Metallurgiya 2 (1975) 8.

[55] G. I. Batalin, T. P. Bondarenko, V. S. Sudavtsova, Sov Prog. Chem. 50 (1984) 69.

[56] Yu. V. Gorbunov, Yu. O. Esin, Russ. J. Phys. Chem. 48 (1974) 1244.

[57] P. Liang, T. Tarfa, J. A. Robinson, S. Wagner, P. Ochin, M. G. Harmelin, H. J. Seifert, H. L. Lukas, F. Aldinger, Thermochim. Acta. 314 (1998) 87.

[58] A. D. Pelton, Calphad, 25 (2001) 319.

[59] F. Bollenrath, H. Grober, Metallfroschung 1 (1946) 116.

[60] J. Tibbals, COST 507 – Thermochemical Databases for Light Metal Alloys, I. Ansara, A.T. Dinsdale, M.H. Rand (eds.), EUR 18499, 2 (1998) 215.

[61] J. Gröbner, D. Mirkovic, M. Ohno and R. Schmid-Fetzer, J. Phase Equilib. 26 (2005) 234.

Table 5.1. Optimized parameters of the Si-Zn and Mn-Si systems from the present work, and of the liquid phase in the Mg-Zn system from Spencer [9].

Liquid:

Co-ordination numbers:

Si-Zn: $Z^{Si}_{SiSi} = Z^{Zn}_{ZnZn} = Z^{Si}_{SiZn} = Z^{Zn}_{ZnSi} = 6$

Mn-Si : $Z^{Si}_{SiSi} = Z^{Mn}_{MnMn} = Z^{Si}_{SiMn} = Z^{Mn}_{MnSi} = 6$

Mg-Zn : $Z^{Mg}_{MgMg} = Z^{Zn}_{ZnZn} = Z^{Mg}_{MgZn} = Z^{Zn}_{ZnMg} = 6$

Optimized values for Δg_{AB} (Eq 1), in Joules:

Δg_{Si-Zn} : $2299 + 1946\ X_{ZnZn}$

Δg_{Mn-Si} : $(-33054 + 6.694\ T) + (-20920)\ X_{MnMn} + (1.674\ T)\ X_{SiSi} +$
$(11715 - 4.184\ T)\ X_{MnMn}^{2}$

Δg_{Mg-Zn} : $(-6778 + 3.128\ T) + (-1996 + 2.008\ T)\ X_{MgMg} + (-2975 + 1.674)$
X_{ZnZn}

Solid solutions :

Excess Gibbs energy (Joules/mol of atoms):

CUB: $X_{Si}X_{Mn}\ [(-157737 + 26.778\ T) + (-41003 + 21.338\ T)\ (X_{Si} - X_{Mn})] +$
$X_{Si}\ (5.021T)$

CBCC: $X_{Si}X_{Mn}\ [(-151042 + 26.778\ T) + (-32217 - 8.368\ T)\ (X_{Si} - X_{Mn})]$

BCC: $X_{Si}X_{Mn}\ [-83680 + 26778\ (X_{Si} - X_{Mn})]$

FCC: $X_{Si}X_{Mn}\ [-101253 + 17991\ (X_{Si} - X_{Mn})]$

Stoichiometric compounds :

Compounds	ΔH^{0}_{298} [*] J /(mol of atoms)	S^{0}_{298} [**] J/[(mol of atoms)·K]	ΔS^{0}_{298} [*] J/[(mol of atoms)·K]	Cp J/[(mol of atoms)·K]
Mn_6Si	-18094	29.471	-0.834	0.857 C_p (Mn, CBCC) + 0.143 C_p (Si, Dia.)
Mn_9Si_2	-23091	27.745	-2.038	0.818 C_p (Mn, CBCC) + 0.181 C_p (Si, Dia.)
Mn_3Si	-27900	27.000	-1.868	0.375 C_p (Mn, CBCC) + 0.125 C_p (Si, Dia)
Mn_5Si_3	-35250	25.562	-1.630	0.625 C_p (Mn, CBCC) + 0.375 C_p (Si, Dia.)
MnSi	-38000	20.800	-4.716	0.500 C_p (Mn, CBCC) + 0.500 C_p (Si, Dia.)
$Mn_{11}Si_{19}$	-32333	17.267	-6.460	0.366 C_p (Mn, CBCC) + 0.633 C_p (Si, Dia.)

[*] Enthalpy and entropy of formation from the elements at 298.15 K
[**] Absolute Third-Law entropy at 298.15 K

Table 5.2. Crystallographic data [14] of all phases in the Si-Zn, Mn-Si, Mg-Si-Zn and

Mg-Mn-Si systems considered in the present optimization.

| Phase	Struktur-bericht	Prototype	Pearson symbol	Space group	Comments
Liquid	-	-	-	-	
FCC	$A1$	Cu	$cF4$	$Fm\bar{3}m$	Mn is stable phase
BCC	$A2$	W	$cI2$	$Im\bar{3}m$	Mn is stable phase
CUB	$A13$	Mn	$cP20$	$P4_132$	Mn is stable phase
CBCC	$A12$	Mn	$cI58$	$I\bar{4}3m$	Mn is stable phase
HCP	$A3$	Mg	$hP2$	$P6_3/mmc$	Mg and Zn are stable phases
Si (Dia.)	$A4$	C (Dia.)	$cF8$	$Fd\bar{3}m$	
$Mg_{51}Zn_{20}$	-	$Mg_{51}Zn_{20}$	$oI158$	$Immm$	
$Mg_{12}Zn_{13}$	-	-	-	-	
Mg_2Zn_3	-	-	$mC110$	$B2/m$	
$MgZn_2$	$C14$	$MgZn_2$	$hP12$	$P6_3/mmc$	
Mg_2Zn_{11}	$D8_c$	Mg_2Zn_{11}	$cP39$	$Pm\bar{3}$	
Mg_2Si	$C1$	CaF_2	$cF12$	$Fm\bar{3}m$	
Mn_6Si	-	-	$hR53$	$R\bar{3}$	
Mn_9Si_2	-	Si_2U_3	$tP10$	$P4/mbm$	
Mn_3Si	$D0_3$	BiF_3	$cF16$	$Fm\bar{3}m$	High temperature form
Mn_3Si	-	-	-	-	Low temperature form
Mn_5Si_3	$D8_8$	Mn_5Si_3	$hP16$	$P6_3/mcm$	
$MnSi$	$B20$	$FeSi$	$cP8$	$P2_13$	
$Mn_{11}Si_{19}$	-	-	$tP120$	$P\bar{4}n2$	
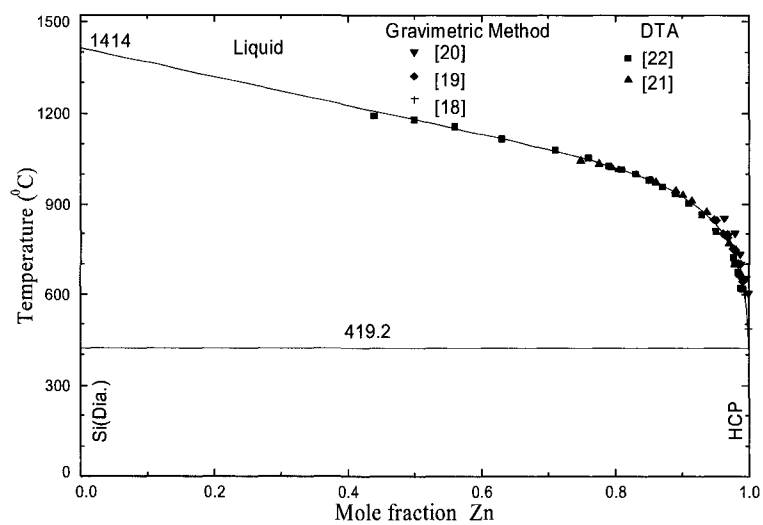
Fig. 5.1.   Optimized phase diagram of the Si-Zn system.
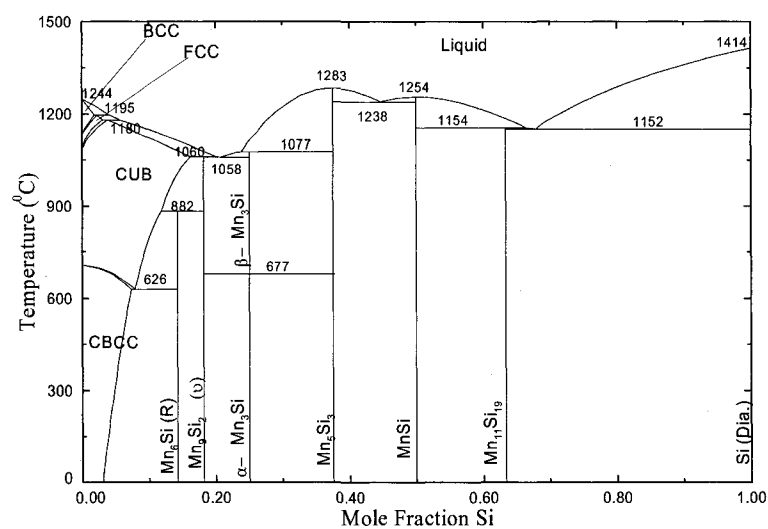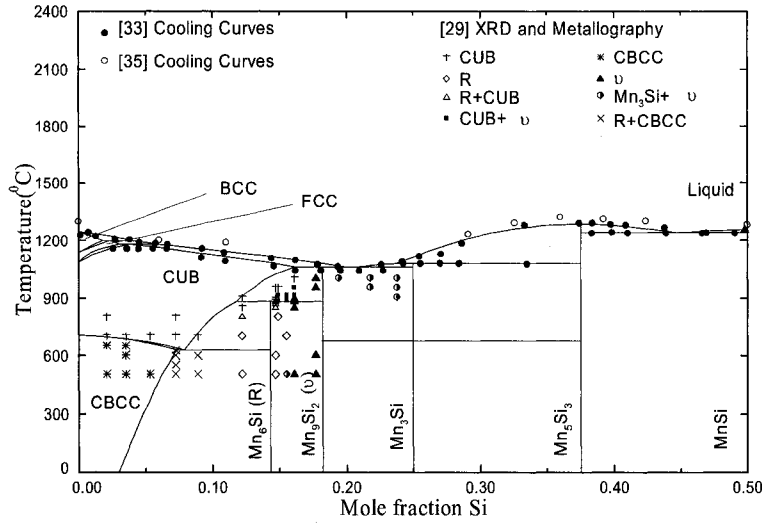

Fig. 5.2.   Optimized phase diagram of the Mn-Si system.

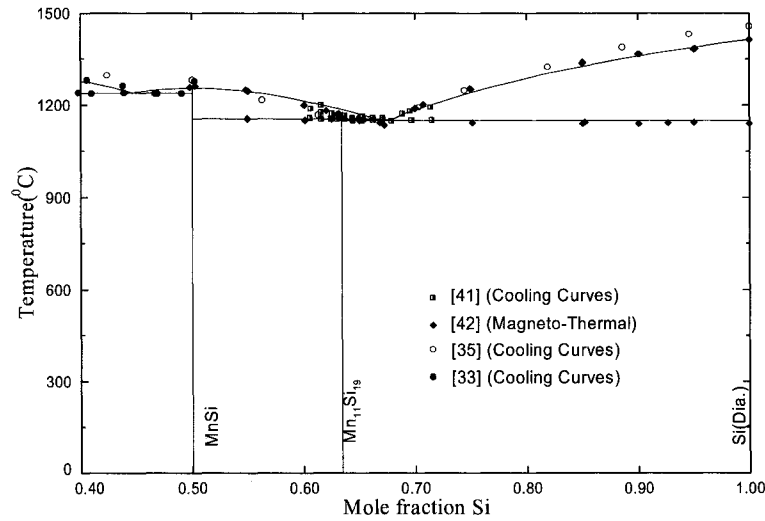Fig. 5.3. Optimized phase diagram of the Mn-Si system for the region X_{Si} = 0.0 to 0.5.

Fig. 5.4. Optimized phase diagram of the Mn-Si system for the region X_{Si} = 0.4 to 1.
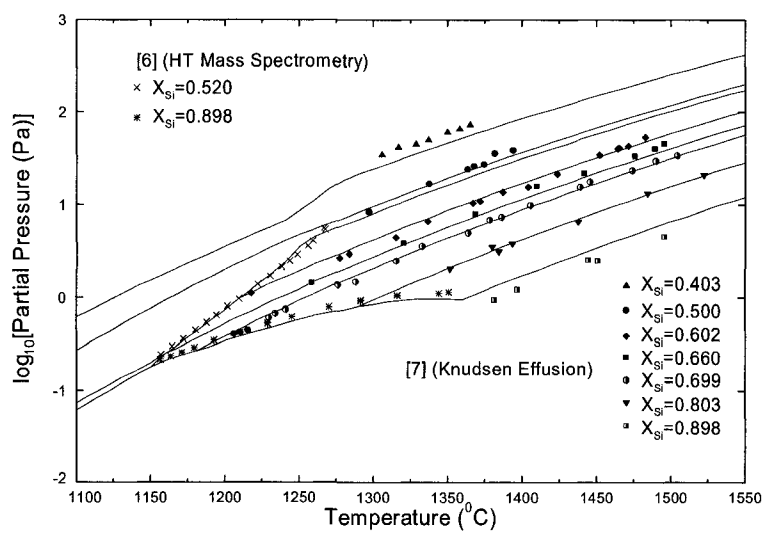
Fig. 5.5a
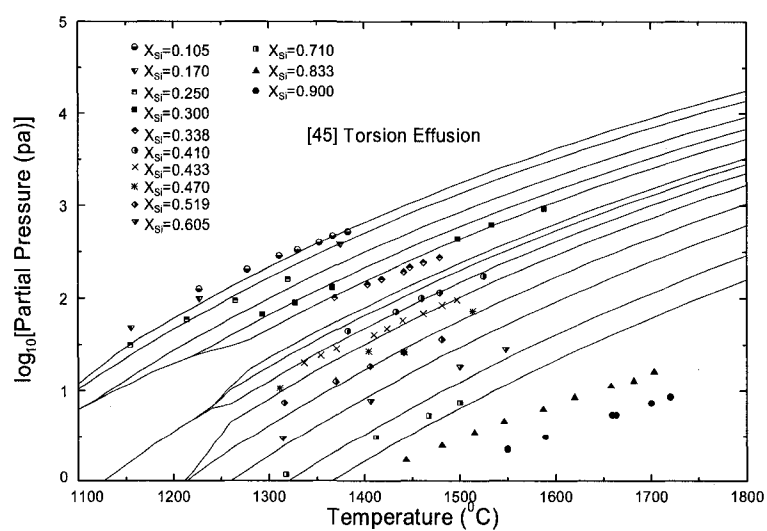
Fig. 5.5b
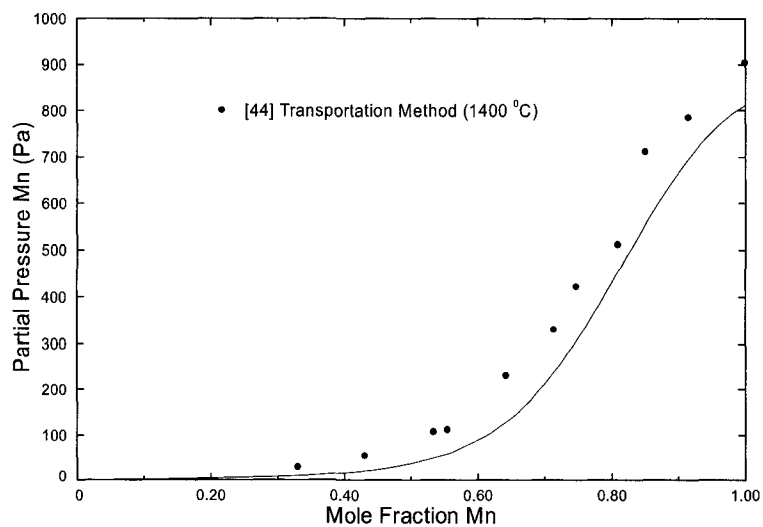
Fig. 5.5c

Fig. 5.5.   Optimized vapor pressure of monatomic Mn over liquid Mn-Si alloys.
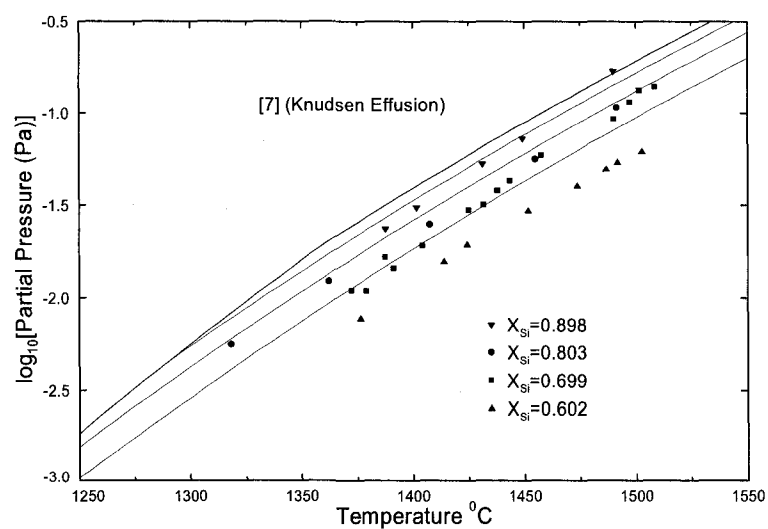
Fig. 5.6.   Optimized vapor pressure of monatomic Si over liquid Mn-Si alloys.
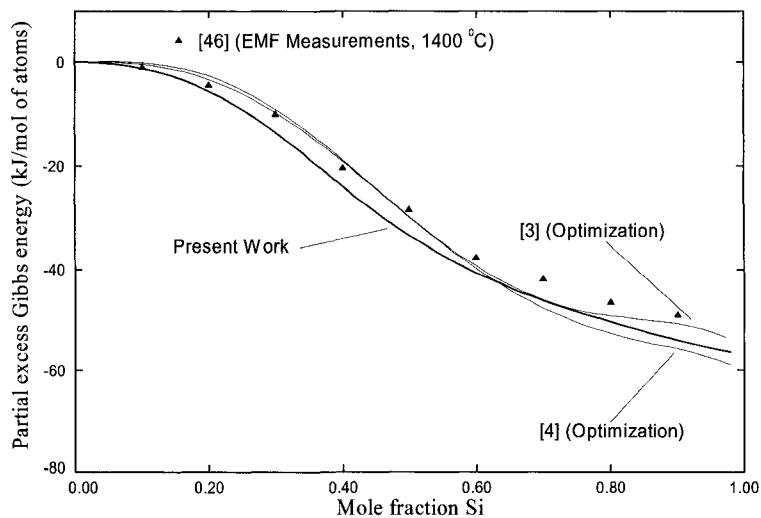
Fig. 5.7. Optimized excess Gibbs energy of Mn in liquid Mn-Si alloys at 1400 ^{0}C.
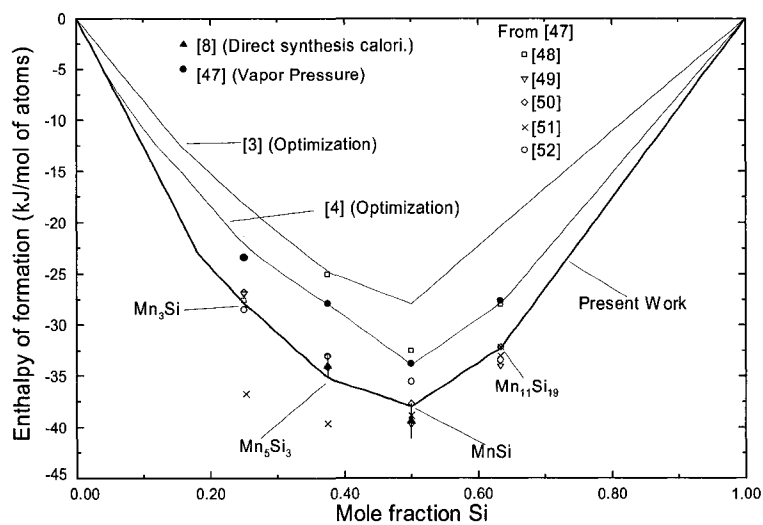
Fig. 5.8. Optimized standard enthalpy of formation of the intermediate compounds in the Mn-Si system.
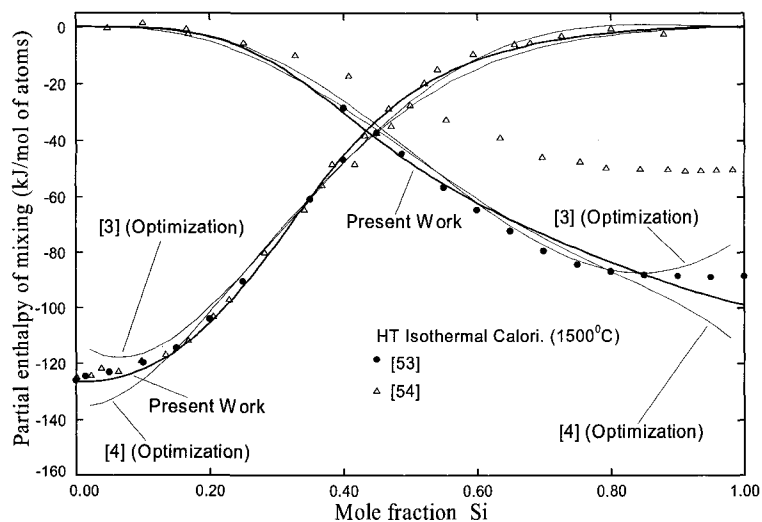
Fig. 5.9. Optimized partial enthalpies of mixing at 1500 ^{0}C in liquid Mn-Si alloys.
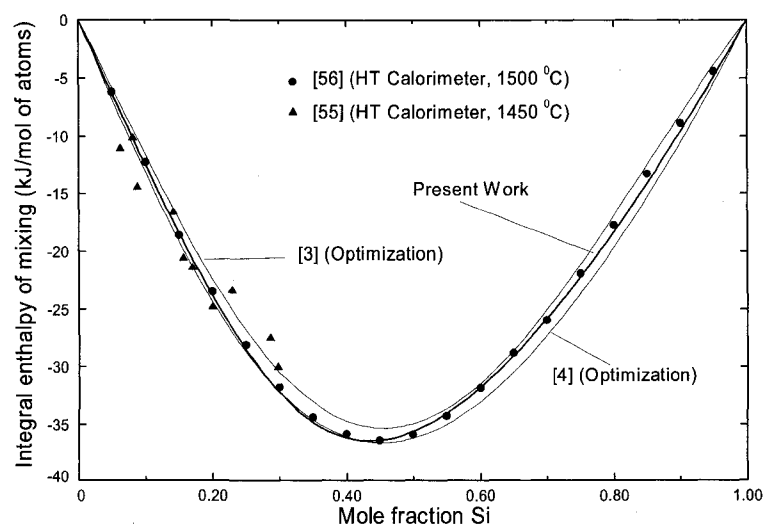
Fig. 5.10. Optimized integral enthalpy of mixing at 1500 ^{0}C in liquid Mn-Si alloys.
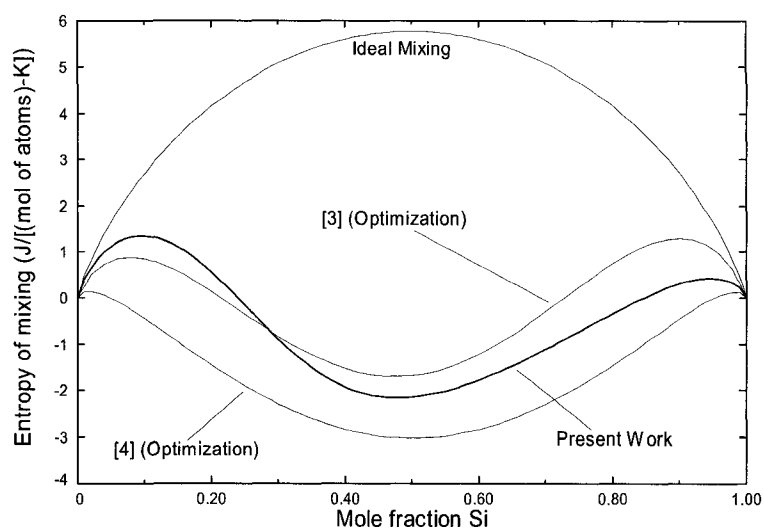
Fig. 5.11. Optimized entropy of mixing at 1500 ^{0}C in liquid Mn-Si alloys.
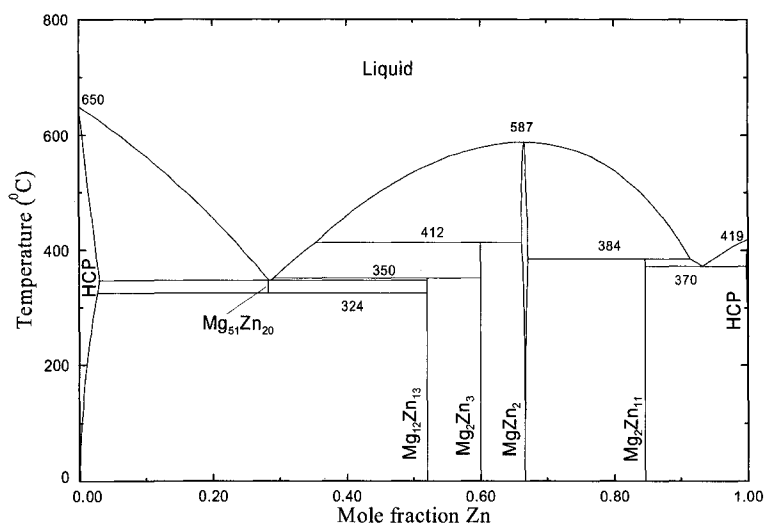
Fig. 5.12. Previously optimized phase diagram of the Mg-Zn system [9].
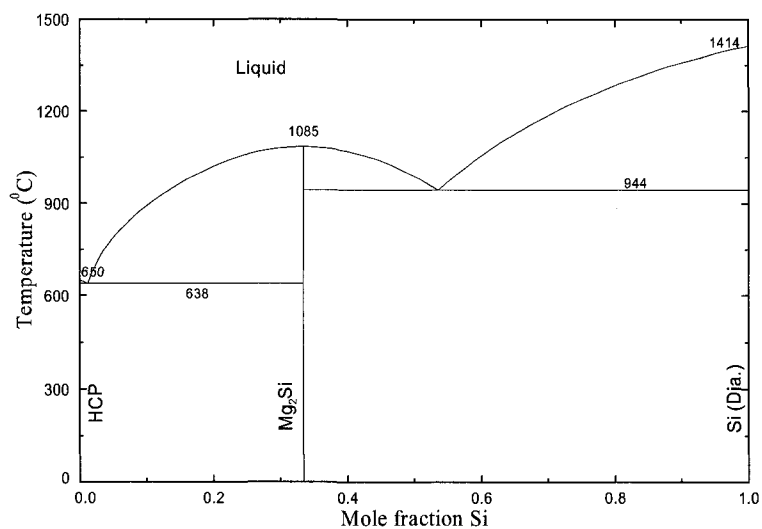
Fig. 5.13. Previously optimized phase diagram of the Mg-Si system [11].
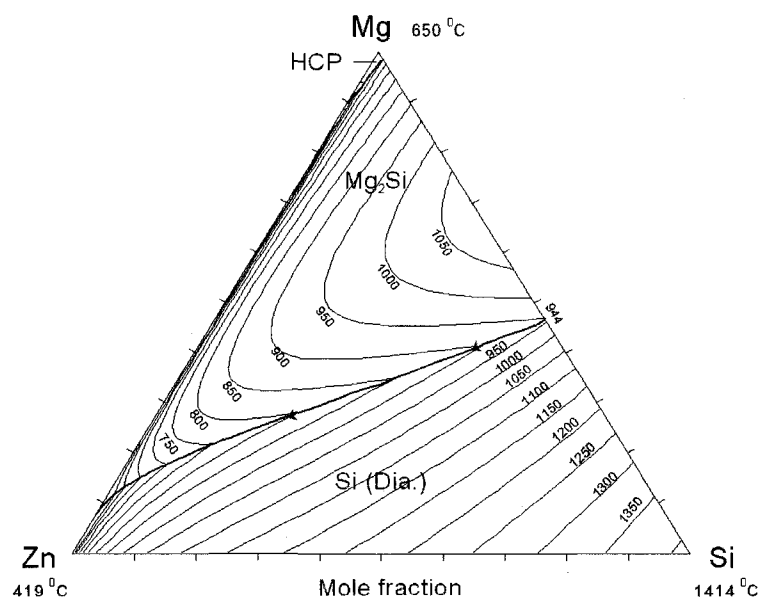
Fig. 5.14. Predicted liquidus projection of the Mg-Si-Zn system.
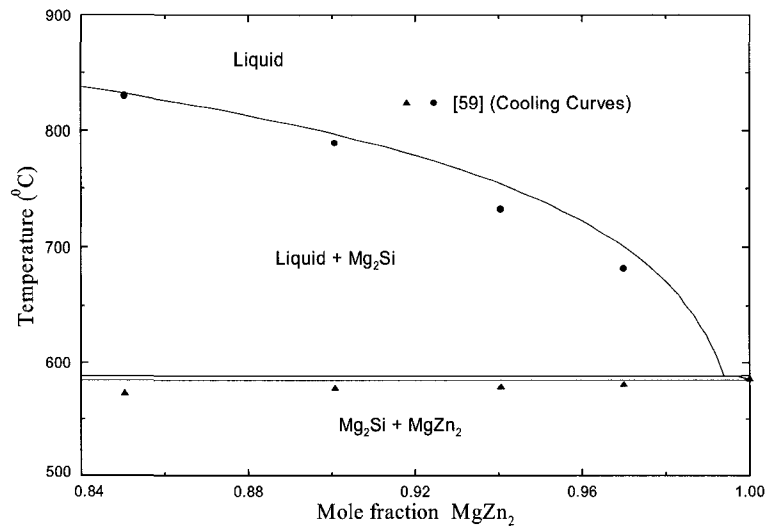
Fig. 5.15. Optimized section of the Mg-Si-Zn phase diagram along the Mg₂Si-MgZn₂ join.
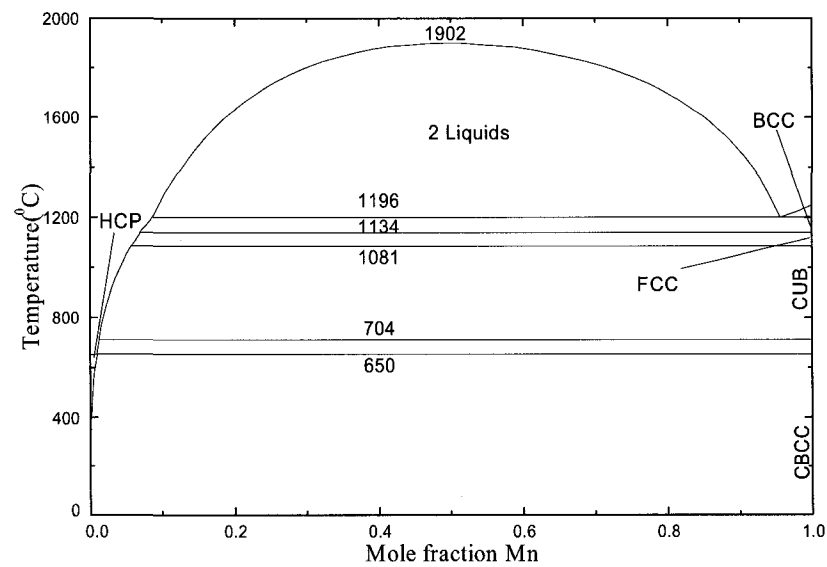
Fig. 5.16. Previously optimized phase diagram of the Mg-Mn system [10].
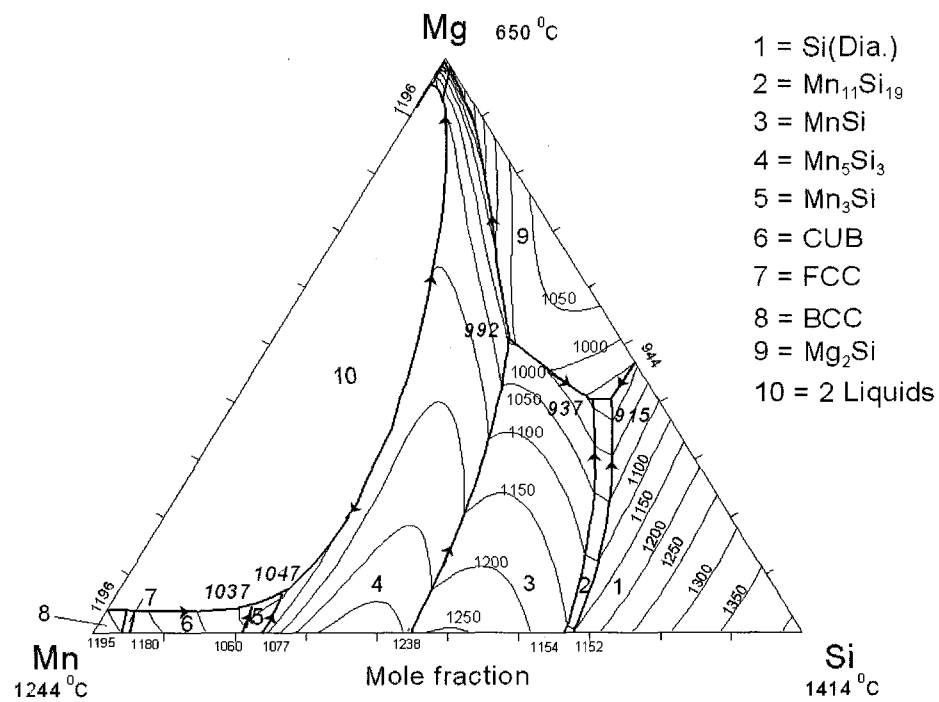
Fig. 5.17. Predicted liquidus projection of the Mg-Mn-Si system. Calculated temperatures of invariants points are shown (^{0}C).

Chapter 6:   Article 3

Adarsh Shukla and Arthur D. Pelton

Centre de Recherche en Calcul Thermochimique, Département de Génie Chimique,

Ecole Polytechnique, Montréal, Québec, Canada

Thermodynamic assessment of the Al-Mn and Mg-Al-Mn systems

The binary Al-Mn system has been critically evaluated based upon available phase

equilibrium and thermodynamic data, and optimized model parameters have been

obtained giving the Gibbs energies of all phases as functions of temperature and

composition. The liquid solution has been modeled with the Modified Quasichemical

Model (MQM) to account for short-range ordering. The results have been combined with

those of our previous optimizations of the Al-Mg, and Mg-Mn systems to evaluate and

optimize the Mg-Al-Mn system. All available data for the ternary system are reproduced

with only one small ternary model parameter for the liquid phase.

6.1 Introduction

Although magnesium-based materials have a long history of important commercial applications, including automotive, there remains much to be learned about the basic properties of the metal and its alloys. With the recent renewed interest in lightweight wrought materials, including both sheet and tube applications, there has been an increased focus on developing a better understanding of novel magnesium alloys, including those that incorporate additions of Mn and Al. These alloy systems, along with other potential candidates, are being actively pursued as possible routes to develop magnesium materials with improved ductility, or even practical room temperature formability.

The properties of cast or wrought material depend first and foremost upon the phases and microstructural constituents (eutectics, precipitates, solid solutions, etc.) which are present. In an alloy with several alloying elements, the phase relationships are very complex. In order to investigate and understand these complex phase relationships effectively, it is very useful to develop thermodynamic databases containing model parameters giving the thermodynamic properties of all phases as functions of temperature and composition. Using Gibbs free energy minimization software such as FactSage[1, 2], the automotive and aeronautical industries and their suppliers will be able to access the databases to calculate the amounts and compositions of all phases at equilibrium at any temperature and composition in multicomponent alloys, to follow the course of equilibrium or non-equilibrium cooling, to calculate corresponding heat effects, *etc.*

Such thermodynamic databases are prepared by critical evaluation, modeling, and optimization. In a thermodynamic "optimization," adjustable model parameters are calculated using, simultaneously, all available thermodynamic and phase-equilibrium data in order to obtain one set of model equations as functions of temperature and composition. Thermodynamic data, such as activities, can aid in the evaluation of the phase diagrams, and information on phase equilibria can be used to deduce thermodynamic properties. Thus, it is frequently possible to resolve discrepancies in the available data. From the model equations, all of the thermodynamic properties and phase diagrams can be back-calculated, and interpolations and extrapolations can be made in a thermodynamically correct manner. The data are thereby rendered self-consistent and consistent with thermodynamic principles, and the available data are distilled into a small set of model parameters, ideal for computer storage.

As part of a broader research project to develop a thermodynamic database for Mg-alloys containing up to 25 potential alloying elements, the present study reports on evaluations and optimizations of the Al-Mn and Mg-Al-Mn systems. Previous optimizations[3-5] were based upon a Bragg-Williams (BW) random-mixing model for the liquid phase. However, the liquid phase in the Al-Mn binary system is expected to exhibit short-range ordering (SRO) as evidenced by the relatively large negative enthalpy of mixing[6]. As has been shown by the present authors[7], the use of the BW model in liquids with a high degree of SRO generally results in unstatisfactory results and in poor predictions of

ternary properties from binary model parameters. Hence the Al-Mn system was reoptimized with the Modified Quasichemcial Model (MQM) for the liquid phase; the present optimization reproduces all available data in the ternary Mg-Al-Mn system with only one very small ternary model parameter for the liquid solution. Care was taken to ensure that all optimized properties, such as for example the entropies of formation of intermetallic compounds, have physically reasonable values.

6.2 Modified Quashichemical Model (MQM)

The Modified Quasichemical Model (MQM) in the pair approximation[8] was used to model the liquid Al-Mn alloys. The liquid phases in the Mg-Al and Mg-Mn sub-systems of the Mg-Al-Mn system were also modeled previously with the MQM[9, 10]. This model, which takes short-range-ordering (SRO) into account, has been used extensively for molten salts[11-13], slags[14] and sulfides[15-17]. All details of the model and notation have been described previously [8] and only a brief summary is given here.

In the MQM in the pair approximation, the following pair exchange reaction between atoms A and B on neighboring lattice sites is considered:

$$(A-A)+(B-B)=2(A-B); \quad \Delta g_{AB} \quad \text{(Eq 1)}$$

where $(i-j)$ represents a first-nearest-neighbor pair. The non-configurational Gibbs energy change for the formation of two moles of $(A-B)$ pairs is Δg_{AB}.

Let n_A and n_B be the number of moles of A and B, n_{ij} be the number of moles of $(i-j)$ pairs, and Z_A and Z_B be the coordination numbers of A and B. The pair fractions, mole fractions, and "coordination-equivalent" fractions are defined respectively as:

$$X_{ij} = n_{ij}/(n_{AA} + n_{BB} + n_{AB}) \qquad \text{(Eq 2)}$$

$$X_A = n_A/(n_A + n_B) = 1 - X_B \qquad \text{(Eq 3)}$$

$$Y_A = Z_A n_A/(Z_A n_A + Z_B n_B) = Z_A X_A/(Z_A X_A + Z_B X_B) = 1 - Y_B \qquad \text{(Eq 4)}$$

The following equations may be written:

$$Z_A X_A = 2n_{AA} + n_{AB} \qquad \text{(Eq 5)}$$

$$Z_B X_B = 2n_{BB} + n_{AB} \qquad \text{(Eq 6)}$$

The Gibbs energy of the solution is given by:

$$G = \left(n_A g_A^\circ + n_B g_B^\circ\right) - T\Delta S^{\text{config}} + \left(n_{AB}/2\right)\Delta g_{AB} \qquad \text{(Eq 7)}$$

where g_A° and g_B° are the molar Gibbs energies of the pure components, and ΔS^{config} is the configurational entropy of mixing given by randomly distributing the $(A-A)$, $(B-B)$ and $(A-B)$ pairs in the one-dimensional Ising approximation[8]:

$$\Delta S^{\text{config}} = -\text{R}\left(n_A \ln X_A + n_B \ln X_B\right)$$
$$- \text{R}\left[n_{AA} \ln\left(X_{AA}/Y_A^2\right) + n_{BB} \ln\left(X_{BB}/Y_B^2\right) + n_{AB} \ln\left(X_{AB}/2Y_A Y_B\right)\right] \qquad \text{(Eq 8)}$$

Δg_{AB} is expanded in terms of the pair fractions:

$$\Delta g_{AB} = \Delta g_{AB}^\circ + \sum_{i \geq 1} g_{AB}^{i0} X_{AA}^i + \sum_{j \geq 1} g_{AB}^{0j} X_{BB}^j \qquad \text{(Eq 9)}$$

where Δg°_{AB}, g^{i0}_{AB} and g^{0j}_{AB} are the parameters of the model which can be functions of temperature.

The equilibrium pair distribution is calculated by setting

$$\left(\partial G/\partial n_{AB}\right)_{n_A,n_B} = 0 \qquad \text{(Eq 10)}$$

This gives the "equilibrium constant" for the "quasichemical reaction" of (Eq 1):

$$\frac{X^2_{AB}}{X_{AA}X_{BB}} = 4\exp\left(-\frac{\Delta g_{AB}}{RT}\right) \qquad \text{(Eq 11)}$$

As Δg_{AB} becomes progressively more negative, the reaction (Eq 1) is shifted progressively to the right, and the calculated enthalpy and configurational entropy of mixing assume, respectively, the negative "V" and "m" shapes characteristic of SRO.

The composition of maximum SRO is determined by the ratio of the coordination numbers Z_B/Z_A, as given by the following equations[8]:

$$\frac{1}{Z_A} = \frac{1}{Z^A_{AA}}\left(\frac{2n_{AA}}{2n_{AA}+n_{AB}}\right) + \frac{1}{Z^A_{AB}}\left(\frac{n_{AB}}{2n_{AA}+n_{AB}}\right) \qquad \text{(Eq 12)}$$

$$\frac{1}{Z_B} = \frac{1}{Z^B_{BB}}\left(\frac{2n_{BB}}{2n_{BB}+n_{AB}}\right) + \frac{1}{Z^B_{BA}}\left(\frac{n_{AB}}{2n_{BB}+n_{AB}}\right) \qquad \text{(Eq 13)}$$

where Z^A_{AA} and Z^A_{AB} are the values of Z_A respectively when all the nearest neighbors of an A are A's, and when all nearest neighbors of an A are B's, and where Z^B_{BB} and Z^B_{BA} are defined similarly. (Note that Z^A_{AB} and Z^B_{BA} represent the same quantity and can be used interchangeably.) In order to set the composition of maximum SRO at $X_{Mn} = 0.5$ in the

binary systems we set the $Z_{ij}^i / Z_{ij}^j = 1$ so that the composition of maximum SRO occurs at the equimolar composition. Although the model is sensitive to the ratio of the coordination numbers, it is less sensitive to their absolute values. The use of the one-dimensional Ising model in Eq 8 introduces a mathematical approximation into the model which we have found, by experience, can be partially compensated by selecting values of Z_B and Z_A which are smaller than the actual values. The value of the coordination numbers selected in the present study are listed in Table 6.1. The liquid phase in the Al-Mg and the Mg-Mn systems show maximum SRO near the equimolar composition[9, 10]; hence $Z_{AB}^A = Z_{BA}^B$ in all cases.

From the MQM model parameters for the binary liquid phases, the thermodynamic properties of a ternary liquid phase may be estimated as discussed previously[18]. If ternary experimental data are available, additional ternary model parameters may be added if required.

6.3 The Al-Mn system

All calculations and optimizations in the present study were performed with the FactSage thermochemical software[1, 2].

The optimized model parameters for the binary phases are reported in Table 6.1. Gibbs energies of all stable and metastable phases of the elements were taken from Dinsdale[19].

Crystallographic data [20-22] for the phases are listed in Table 6.2. The optimized phase diagram of this system is shown in Fig. 6.1.

McAlister and Murray[23] presented an extensive literature review of the system up to 1987. Jansson[3] performed the first thermodynamic optimization of the system, treating the liquid phase with a BW random-mixing model. Liu et al.[4] re-optimized the system in the light of their new data[24] for the HCP phase. Du et al.[5] optimized the Al-Mn system as a first step in their assessment of the Mg-Al-Mn system.

The solid solution phases CBCC, CUB, FCC, BCC, γ (BCC) and ε (HCP) (Fig. 6.1) were modeled by a single-sublattice substitutional model. There are numerous data[25-34] for the solubility of Mn in FCC-Al obtained by various techniques (electrical resistivity (ER), optical microscopy (OM), lattice parameter (LP), hardness measurements (HD), electron probe microanalysis (EPMA)). Fig. 6.2 compares the present optimization with these data.

The optimized phase diagram for $X_{Mn} \leq 0.2$ is compared with experimental data in Fig. 6.3. Schaefer et al.[35], by XRD and metallography, identified $Al_{12}Mn$ as a stable phase. They reported the pertectoid decomposition of $Al_{12}Mn$ into Al and Al_6Mn between 504 and 521 ^0C. The present calculated temperature for this reaction is 511 ^0C.

Dix et al.[34] and Phillips[36] studied the system by metallography and thermal analysis. They reported the intermetallic compounds Al_6Mn and Al_4Mn (μ-Al_4Mn in Fig. 6.1). Godecke and Koster[37] studied the system by the same techniques. They confirmed the presence of $Al_{11}Mn_4$ which was also noted by Philips[36]. They reported high- and low-temperature allotropes of $Al_{11}Mn_4$, the high-temperature form with a single-phase composition range of approximately 4 at. %. As the exact nature of the phase boundaries of the high-temperature form are unknown, this compound is treated as two stoichiometric phases $Al_{11}Mn_4$ in the present calculations with a transition temperature of $916\ ^0C$[37]. The Gibbs energy of the transformation was assumed to be zero.

Taylor[38] by XRD and thermal analysis, and Murray et al.[39] by thermal analysis, reported the existence of a second phase close to μ-Al_4Mn. Du et al.[5] by XRD and DTA confirmed the presence of two distinct phases: μ-Al_4Mn at X_{Mn}= 0.2 and λ-Al_4Mn at X_{Mn}= 0.186. They modeled the phase λ-Al_4Mn as stoichiometric $Al_{461}Mn_{107}$ based on the crystallographic data of Kreiner and Franzen[21].

Koch et al.[40] studied the system by thermal analysis in the range 25-100 at. % Mn. Koster and Wachtel[41] studied the system in the range 30-100 at. % Mn by thermal and magnetic analysis, microhardness, and XRD. Later, Godecke and Koster[37], by metallography and thermal analysis, reported three phases in the region from 30 to 50 at. % Mn: γ, $\gamma1$, and $\gamma2$ (In Fig. 6.1, γ is denoted γ (BCC), while $\gamma1$ and $\gamma2$ are the Al_8Mn_5 phase). Ellner[20], using high temperature XRD, showed that the γ phase has a BCC

structure. As very little information is available about the γ1 and γ2 phases, they were modeled as a single phase "Al_8Mn_5" (Fig. 6.1), as was also done in previous optimizations[4, 5]. Following the suggestion, based on crystallographic data[20], of Du et al.[5], the Al_8Mn_5 phase was modeled by the compound energy formalism[42,43] as $Al_{12}Mn_5(Al,Mn)_9$ (the first sublattice containing only Al, the second only Mn and the third a random mixture of Al and Mn).

The optimized phase diagram for the region from $0.2 \leq X_{Mn} \leq 0.5$ is compared with experimental data in Fig. 6.4. In the absence of any further experimental evidence, the order-disorder transformation in the γ (BCC) phase suggested by Liu et al.[4] based upon preliminary DSC results[44] was ignored. For modeling purpose, γ (BCC) was formally treated as the same phase as the terminal BCC solid solution of Al and Mn, but for clarity of representation, this region has been denoted as γ (BCC) in the figures.

The optimized phase diagram in the region from $0.5 \leq X_{Mn} \leq 0.1$ is compared with the experimental data in Fig. 6.5. The phase equilibria for the ε (HCP) phase were first studied by XRD and specific heat measurements by Kono[45]. Koster and Wachtel[41] studied the boundaries of the phase by magnetic analysis, micro-hardness, XRD and thermal analysis, and denoted the phase as ε. Muller et al.[46] established phase equilibria for this phase by DTA. Liu et al.[24] investigated the phase mainly by a diffusion couple technique, and also by metallography, XRD, DSC and TEM. They reported a wider single-phase region than Koster and Wachtel[41], attributing the difference to the

transformation of ε (HCP) at compositions richer in Mn than 58 at. % into the CUB phase during the quenching experiments.

Meschel and Kleppa[47], by direct synthesis calorimetry, reported the enthalpy of formation at 25 ^{0}C for alloys at 60 and 80 at. % Mn. Kubaschewski and Heymer[48], by high temperature reaction calorimetery, reported enthalpies of formation for four compositions: Al_6Mn, Al_4Mn, $Al_{11}Mn_4$ and $AlMn$. The optimized standard enthalpy of formation of the intermediate compounds is compared with the experimental data and the previous optimizations in Fig. 6.6.

Partial enthalpies of mixing in the liquid phase at 1353 ^{0}C were measured by high-temperature vacuum isothermal calorimetry by Esin et al.[6] who reported only smoothed data. The present optimized enthalpy of mixing is compared with these data and with previous optimizations in Fig. 6.7.

Batalin et al.[49] performed EMF measurements in the liquid phase at 1297 ^{0}C, reporting activities of Mn, while Kematick and Myers[50] measured Al and Mn activities at 902 ^{0}C by Knudsen cell /mass spectrometry in the range 42-62 at. % Mn. These data are inconsistent with the other data for the system and were ignored. Chastel and co-workers[51] determined activities of Mn and Al in the melt in the range from 0 to 50 at. % Mn at 1247 ^{0}C by Knudsen cell/mass spectrometry. The optimized activities are compared with the experimental data and previous optimizations in Fig. 6.8.

The optimized entropy of mixing in the liquid phase at 1400 ^{0}C is compared with the previous optimizations in Fig. 6.9. The optimized standard entropies of formation of the solid alloys from the elements at 25 ^{0}C are compared with previous optimizations in Fig. 6.10 (see also Table 6.1). Generally, such entropies of formation are expected to be small, as in the case in the present study.

6.4 The Mg-Al-Mn System

The previously optimized phase diagrams of the Al-Mg[9] and Mg-Mn[10] systems are shown in Figs. 6.11 and 6.12 respectively. The parameters optimized by Chartrand[9] for the phases in the Al-Mg system pertinent to the present work are given in Table 6.3. Crystallographic data of all the solid phases appearing in the Mg-Al-Mn system are in Table 6.2. It may be noted that the calculated consolute temperature of the misciblity gap in the Mg-Mn system, Fig. 6.9, is about 1500-2000 ^{0}C lower than in the previous optimizations[52,53] of this binary system.

Our previous optimizations[9, 10] of the Al-Mg and Mg-Mn systems were combined with the present optimization of the Al-Mn system in order to calculate the polythermal projection of the liquidus of the Mg-Al-Mn system shown in Fig. 6.13. The thermodynamic properties of the ternary liquid phase were calculated by the MQM from the binary model parameters. The "asymmetric approximation"[18, 54] with Al as "asymmetric component" was used, since the Mg-Mn liquid exhibits positive deviations

from ideality, whereas the Al-Mg and Al-Mn liquids exhibit negative deviations. A small ternary interaction parameter (Table 6.1) was included for the liquid phase.

The HCP phase in the Al-Mg and Mg-Mn systems[9, 10] and the FCC phase in the Al-Mg system were modeled with single-sublattice substitutional models. For modeling purposes, the Mg-rich HCP phase in the Al-Mg and Mg-Mn systems and the ε (HCP) phase in the Al-Mn system were formally treated as the same phase. The thermodynamic properties of the ternary HCP and FCC phases were estimated from the binary model parameters. The "symmetric" (Kohler) approximation[54] was used with no ternary interaction parameters. The predicted stability of the ε (HCP) phase at 1200 ^{0}C is shown in Fig. 6.14.

γ-AlMg has the same structure as the CBCC-Mn phase (Table 6.2). A small solubility of Mn in this compound or combined solubility of Al and Mg in CBCC-Mn might therefore be expected. No data for these solubilities could be found. Pending further experimental work, the binary phase γ-AlMg and CBCC-Mn were treated as separate phases. Possible mutual solubilities between any other intermetallic phases were assumed to be negligible in the absence of any experimental evidence and since they all have different structures and stoichiometries.

6.4.1 Mg-Rich Alloys

The solubilities of Mn in liquid Mg reported by Hanawalt et al.[55] are significantly lower than later findings[56,57] and have been rejected. Beerwald[56] and Nelson[57] used a settling technique to determine solubilities. Oberländer et al.[58], and later Simensen et al.[59] from the same laboratory, identified the composition of precipitated solids around 700-750 ^{0}C by a centrifuging technique supplemented with XRD and metallography. They concluded that at 700-750 ^{0}C, CUB and Al_8Mn_5 are the equilibrium phases at compositions $0 \leq$ wt. % Mn ≤ 3 and $0 \leq$ wt. % Al ≤ 15. The present calculations agree well with these data. In another work, Simensen et al.[60] reported solubilities at 750, 710 and 670 ^{0}C by the same technique. Thorvaldsen and Aliravci[61] measured the solubility of Mn in the liquid phase by settling and decantation followed by emission spectrometry and ICP.

The data of Nelson[57], Beerwald[56], Simensen et al.[60] and Thorvaldsen and Aliravci[61] are compared with the present calculations in Fig. 6.15. All data except those of Simensen et al.[60] are reasonably well reproduced below 780 ^{0}C. The solubilities reported by Simensen et al.[60] are lower than the present calculations and the disagreement increases with increasing temperature. This same trend was noted by Ohno and Schmid-Fetzer[62] in their assessment. Thorvaldsen and Aliravci[61] reported that the results of Simensen et al.[60] may have been influenced by iron contamination. A calculated isopleth at 5.05 wt. % Al is compared with the data of Thorvaldsen and Aliravci[61] in Fig. 6.16.

Mirgalovskaya et al.[63], by microstructural and microhardness tests, studied liquid-solid and solid-solid phase equilibria in Mg-rich alloys. Their data are compared with the present calculations in Fig. 6.17. Their results at 850 ^{0}C are inconsistent with the measurements of other authors as can be seen by comparing Figs. 6.17b and 6.15c. Other measurements of Mirgalovskaya et al.[63] and Ageev et al.[64] in Mg-rich alloys at temperatures below 400 ^{0}C were rejected because they report large solublities of Mn and Al in Mg which are inconsistent with the other data.

The solidus measurements of Nelson[57] are compared with the calculations in Fig. 6.18. The disagreement is due to the fact that these measurements are inconsistent with other data in the binary Al-Mg system (wt. % Mn = 0 in Fig. 6.18) which were used in the optimization of this binary system.

In the present work, for all practical purposes the solubility data up to 760 ^{0}C can be reproduced without any ternary interaction parameters. The small ternary term shown in Table 6.1 is only required to refine the optimization at the higher temperatures.

6.4.2 Al-Rich Alloys

Leemann and Hanemann[65] studied Al-rich alloys by metallography and thermal analysis. Wakeman and Raynor[66] doubted the attainment of equilibrium in Leemann and Hanemann's work[65] and carried out microstructural observations of alloys annealed at 400 ^{0}C. These authors[66] reported a ternary compound by XRD and tentatively reported

its composition to be $MnMg_2Al_{10}$. Later, Fun et al.[67] determined the crystal structure of this phase by XRD and reported its composition to be $Mn_2Mg_3Al_{18}$. This phase is denoted as **T** in the present work. Du et al.[5] reported the enthalpy of formation of **T** as -10.2 kJ/(mol of atoms) by first principles calculations and as -8.7 kJ/(mol of atoms) by a CALPHAD-type assessment. The present optimization gives the enthalpy of formation as -9.9 kJ/(mol of atoms).

Barlock and Mondolfo[68] reported a eutectic invariant reaction L = (Al) + β-AlMg + **T** at 447 ^{0}C. The present computed temperature for this reaction is 451 ^{0}C. According to the present calculations, the **T** phase should melt peritectically near 471 ^{0}C. The primary crystallization field for this ternary phase is extremely small and is very close to the Mg-Al binary edge of the composition triangle. It is not visible on the scale of Fig. 6.13.

Ohnishi et al.[69] studied Al-rich alloys at 400 ^{0}C and 450 ^{0}C by metallography and XRD. Isothermal sections at 400 ^{0}C and 450 ^{0}C are compared with the experimental data in Figs. 6.19 and 6.20. Ohnishi et al.[69] also reported two-phase (FCC + Al_6Mn) regions (not shown here) at very low Mg and Mn contents at 400 ^{0}C and 450 ^{0}C which are inconsistent with the optimized Al-Mn binary phase diagram. In a different work, Ohnishi et al.[70] studied six Al-rich alloys, showing the two-phase FCC+Al_6Mn region to be stable for 1≤ wt. % Mn≤ 2 and 0≤wt. % Mg ≤4, in agreement with the present calculations.

Butchers *et al.*[71], from cooling curves, reported smoothed liquidus curves between 630

and 650 ^{0}C. The data at 650 ^{0}C are compared with the present calculations in Fig. 6.20.

Little *et al.*[72] by microstructure observations, and Fahrenhorst and Hoffman[25] by

electrical resistance measurements, reported solubilities of Mn and Mg at 500 ^{0}C in the

FCC-Al phase. These data are compared with the present calculations in Fig. 6.21.

6.5 Conclusions

Gibbs energy functions for all phases in the Al-Mn system have been obtained. All

available thermodynamic and phase equilibrium data have been critically evaluated in

order to obtain one set of optimized model parameters of the Gibbs energies of all phases

which can reproduce the experimental data within experimental error limits. Tentative

calculated phase diagrams of the Mg-Al-Mn system have been given. For all practical

purposes, the available data below 760 ^{0}C in the Mg-Al-Mn system can be reproduced

solely from the optimized binary model parameters. A small ternary parameter has been

included for the liquid phase to refine the optimization at higher temperatures.

The use of the Modified Quasichemical Model (MQM) for the liquid phase has permitted

short-range ordering to be taken into account. Use of this model results in a better fitting

of the data for the liquid phase than is the case when a Bragg-Williams random-mixing

model is used, as well as a better representations of the partial properties of solutes in

dilute solution in magnesium, the activities of solutes in dilute solution being of much

practical importance. As shown by the present authors[7], the use of the MQM generally also results in better estimations of the properties of ternary and higher-order liquid alloys. These estimations of phase equilibria in magnesium alloys will aid in the design of novel magnesium alloys.

6.6 Acknowledgements

6.7 References:

[1] C. W. Bale, P. Chartrand, S. A. Degterov, G. Eriksson, K. Hack, R. Ben Mahfoud, J. Melançon, A. D. Pelton and S. Petersen, FactSage Thermochemical Software and Databases, *Calphad*, 2002, **26(2)**, 189-228

[2] C.W.Bale, A.D. Pelton, W. Thompson, Factsage thermochemcial software and databases, http:// www.crct.polymtl.ca (2008)

[3] A. Jansson, Thermodynamic Evaluation of the Al-Mn System, *Metall. Mater. Trans. A*, 1992, **23A**, 2953

[4] X. J. Liu, I. Ohnuma, R. Kalnuma, and K. Ishida, Thermodynamic Assessment of the Al-Mn Binary Phase Diagram , *J. Phase Equilib.*, 1999, **20(1)**, p 45

[5] Y. Du, J. Wang, J. Zhao, J. C. Schuster, F. Weitzer, R. Schmid-Fetzer, M Ohno, H. Xu, Z. Liu, S. Shang and W. Zhang, Reassessment of the Al–Mn system and a thermodynamic description of the Al–Mg–Mn system, *Int. J. Mat. Res.*, 2007, **98**, p 9

[6] Y. O. Esin, N. T. Bobrov, M. S. Petrushevskii and P. V. Geld, Concentration Variation of the Enthalpies of Formation of Mn-Al melts at 1626 K, *Russ. J. Phys. Chem.* 1973, **47**, p 1103

[7] A. D. Pelton and Y. -B. Kang, Modeling Short-range Ordering in Solutions, *Int. J. Mat. Res.*, 2007, **10**, 905

[8] A. D. Pelton, S. A. Degterov, G. Eriksson, C. Robelin and Y. Dessureault, The Modified Quasichemical Model I – Binary Solutions, *Metall. Mater. Trans. B.*, 2000, **31B (6)**, p 651-659

[9] P. Chartrand, CRCT, Ecole Polytechnique, Montreal, 2006 (Unpublished Work)

[10] Y.-B. Kang, A. D. Pelton, P. Chartrand, P. Spencer and C. D. Fuerst, Critical Evaluation and Thermodynamic Optimization of the Binary Systems in the Mg-Ce-Mn-Y System, *J. Phase Equilib. Diffus.*, 2007, **28 (4)**, 342-354

[11] P. Chartrand and A. D. Pelton, Thermodynamic Evaluation and Optimization of the LiCl-NaCl-KCl-RbCl-CsCl-MgCl$_2$-CaCl$_2$ System Using the Modified Quasi-chemical Model, *Metall. Mater. Trans. A.*, 2001, **32A (6)**, p 1361-1383

[12] P. Chartrand and A. D. Pelton, Thermodynamic Evaluation and Optimization of the LiF-NaF-KF-MgF$_2$-CaF$_2$ System Using the Modified Quasi-chemical Model, *Metall. Mater. Trans. A.*, 2001, **32A (6)**, p 1385-1396

[13] P. Chartrand and A.D. Pelton, Thermodynamic Evaluation and Optimization of the Li, Na, K, Mg, Ca//F, Cl Reciprocal System Using the Modified Quasichemical Model, *Metall. Mater. Trans. A.*, 2001, **32A (6)**, p 1417-1430

[14] S. A. Decterov, I.-H. Jung, E. Jak, Y.-B. Kang, P. Hayes and A. D. Pelton, Thermodynamic Modelling of the Al_2O_3-CaO-CoO-CrO-Cr_2O_3-FeO-Fe_2O_3-MgO-MnO-NiO-SiO_2-S System and Application in Ferrous Process Metallurgy, *Proc. VII International Conference on Molten Slags, Fluxes and Salts*, C. Pistorius, ED., The South African Institute of Mining and Metallurgy, Johannesburg, South Africa, 2004, p 839-850

[15] P. Waldner and A. D. Pelton, Thermodynamic Modeling of the Ni-S System, *Z. Metallkunde*, 2004, **95**, p 672-681

[16] P. Waldner and A. D. Pelton, Critical Thermodynamic Assessment and Modeling of the Fe-Ni-S System, *Metall. Mater. Trans. B.*, 2004, **35B (5)**, p 897-907

[17] P. Waldner and A.D. Pelton, Thermodynamic Modeling of the Fe-S System, *J. Phase Equilib. Diffus.*, 2005, **26 (1)**, p 23-38

[18] A. D. Pelton and P. Chartrand, The Modified Quasichemical Model: Part II. Multicomponent solutions, *Metall. Mater. Trans. A.*, 2001, **32A(6)**, p 1355

[19] A. T. Dinsdale, SGTE Data for Pure Elements, *Calphad*, 1991, **15 (4)**, p 317-425 plus updates (private communication), 2000, http:// www.sgte.org

[20] M. Ellner, The Stucture of the High-Temperature Phase MnAl (h) and the Displacive Transformation from MnAl (h) into Mn_5Al_8, *Metall. Mater. Trans. A*, 1990, **21A**, p 1669

[21] G .Kreiner and H. F. Franzen, The crystal structure of λ-Al_4Mn, *J. Alloys Compd.*, 1997, **261**, p 83-104

[22] P. Villars, L.D. Calvert, *Pearson's Handbook of Crystallographic Data for Intermetallic phases*, 2nd edition, ASM, Materials Park, Ohio, USA (1991)

[23] A. J. McAlister and J. L. Murry, The Al-Mn System, *Bulletin of Alloy Phase Diagrams*, 1987, **8(5)**, p 438

[24] X. J. Liu, I. Ohnuma, R. Kalnuma, and K. Ishida, Phase equilibria in the Mn-rich portion of the binary system Mn-Al, *J. Alloys Compd.*, 1996, **235**, p 256-261

[25] E. Fahrenhorst and W. Hoffman, The solubility of Manganese in Aluminum Containing up to 2 Percent of Magnesium, *Metallwirtschaft*, 1940, **19**, p 891-893

[26] E. Butchers and W. Hume-Rothery, The Solubility of Manganese in Aluminum, *J. Inst. Met.*, 1945, **71**, p 87-91

[27] I. Obinata, E. Hata and K. Yamaji, Chiefly on the Sub-Cooled Al-Mn Alloys, *J. Inst. Met.*, 1953, **17**, p 496-501

[28] G. M. Kuznetsov, A. D. Barsukov and M. I. Abas, Study of manganese, chromium, titanium, and zirconium solubility in solid aluminum, *Sov. Non Ferrous Met. Res.*, 1983, **11**, p 783

[29] Y. Minamino, T. Yamane, H. Araki, N. Takeuchi, Y.-S. Kang, Y. Miyamoto and T. Okamoto, Solid Solubilities of Mn and Ti in Aluminum at 0.1 MPa and 2.1 GPa, *Metall. Mater. Trans. A*, 1991, **22A**, p 783

[30] V. A. Livanov and V. M. Vozdvizhenskii, Recrystallization of aluminum alloys with manganese, *Trudy Moskov. Aviatsion, Tekhnol. Inst.*, 1958, **31**, p 65-83.

[31] E. H. Dix and W. D. Keith, Equilibrium Relations in Al-Mn Alloys of High Purity, *Proc. AIME,* Inst. Metals, Div., 1927, p 315-335

[32] M. E. Drits, E. S. Kadaner, E. M. Padzhnova and N. R. Bochvar, Determination of the Boundaries of Common Solubility of Mn and Cd in Solid Aluminum, *Zh. Neorg. Khim.*, 1964, **9(6)**, p 1397.

[33] C. Sigli, CALPHAD XXIV conference, Kyoto, Japan, 1995, quoted by Du *et al.* [5].

[34] E. H. Dix, W. L. Fink and L. A. Willey, Equilibrium Relations in Al-Mn Alloys of High Purity II, *Trans. AIME*, 1933, **104**, p 335-352

[35] R. J. Schaefer, F.S. Biancaniello and J. W. Cahn , Formation and Stability Range of the G Phase in the Al-Mn System, *Scr. Metall.*, 1986, **20(10)**, p 1439-44

[36] H.W.L. Phillips, The Constitution of Alloys of Aluminium with Manganese ,Silicon and Iron., *J. Inst. Met*, 1942, **69**, p 275-316

[37] T. Godecke and W.Koster, A supplement to the Constitution of the Al-Mn system, *Z. Metallkd.*, 1971, **62(10)**, p 727-32.

[38] M. A. Taylor, Intermetallic Phases in the Al-Mn Binary system, *Acta. Metall.*, 1960, **8**, p 256-262.

[39] J. L. Murray, A. J. McAlister, R. J. Schaefer, L. A. Bendersky, F. S. Biancaniella and D. L. Moffatt, Stable and Metastable Phase Equilibria in the Al-Mn System, *Metall. Trans. A*, 1987, **18A**, 385

[40] A. J. J. Koch, P. Hokkeling, M.G.v.d. Steeg, and K. J. Devos, New Material for Permanent Magnets on a Base of Mn and Al, *J.Appl. Phys.*, 1960, **31(5)**, p 75S-77S

[41] W. Koster and E. Wachtel, Magnetic Investigation of Al-Mn Alloys Containing More than 25 at. % Mn, *Z. Metallkd.*, 1960, **51**, p 271-280

[42] M. Hillert and L. -I. Staffansson, Regular solution model for stoichiometric phases and ionic melts, *Acta Chem. Scand.*, 1970, **24(10)**, p 3618-26.

[43] J.O. Andersson, A. F Guillermet, M. Hillert, B. Jansson, B. Sundman, A compound-energy model of ordering in a phase with sites of different coordination numbers, *Acta Metall.* 1986, **34(3)**, p 437-45.

[44] X. J. Liu, Ph. D. Thesis, Tohoku University, Japan, 1998

[45] H. Kono, On the Ferromagnetic Phase in Mn-Al system, *J. Phys. Soc. Jpn.*, 1958, **13**, p 1444

[46] C. Muller, H.Stadelmaier. B.Reinsch and G Petzow, Metallurgy of the Magnetic τ-Phase in Mn-Al and Mn-Al-C, *Zeitschrift fuer Metallkunde* , 1996, 87(7), p 594-597

[47] S. V. Meschel and O. J. Kleppa, The Standard Enthalpies of Formation of Some 3d Transition Metal Aluminides by High-Temperature Direct Synthesis Calorimetery, *NATO ASI Series, Ser.E*, 1994, **256**, p 103-112

[48] O. Kubaschewski and G. Heymer, Heats of Formation of Transition-Metal Aluminides, *Trans. Faraday Soc.* 1960, **56**, p 473

[49] G. I. Batalin, E. A. Beloborodova, V. A. Stukalo and A. A. Chekhovskii, Thermodynamic Properties of Molten Alloys of Aluminum with Manganese, *Ukr. Khim Zh.* 1972, **38(8)**, p 825

[50] R. J. Kematick and C. E. Myers, Thermodynamics and Phase Equilibria in the Al-Mn System, *J. Alloys and Comp*, 1992, **178**, p 343-349

[51] R. Chastel, M. Saito and C. Bergman, Thermodynamic Investigation on $Al_{1-x}Mn_x$ melts by Knudsen Cell Mass Spectrometry, *J. Alloys and Comp.* 1994, **205**, p 39

[52] J. Tibbals, Mg-Mn System, *COST 507 – Thermochemical Databases for Light Metal Alloys*, I. Ansara, A.T. Dinsdale, M.H. Rand (eds.), Vol 2, EUR 18499, 1998, p 215-217

[53] J. Gröbner, D. Mirkovic, M. Ohno and R. Schmid-Fetzer, Experimental Investigation and Thermodynamic Calculation of Binary Mg-Mn Phase Equilibria, *J. Phase Equilib. Diffus.*, 2005, **26(3)** p 234-239

[54] A. D. Pelton, A General "Geometric" Thermodynamic Model for Multicomonent Solutions, *Calphad*, 2001, **25(2)**, p 319-328

[55] J. D. Hanawalt, C. E. Nelson and G. E. Holdeman, Removal of Iron from Mg-base Alloys, US Patent No. 2267862, Dec.30, 1941

[56] A. Beerwald, On the Solubility of Iron and Manganese in Magnesium and in Magnesium-Aluminium Alloys, *Metallwirtschaft*, 1944, **23**, p 404-407

[57] B. J. Nelson, Equilibrium Relations in Mg-Al-Mn Alloys, *J. Metals* 1951, **3**, p 797

[58] B. C. Oberländer, C. J. Simensen, J. Svalestuen and A. Thorvaldsen, Phase Diagram of Liquid Magnesium - Aluminium - Manganese Alloys, *Magnesium Technology*, Pros. Conf., London, 1986, p 133-137,

[59] C. J. Simensen, B. C. Oberländer, J. Svalestuen and A. Thorvaldsen, Determination of the Equilibrium Phases in Molten Mg - 4 wt.% Al-Mn Alloys, *Z. Metallkd.*, 1988, **79**, p 537-540

[60] C. J. Simensen, B. C. Oberländer, J. Svalestuen and A. Thorvaldsen, The Phase Diagram for Magnesium - Aluminium - Manganese above 650°C, *Z. Metallkd.*, 1988, **79**, p 696-699

[61] A. Thorvaldsen and C. A. Aliravci, Solubility of Mn in Liquid Mg-Al Alloys, *Proc Int. Symp*, A*dv. Prod. Fabr. Light Met. Met. Matrix Comp.* 1992, p 277

[62] M. Ohno and R. Schmid-Fetzer, Thermodynamic Assessment of Mg-Al-Mn Phase Equilibira on Mg-Rich Alloys, *Z. Metallkd.*, 2005, **96(8)**, p 857

[63] M. S. Mirgalovskaya, L. N. Matkova and E. M. Komova, The System Mg-Al-Mn, *Trudy Inst. Met. Im. A.A. Baikova, Akad. Nauk*, 1957, **2**, 139-148

[64] N. V. Ageev, I. I. Kornilov and A. N. Khlapova, Magnesium-Rich Alloys of the System Magnesium-Aluminium-Manganese, *Izv. Inst. Fiz.-Khim. Anal., Inst. Obshcheii Neorg. Khim., Akad. Nauk SSSR*, 1948, **14**, p 130-143

[65] W. G. Leemann and H. Hanemann, The Ternary System Aluminium-Magnesium-Manganese, *Aluminium Arch.*, 1938, **9**, p 6-17

[66] D. W. Wakeman and G. V. Raynor, The Constitution of Aluminium-Manganese-Magnesium and Aluminium-Manganese-Silver Alloys, with Special Reference to Ternary Compound Formation, *J. Inst. Met.*, 1948, **75**, p 131-150

[67] H. -K. Fun, H.-C. Lin, T. -J Lee and B.-C. Yipp, T-Phase $Al_{18}Mg_3Mn_2$, *Acta Crystallogr.*, 1994, **C50**, p 661-663

[68] J. G. Barlock and L.F. Mondolfo, Structure of some aluminum-iron-magnesium-manganese-silicon alloys. *Z. Metallkd.* 1975, **66(10)**, p 605-11.

[69] T. Ohnishi, Y. Nakatani and K. Shimizu, Phase Diagrams and Ternary Compounds of the Al-Mg-Cr and the Al-Mg-Mn Systems in Al-Rich Side, *Light Metals Tokyo*, 1973, **23**, p 202-209

[70] T. Ohnishi, Y. Nakatani and K. Shimizu, Phase Diagram in the Al-Rich Side of the Al-Mg-Mn-Cr Quaternary System, *Light Metals Tokyo*, 1973, **23**, p 437-443

[71] E. Butchers, G.V. Raynor and W. Hume-Rothery, The Constitution of Magnesium-Manganese-Zinc-Aluminium Alloys in the Range 0-5 % Magnesium, 0-2 % Manganese, 0-8 % Zinc, I-The Liquidus, *J. Inst. Met.*, 1943, **69**, p 209-228

[72] A.T. Little, G.V. Raynor, W. Hume-Rothery, The Constitution of Magnesium-Manganese - Zinc - Aluminium Alloys in the Range 0-5 % Magnesium, 0-2 %

Manganese and 0-8 % Zinc, III-The 500 ^{0}C and 400 ^{0}C Isothermals, *J. Inst. Met.*, 1943, **69**, p 423-440

Table 6.1. Model parameters of the Al-Mn and Mg-Al-Mn systems optimized in the present study.

Liquid:

Co-ordination numbers: $Z_{AlAl}^{Al} = Z_{MnMn}^{Mn} = Z_{AlMn}^{Al} = Z_{MnAl}^{Mn} = 6$

Δg_{Al-Mn} : $(-16945 + 3.012\ T) + (-5857 + 0.418\ T)\ X_{Al-Al} + (-1674 + 2.761\ T)\ X_{Mn-Mn}$ Joules

Ternary interaction term for Δg_{Al-Mn}: $\ 0.837\ T\ (\dfrac{X_{Mg}}{X_{Mg}+X_{Mn}})\ $ Joules

Solid solutions :

Excess Gibbs energy terms, $G^E/X_{Mn}X_{Al}$ (Joules/mol of atoms)

CUB	$(-121838 + 46.861\ T) + (-5021 + 10.627\ T)\ (X_{Mn}-X_{Al})$
CBCC	$(-79536 + 27.614\ T) + (-10042)\ (X_{Mn}-X_{Al})$
BCC	$(-108700 + 32.510\ T) + (44769 - 19.246\ T)\ (X_{Mn}-X_{Al})$
FCC	$(-84517 + 29.999\ T) + (-19665 + 12.552\ T)\ (X_{Mn}-X_{Al})$
HCP	$(-87027 + 17.154\ T) + (-5774 + 8.786\ T)\ (X_{Mn}-X_{Al}) + (83931 - 47.279\ T)$ $(X_{Mn}-X_{Al})^2$

"Al_8Mn_5" $\{Al_{12}Mn_5(Al,Mn)_9\}$ (Joules/mol of atoms)

$^0G_{Al:Mn:Al}$ [a]	$\frac{21}{26}\ ^0G_{FCC}^{Al} + \frac{5}{26}\ ^0G_{CBCC}^{Mn} + (-13634 + 1.579\ T)$
$^0G_{Al:Mn:Mn}$ [a]	$\frac{12}{26}\ ^0G_{FCC}^{Al} + \frac{14}{26}\ ^0G_{CBCC}^{Mn} + (-23566 + 2.502\ T)$
Excess Gibbs energy, $G^E/y_{Al}y_{Mn}$	$(-31621 + 14.792\ T) + (-7870 + 10.024\ T)\ (y_{Mn}-y_{Al})$ [b]

Stoichiometric compounds :				
Compounds	ΔH^0_{298} [c] J/(mol of atoms)	S^0_{298} [d] J/[(mol of atoms)-K]	ΔS^0_{298} [c] J/[(mol of atoms)-K]	Cp J/[(mol of atoms)-K]
$\frac{1}{13}Al_{12}Mn$	-8818	26.208	-2.394	0.923 C_p(Al, FCC) + 0.077 C_p(Mn, CBCC)
$\frac{1}{7}Al_6Mn$	-15714	25.243	-3.617	0.857 C_p(Al, FCC) + 0.143 C_p(Mn, CBCC)
$\frac{1}{568}\lambda$-Al_4Mn (modeled as $Al_{461}Mn_{107}$)	-20450	24.325	-4.714	0.812 C_p(Al, FCC) + 0.188 C_p(Mn, CBCC)
$\frac{1}{5}\mu$-Al_4Mn	-20880	24.860	-4.224	0.800 C_p(Al, FCC) + 0.200 C_p(Mn, CBCC)
$\frac{1}{15}Al_{11}Mn_4$	-23913	25.400	-3.946	0.733 C_p(Al, FCC) + 0.267 C_p(Mn, CBCC)
$\frac{1}{23}Mn_2Mg_3Al_{18}$ (T)	-9887	28.391	-0.820	0.783 C_p(Al, FCC) + 0.111 C_p(Mn, CBCC) + 0.106 C_p(Mg, HCP)

[a] Gibbs energy of end-members [42, 43]
[b] y_{Al} and y_{Mn} are the site fractions of Al and Mn in the sublattcie $(Al,Mn)_9$
[c] Enthalpy and entropy of formation from the elements at 298.15 K
[d] Absolute Third-Law entropy at 298.15 K

Table 6.2. Crystallographic data of all phases in the Mg-Al-Mn system considered in the present optimization.

Phase	Prototype	Pearson symbol	Space group	Comments, Reference
FCC	Cu	$cF4$	$Fm\overline{3}m$	Al, Mn are stable phases,[22]
BCC	W	$cI2$	$Im\overline{3}m$	Mn is stable phase, [22]
CUB	Mn	$cP20$	$P4_132$	Mn is stable phase, [22]
CBCC	Mn	$cI58$	$I\overline{4}3m$	Mn is stable phase, [22]
HCP	Mg	$hP2$	$P6_3/mmc$	Mg and ε (HCP) phases are stable phases, [22]
$Al_{12}Mn$	$Al_{12}W$	$cI26$	$Im3$	[22]
Al_6Mn	Al_6Mn	$oC28$	$Cmcm$	[22]
λ-Al_4Mn	....	$hP586$	$P6_3/m$	[21]
μ-Al_4Mn	Al_4Mn	$hP574$	$P6_3/mmc$	[21]
$Al_{11}Mn_4$	$Al_{11}Mn_4$	$aP15$	$P\overline{1}$	Low temperature form, [22]
"Al_8Mn_5"	Al_8Cr_5	$hR26$	$R3m$	[20]
$Al_{30}Mg_{23}$	$Mn_{44}Si_9$	$hR159$	$R\overline{3}h$	[22]
β-AlMg	Al_3Mg_2	$cF1168$	$Fd\overline{3}m$	[22]
γ-AlMg	Mn (CBCC)	$cI58$	$I\overline{4}3m$	[22]
$Mn_2Mg_3Al_{18}$	$Al_{18}Mg_3Cr_2$	$cF184$	$Fd\overline{3}m$	[22]

Table 6.3.   Optimized parameters from Chartrand [9] for phases in the Al-Mg system pertinent to the present work

| Phases (Model used)	Optimized Parameters (Joules)
Liquid (MQM)	$\Delta g_{Al\text{-}Mn} = (-2762 + 1.527\ T) + (-418 + 0.628\ T)\ X_{Al\text{-}Al}$ Coordination numbers : $Z^{Mg}_{MgMg} = Z^{Al}_{AlAl} = Z^{Al}_{AlMg} = Z^{Mg}_{MgAl} = 6$
Solid solutions	Excess Gibbs energy terms, $G^E/X_{Mg}X_{Al}$ (Joules/mol of atoms)
FCC (Single-sublattice random mixing)	$(4971 - 3.500\ T) + (-900 - 0.423\ T)\ (X_{Mg}\text{-}X_{Al})$
HCP (Single-sublattice random mixing)	$(1950 - 1.999\ T) + (-1480 + 2.079\ T)\ (X_{Mg}\text{-}X_{Al}) + 3500\ (X_{Mg}\text{-}X_{Al})^2$
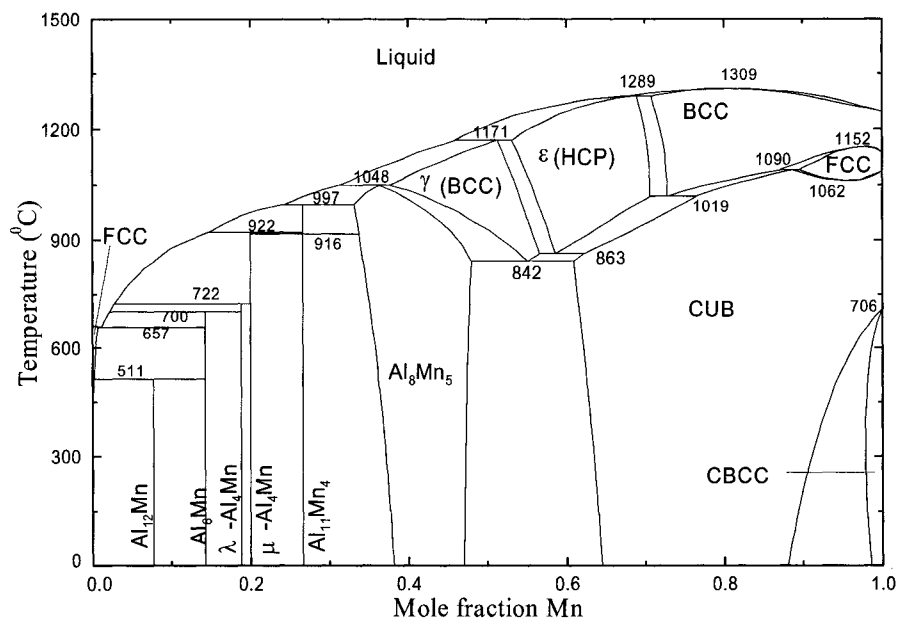
Fig. 6.1. Optimized phase diagram of the Al-Mn system.
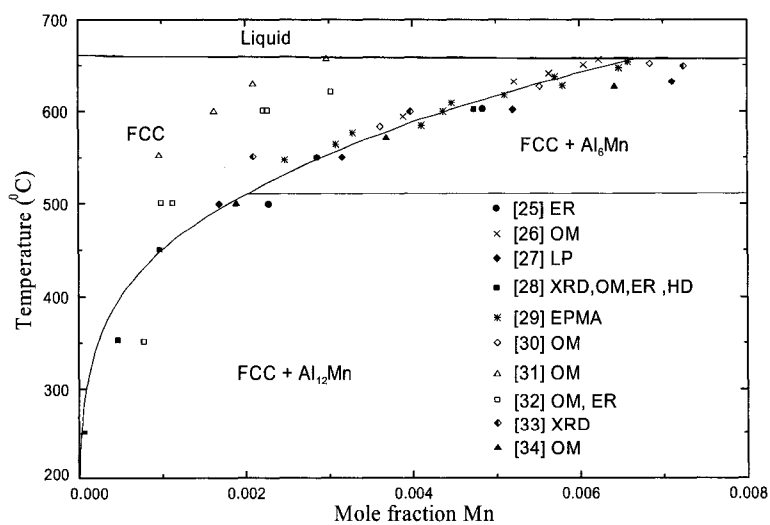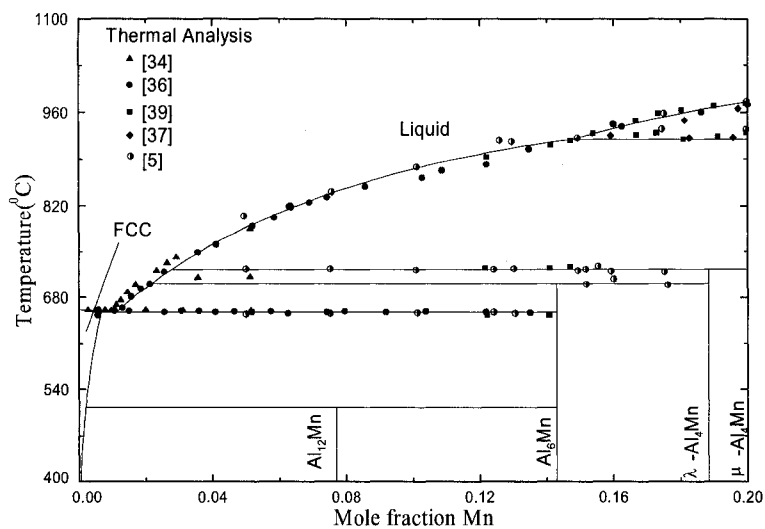

Fig. 6.2. Optimized solubility of Mn in the FCC phase.

Fig. 6.3. Optimized phase diagram of the Al-Mn system for $X_{Mn} \leq 0.2$.
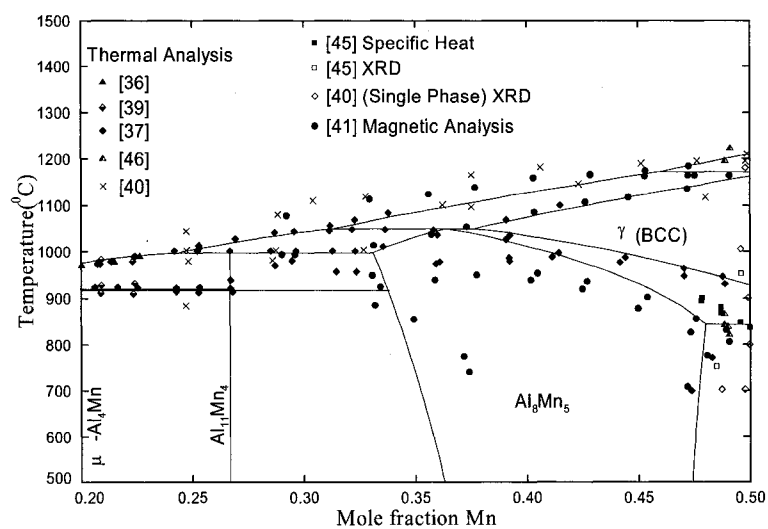

Fig. 6.4. Optimized phase diagram of the Al-Mn system for $0.2 \leq X_{Mn} \leq 0.5$.
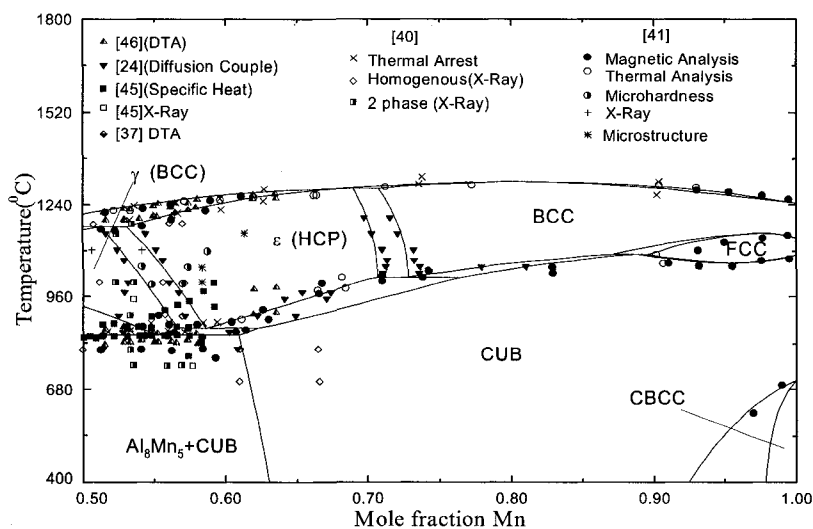
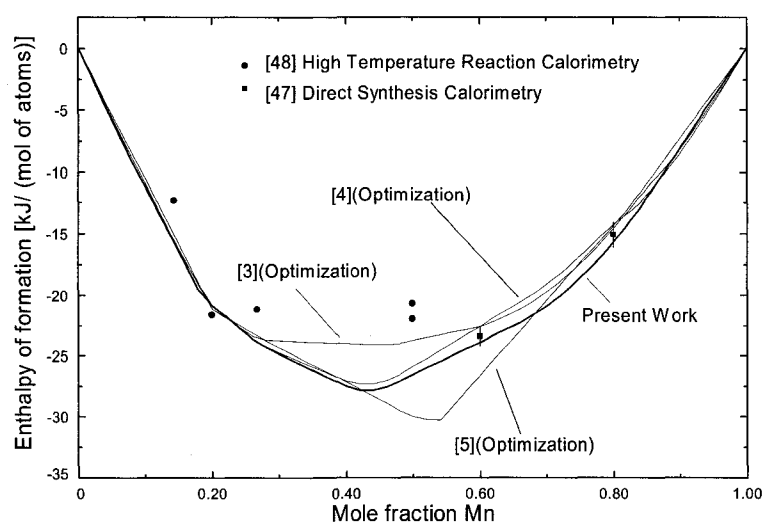Fig. 6.5. Optimized phase diagram of the Al-Mn system for $0.5 \leq X_{Mn} \leq 1.0$.

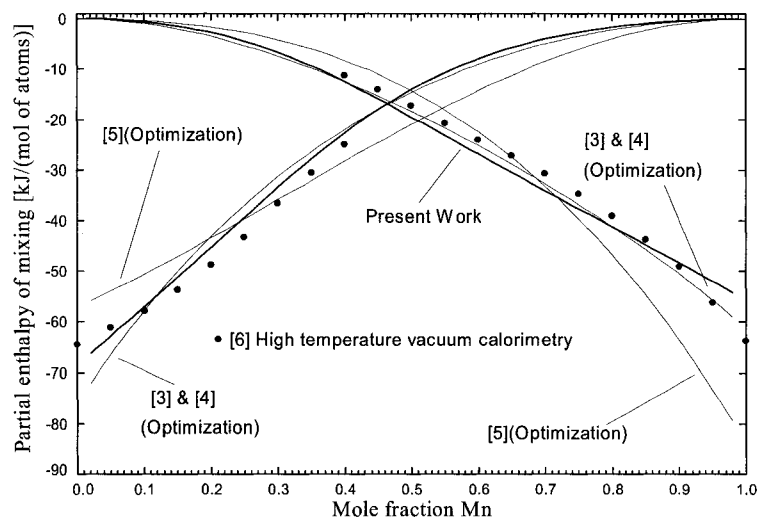Fig. 6.6. Optimized standard enthalpies of formation of solid Al-Mn alloys.

Fig. 6.7 Optimized partial enthalpies of mixing in liquid Al-Mn alloys at 1353 ^{0}C.
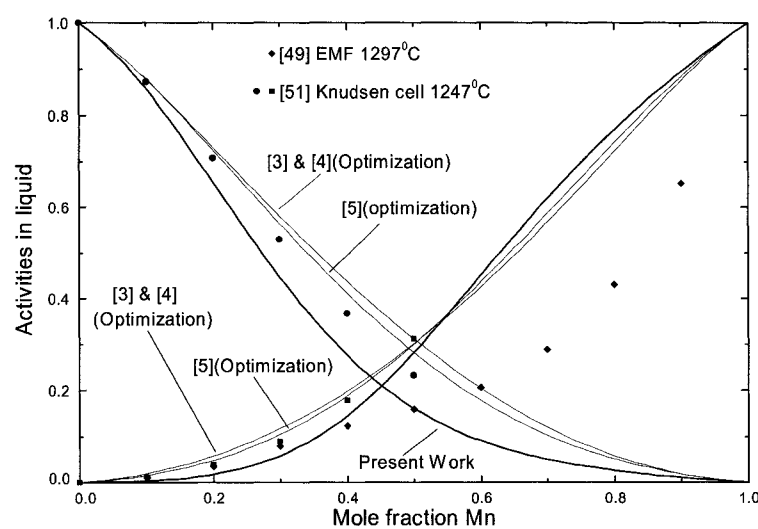

Fig. 6.8. Optimized activity of Al and Mn in liquid Al-Mn alloys at 1247 ^{0}C.
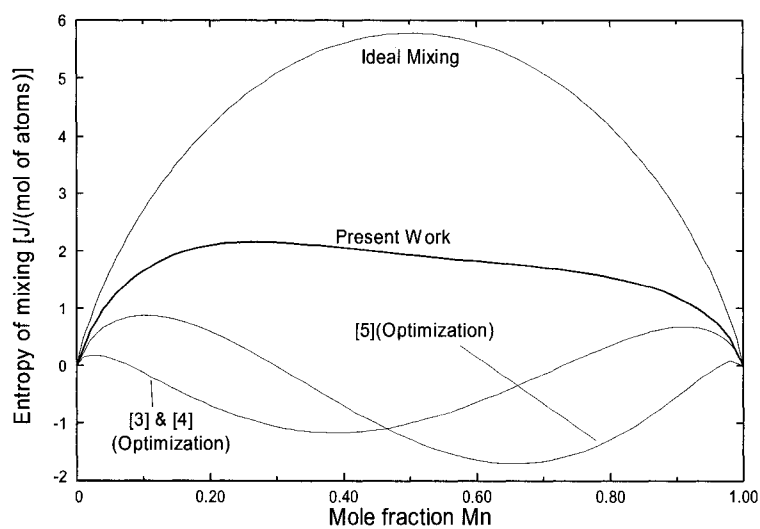
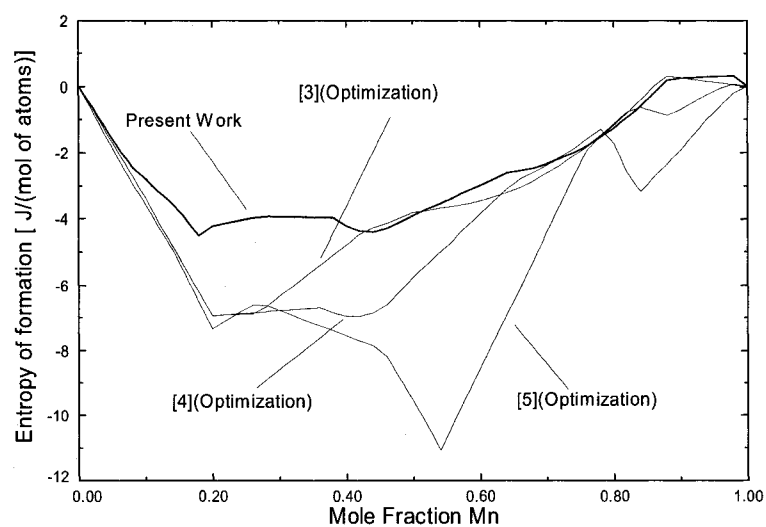Fig. 6.9. Optimized entropy of mixing in liquid Al-Mn alloys at 1400 ^{0}C.

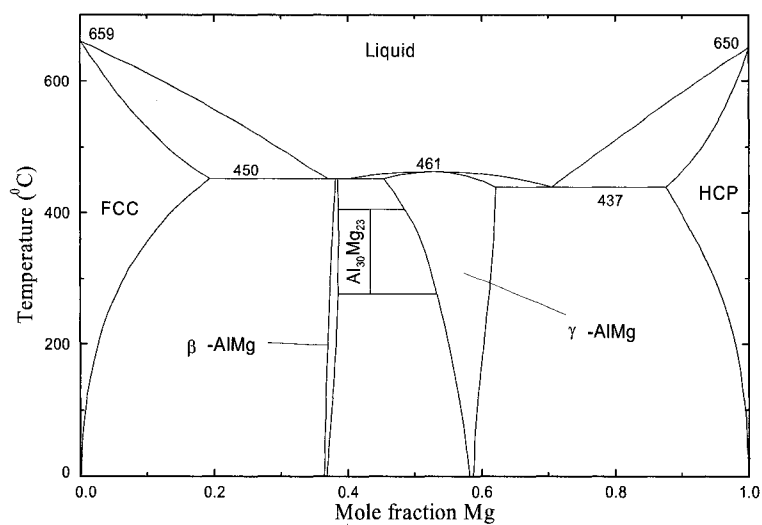Fig. 6.10. Optimized standard entropies of formation at 25 ^{0}C of solid Al-Mn alloys from the elements.

Fig. 6.11. Previously optimized phase diagram of the Al-Mg system [9].

Fig. 6.12. Previously optimized phase diagram of the Mg-Mn system [10].

Mg

829
895

11
10

0.8
0.6
0.4
0.2
0.2
0.4
0.6
0.8

1083

9

1083

1238

max

1 = Al₆Mn
2 = λ– Al₄Mn
3 = μ– Al₄Mn
4 = Al₁₁Mn₄
5 = Al₈Mn₅
6 = γ (BCC)
7 = HCP
8 = BCC
9 = 2 Liquids
10 = FCC
11 = CUB

2
1
3   4   5   6   7   8

Al   0.8   0.6   0.4   0.2   Mn
Mole fraction
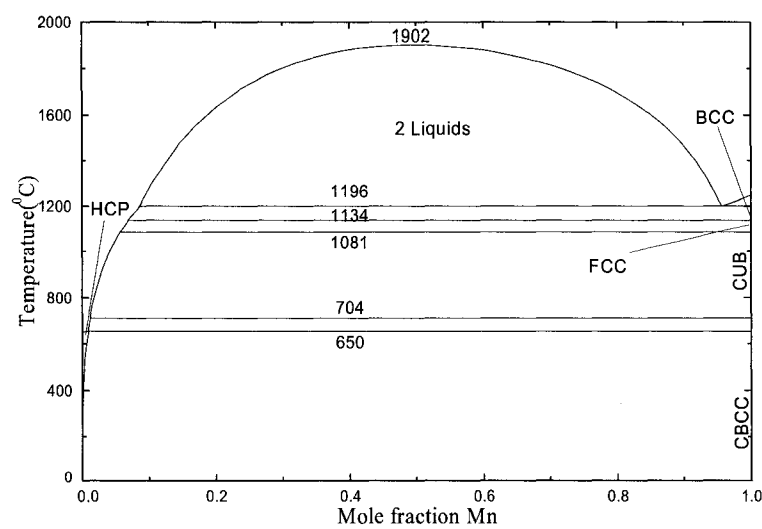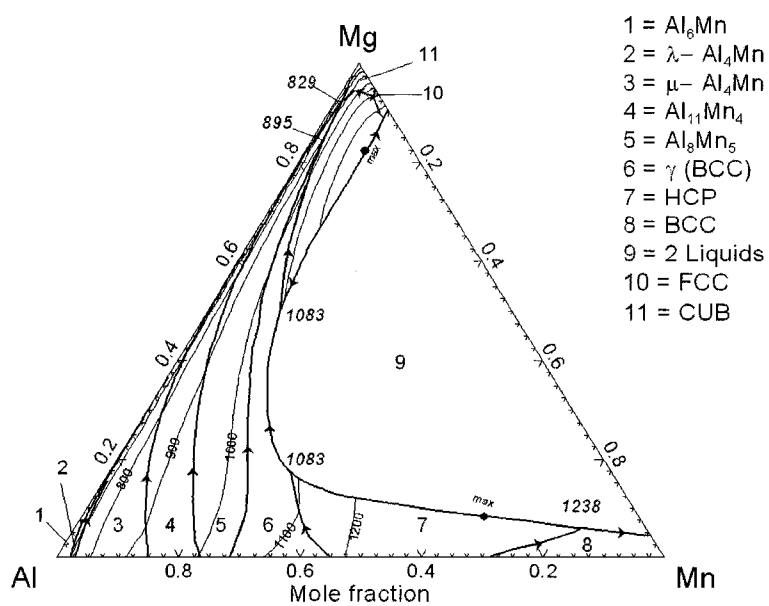
Fig. 6.13. Predicted polythermal projection of the liquidus in the Mg-Al-Mn system.

Calculated invariant temperatures are shown (^{0}C).

Mg

T = 1200 ^{0}C

0.8
0.6
0.4
0.2
0.2
0.4
0.6
0.8

2 Liquids

Liquid

Liquid + BCC

(HCP)

Al   0.8   0.6   0.4   0.2   Mn
Mole fraction
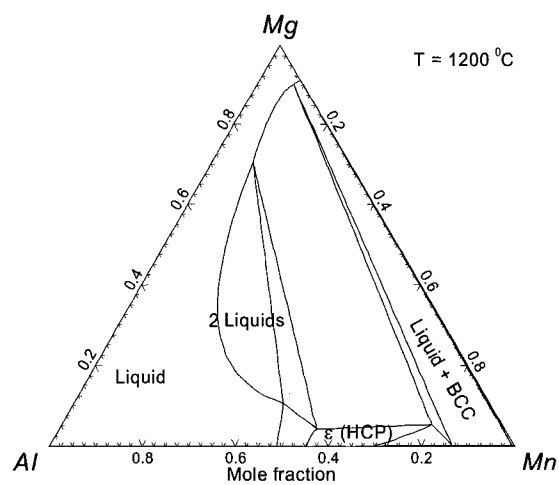
Fig. 6.14. Calculated isothermal section of the Mg-Al-Mn phase diagram at 1200^{0}C
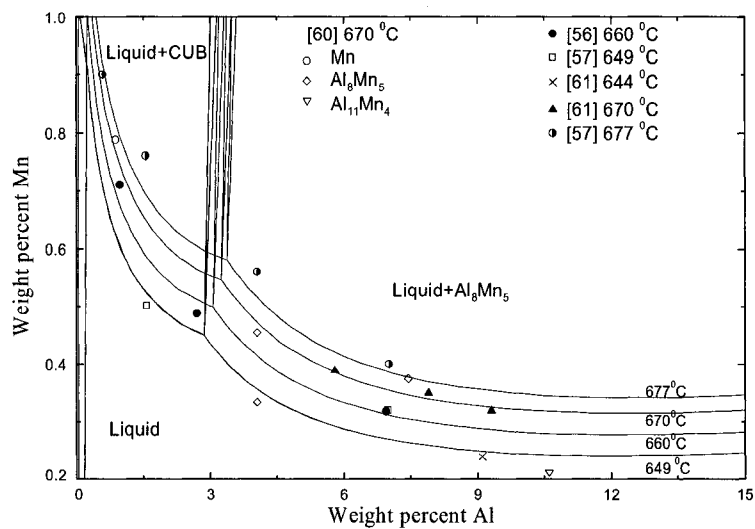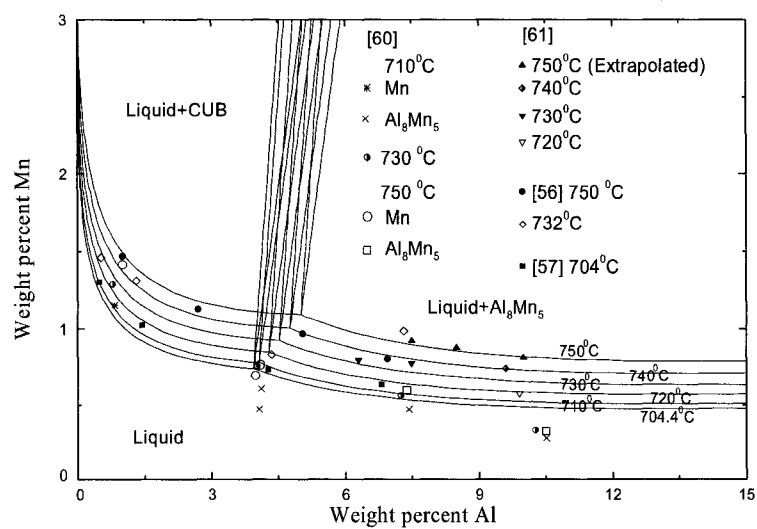
Fig 6.15a

Fig. 6.15b
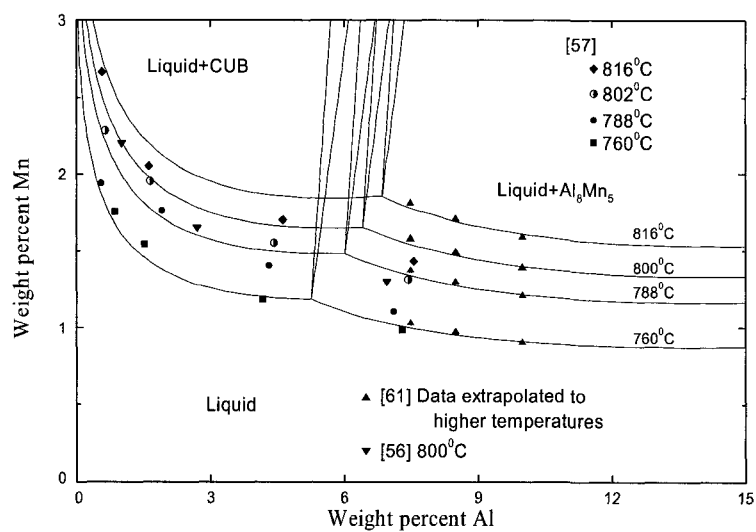
Fig. 6.15c

Fig. 6.15 Optimized liquidus surface in Mg-rich solutions.
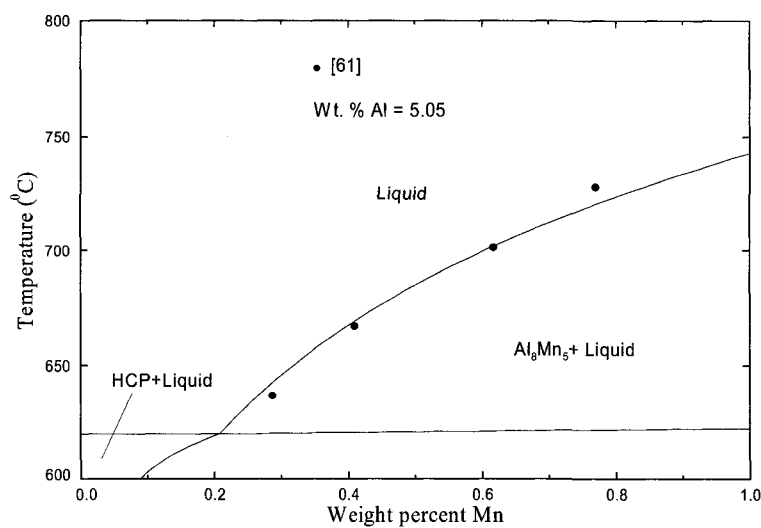
Fig. 6.16 Calculated section of the Mg-Al-Mn phase diagram at constant 5.05 wt. % Al.
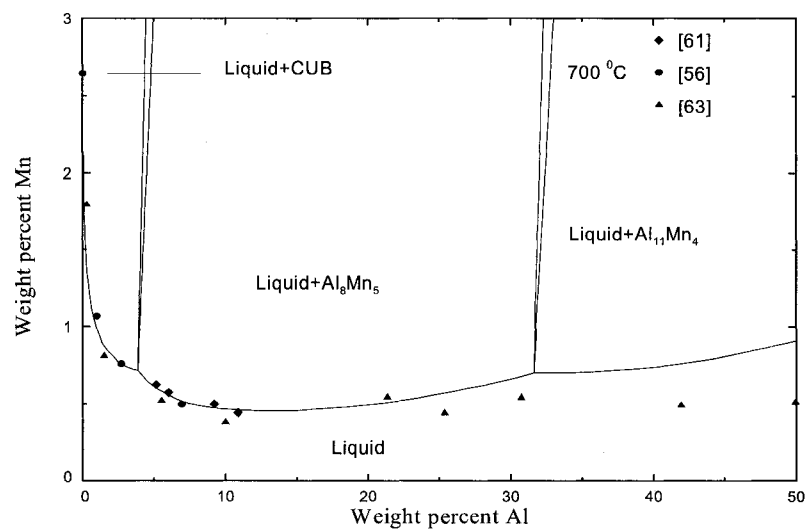
Fig. 6.17a
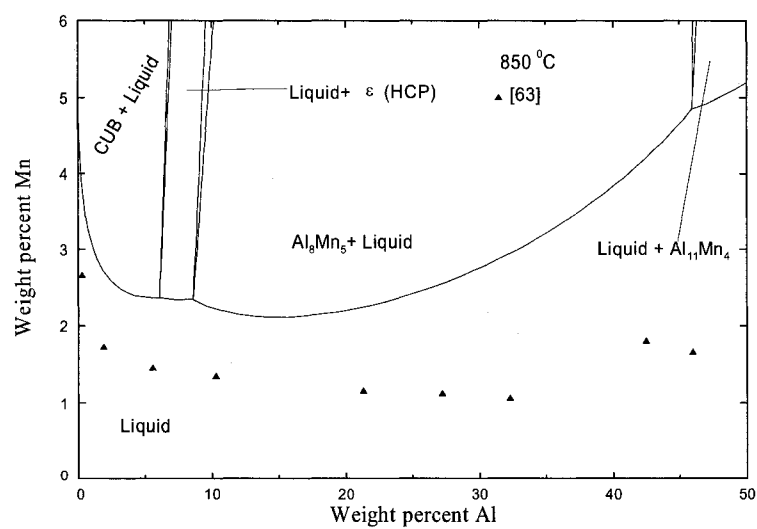
Fig. 6.17b

Fig. 6.17   Calculated liquidus surface in the Mg-Al-Mn system: a) 700 ^{0}C   b) 850 ^{0}C.
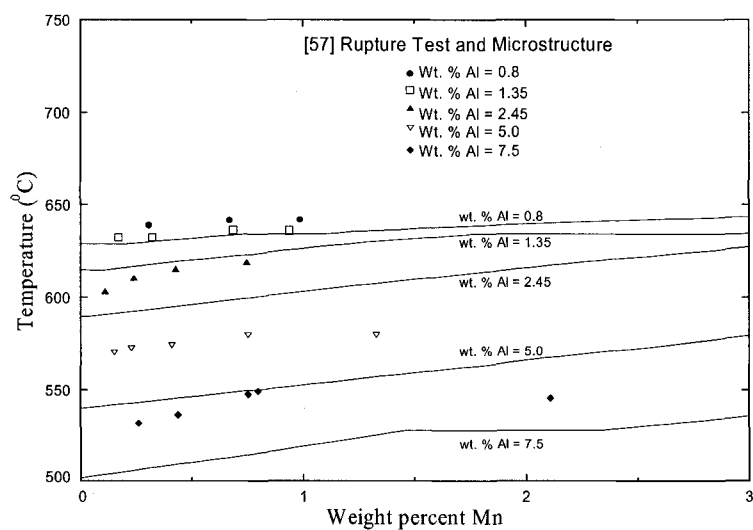
Fig. 6.18   Calculated solidus curves in the Mg-Al-Mn system
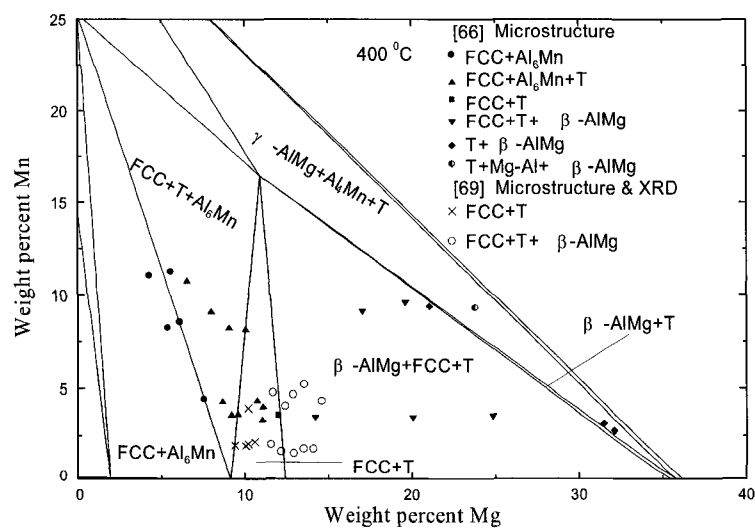
Fig. 6.19a
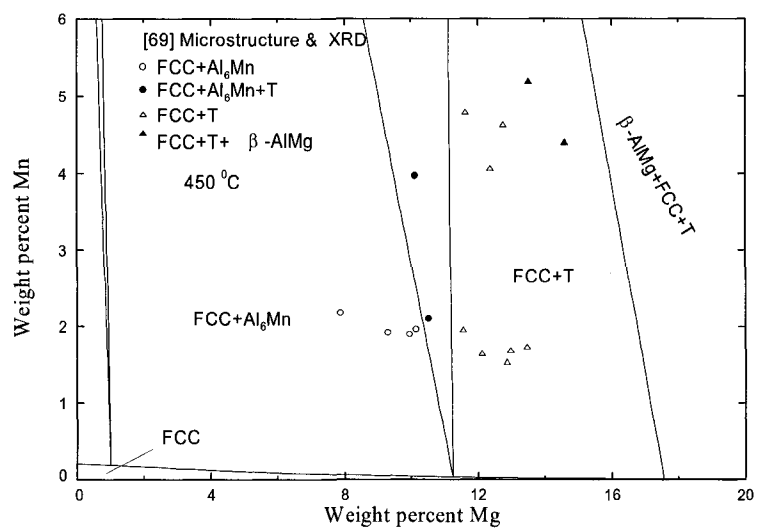
Fig. 6.19b

Fig. 6.19 Calculated isothermal sections of the Mg-Al-Mn phase diagram: a) 400 ^{0}C b)

450 ^{0}C.
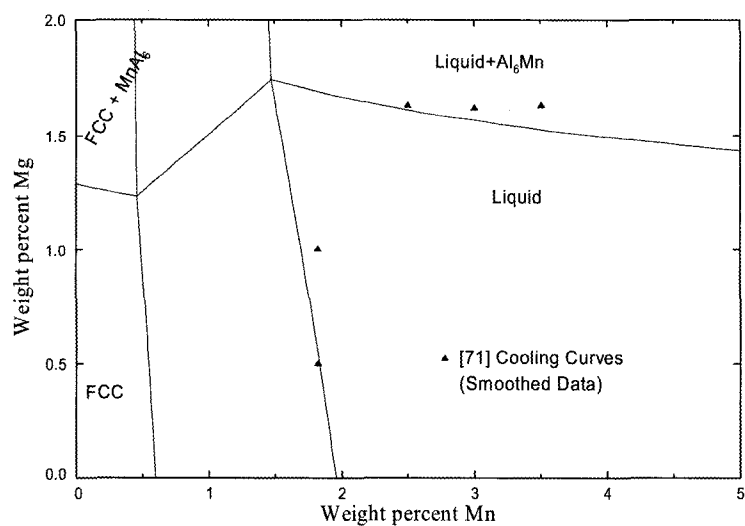
Fig. 6.20   Calculated liquidus surface in the Mg-Al-Mn system.
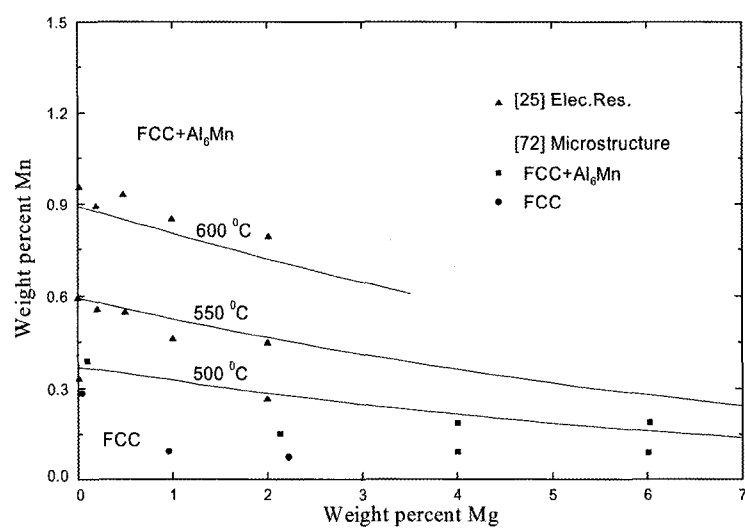
Fig. 6.21   Calculated solubility of Mn and Mg in FCC-Al.

Chapter 7: General discussion

Once the optimized parameters for various phases in a system are obtained they are stored in the computer databases. When these evaluated and optimized databases are used with the FactSage™ thermochemical software (FactSage, 2008), they permit the calculation of phase diagrams, phase equilibria and thermodynamic properties of Mg-alloys. Some examples of such calculations are given here.

*Si may be an impurity in Mg-alloys containing Ce and Y*

Grobner and Schmid-Fetzer (Grobner and Schmid-Fetzer, 2001) listed a number of factors to be considered in the selection of compositions for the development of new Mg-alloys. One of the very important factors they listed was that the primary phase precipitated during solidification should be the HCP (Mg-rich) phase.

In the phase diagram shown in Fig. 7.1, it can be seen that HCP (Mg-rich) is not a primary phase at compositions wt. % Y = 2.0, wt. % Si =0.5 and wt. % Ce < 0.1, because YSi is precipitated first. Metals like Ce or Y are considered to have high potential as alloying materials with Mg as they improve its high temperature stability. The rare-earth silicides like YSi, having a much higher melting temperature than the HCP (Mg-rich) phase, are highly stable and during solidification of the liquid alloy they precipitate before the HCP (Mg-rich) phase. This violates the above condition listed by Grobner and Schmid-Fetzer. The primary precipitated silicides may adversely affect the microstructure

and mechanical properties of Mg-alloys. In this case, Si should be present to the lowest

possible extent in such Mg-alloys.

In Fig. 7.1, it can be seen that $CeMg_{12}$ is the next phase which is precipitated from HCP

(Mg-rich) which can be useful in age-hardening mechanisms of these alloys. Hence,

multi-component phase diagrams as shown in Fig. 7.1 calculated by the presently

developed thermodynamic database can provide vital information.
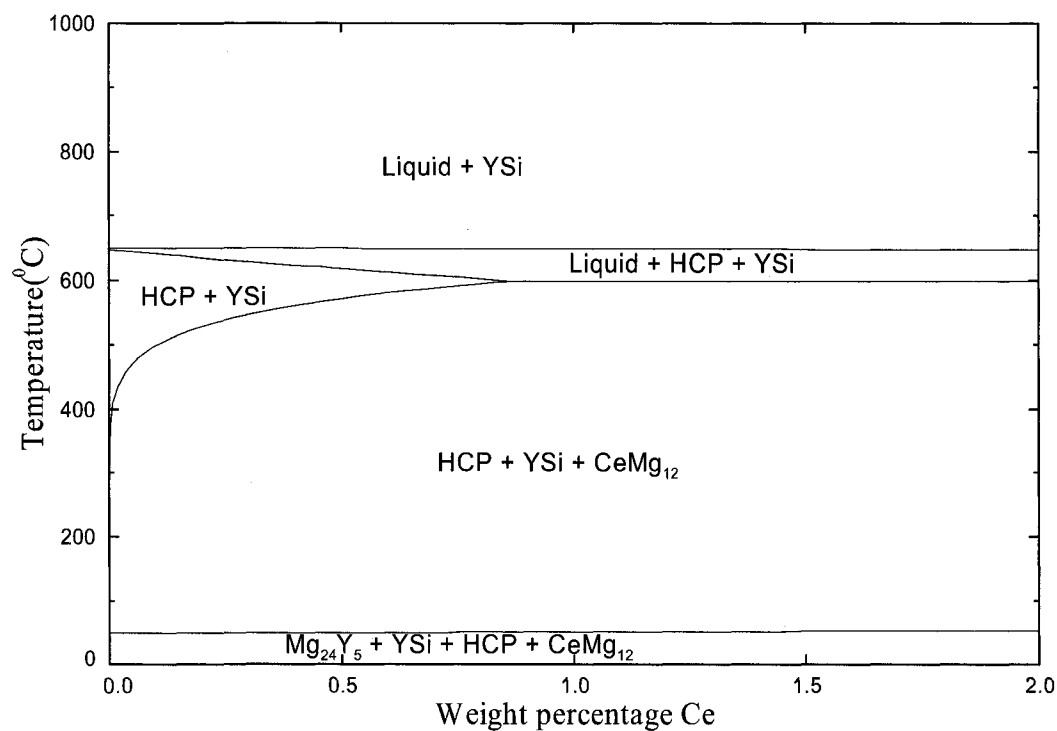
Figure 7.1   Calculated vertical section in the Mg-Y-Si-Ce phase diagram, wt. % Si = 0.5

and wt. % Y = 2.

Equilibrium cooling and non-equilibrium cooling of the Mg-alloys

To show an example, an arbitrary composition of an alloy containing elements from the presently optimized system was chosen. The composition of the alloy was 95 wt. % Mg, 2 wt. % Zn, 1 wt. % Ce, 1 wt. % Y, 0.5 wt. % Si and 0.5 wt. % Mn. Equilibrium cooling was simulated at this composition to calculate the various phases in equilibrium during cooling. Such calculations are of great importance in a casting process. The precipitated phases control the microstructure and hence many physical properties of the alloy. Thus it is very helpful to know the sequence of phases and the amount precipitated out during cooling of an alloy composition. The calculations shown here as examples were performed with the *Equilib* module of FactSage[TM].

It should be noted that the calculations shown below are predictions based upon the presently evaluated and optimized systems. These results can only be validated by experimental results. But these predictions do give a basis for an "educated-guess" based on which the number of experiments required to validate these results can be significantly reduced.

Fig. 7.2 shows the percentage distribution of alloys obtained during cooling of the above alloy from 800 ^{0}C. The liquid phase disappears at around 512 ^{0}C. The YSi phase was in equilibrium with the liquid phase at 800 ^{0}C, the temperature where the calculation was started. As can be seen, Mn_3Si and Ce_3Si_5 phases were precipitated during the course of equilibrium cooling but were soon transformed into other stable phases. According to the

present calculations, the equilibrium phases obtained after the disappearance of the liquid phase are HCP, YSi, $CeMg_{12}$, Mn_5Si_3 and CeSi. The equilibrium amount of these phases can be read from Fig. 7.2 (Due to the large difference in the amount of phase precipitated, the percentage phase distribution is shown on two different scales in Figs. 7.2a and 7.2b).
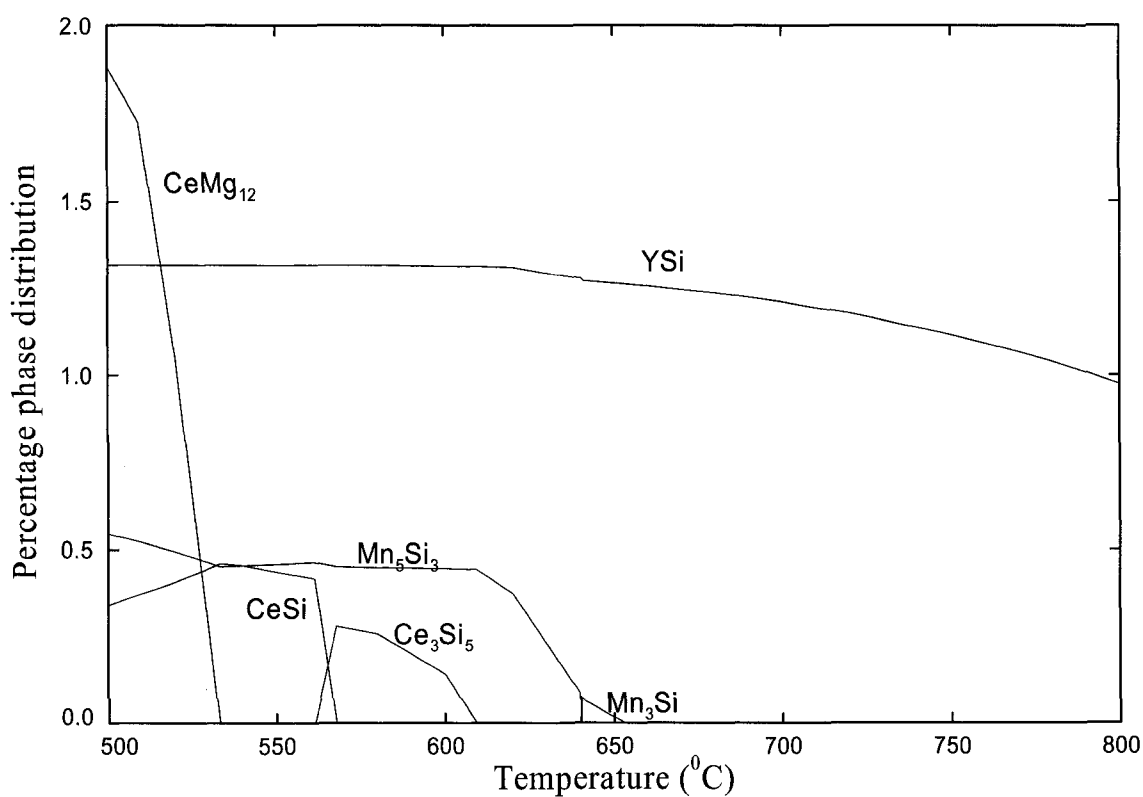
Fig. 7.2a
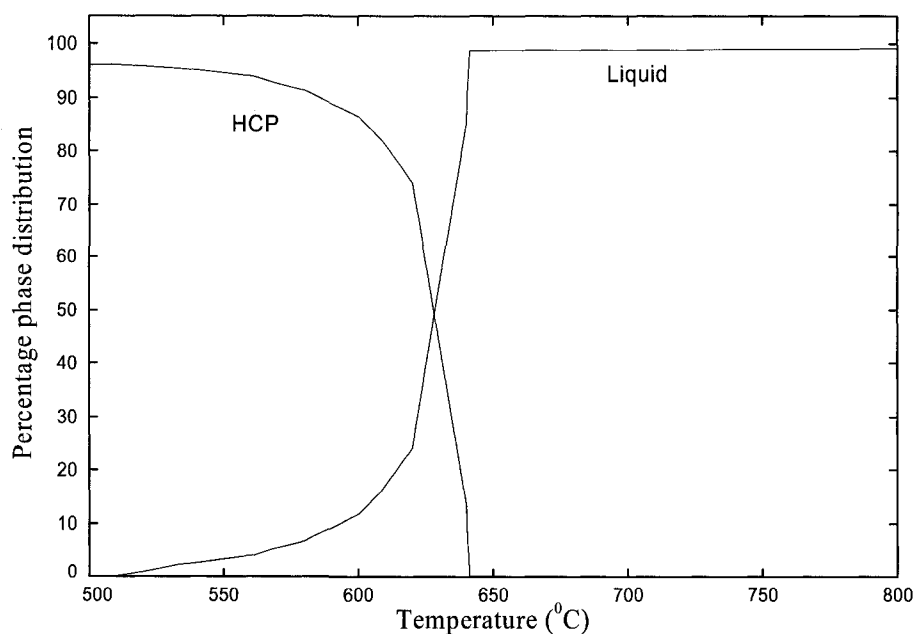
Fig. 7.2b

Figure 7.2   Phase distribution of the phases precipitated during equilibrium cooling of an alloy of composition 95 wt. % Mg, 2 wt. % Zn, 1 wt. % Ce, 1 wt. % Y, 0.5 wt. % Si and 0.5 wt. % Mn.

An equilibrium cooling requires slow cooling of a melt. The opposite of an equilibrium cooling is a Scheil-Gulliver cooling. Under this non-equilibrium condition, it is assumed that once a solid phase is precipitated, it does not react further. In other words, diffusion within solid phases is assumed to be zero. The non-equilibrum Scheil-Gulliver cooling, with cooling steps of 5 ^{0}C, was simulated on the same alloy composition. The results obtained in the form of percentage distributions of various phases are shown in Fig. 7.3.

The liquid disappears in this case at around 342 ^{0}C. It might be noted that in this case, binary Ce-Zn phases were obtained which were absent in the case of equilibrium phases.

The Scheil-Gulliver cooling process can simulate the conditions of non-equilibrium solidification and thus can help by showing the probable non-equilibrium phase that may be obtained. After the solidification, heat treatment is done to attain the final phases and microstructure. The Scheil-Gulliver cooling simulation using optimized databases could be very helpful during solidification studies.
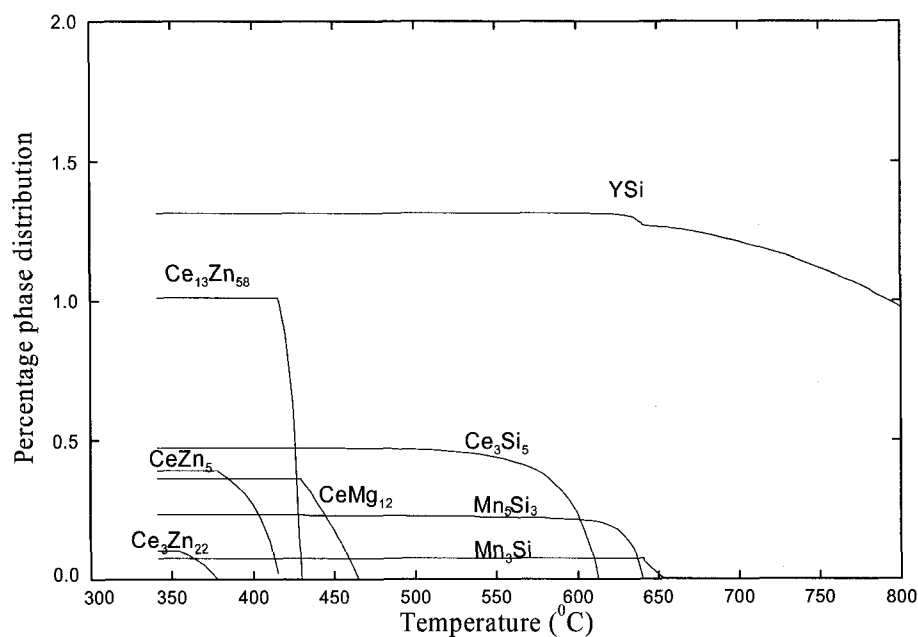
Figure 7.3a
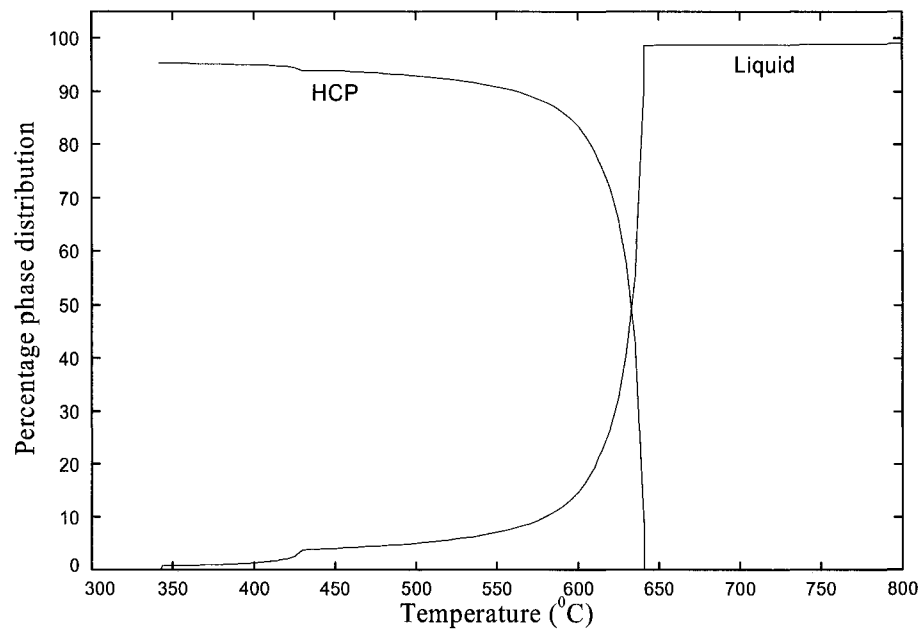
Figure 7.3b

Figure 7.3   The phase distribution of the phases precipitated out during non-equilibrium Scheil-Gulliver cooling of an alloy of composition 95 wt. % Mg, 2 wt. % Zn, 1 wt. % Ce, 1 wt. % Y, 0.5 wt. % Si and 0.5 wt. % Mn (Due to the large differences in the amounts of phases precipitated, the percentage phase distribution are shown on different scales in Figs. 7.3a and 7.3b).

Chapter 8: Conclusions and Recommendations

As the aim of the present work was to prepare a critically evaluated database as part of a broader research project to develop a database for Mg-alloys with 25 potential elements, the Si-Zn, Ce-Si, Y-Si, Mn-Si and Al-Mn systems were critically evaluated and optimized. The Modified Quasichemcial Model (MQM) capable of taking into account short-range ordering in the solutions was used to model the liquid alloys. All the available thermodynamic and phase equilibria data have been critically evaluated in order to obtain one set of optimized model parameters representing the Gibbs energies of all the phases in these binary systems. The experimental data were reproduced within experimental error limits. All the thermodynamic properties obtained in the present work were compared with previous optimizations in the respective systems.

The binary model parameters obtained in the present study were combined with those for the other binary sub-systems optimized previously (at the CRCT, Ecole Polytechnique) to evaluate the Mg-Si-Zn, Mg-Ce-Si, Mg-Y-Si, Mg-Mn-Si and Mg-Al-Mn ternary systems. The thermodynamic properties in the ternary systems were estimated from the optimized binary model parameters using proper "geometric" models. Predictions for these ternary systems were made, and ternary data were satisfactorily reproduced either from just binary model parameters or with the inclusion of a small ternary parameter.

Inclusion of recent data for binary systems on phase equilibria and thermodynamic properties, and the use of MQM for the liquid phase have improved the results obtained in the present work compared to those of previous optimizations. Furthermore, the entropy of mixing in the liquid phase and entropies of formation of intermetallic phases obtained in the present work are physically reasonable.

Previous optimizations of these systems were based on a Bragg-Williams random-mixing model for the liquid phase. In the dilute composition regions, the partial properties obtained by the previous optimizations often deviate from the experimental data, particularly in the case of partial enthalpies of mixing. Partial properties obtained in the present work are smoother and closer to the experimental data. The better optimization of partial properties in dilute liquid solutions will play a crucial role in the development of novel Mg-alloys.

Estimations of the properties of a ternary phase from binary model parameters depend upon the optimized binary model parameters and the techniques used to estimate the ternary properties. The optimized parameters should be able to give a good first estimation of the ternary properties. In the present work, a very small ternary interaction parameter was used to reproduce the ternary data in the Mg-Al-Mn liquid, whereas the previous optimization of this system, based on a Bragg-Williams random-mixing model for the liquid phase, required a much larger ternary interaction parameter. For all practical purposes, the ternary data below 760 ^{0}C in this ternary system can be

reproduced without any ternary interaction parameter. Better estimation of the ternary properties in the present work can be attributed to the use of the "asymmetric approximation" with Al as "asymmetric-component", and the use of the MQM in the present work.

A flat liquidus surface or even a miscibility gap is seen on the A_xB_y-C join in a ternary A-B-C system when the A-B binary liquid phase exhibits considerable short-range ordering while the other two, B-C and A-C, are closer to ideality. Due to the short-range ordering, A and B atoms cluster, excluding C atoms, leading positive deviations on the A_xB_y-C join. In the present work, calculated miscibility gaps on the Mg-CeSi and Mg-YSi joins have been obtained in the Mg-Ce-Si and Mg-Y-Si systems. In these ternary systems, the liquids in the Ce-Si and Y-Si systems exhibit large negative deviations from ideality compared to the other two binary sub systems, and hence are expected to have considerable short-range ordering. In the Mg-Mn-Si system, where the liquid phase in the Mn-Si system exhibits comparatively less short-range ordering than the Y-Si and Ce-Si systems, flat liquidus surfaces have been calculated on the join from Mg towards the Mn-Si system. If a Bragg-Williams model is used to model these ternary systems, it will overestimate the positive deviations and, in fact, can predict a miscibility gap when there is none. An "associate" model for short-range ordering will not at all predict these positive deviations, as the model assumes random mixing of A_xB_y associates and C atoms on the A_xB_y-C join. Thus, the MQM has better predicted the thermodynamic properties of ternary solutions from the binary model parameters.

The extension of a binary miscibility gap into the ternary system depends upon the model used. The MQM predicts a smaller extension of a binary miscibility gap into the ternary system than the Bragg-Williams or "associate" random-mixing model. However, in the MQM, this extension depends upon the coordination numbers used to model the liquid phase. The calculated extension of the binary Mg-Mn liquid immiscibility into the Mg-Mn-Si and Mg-Al-Mn systems are small compared to the extension that would be calculated using a random-mixing model. The consulate temperature obtained in the optimization of the Mg-Mn system, where the MQM was used to model the liquid phase, and which was used in the present work, is lower by approximately $1500\text{-}2000^0$ than in previous optimizations in which a random-mixing model was used. This results in a smaller calculated extension of the binary miscibility gap into the ternary systems.

These optimized systems will help in the calculation of multicomponent phase diagrams, phase fractions charts, and the tracking of solidification of liquid alloys. With the help of these calculations, systems with potential use as alloys and systems with unwanted properties will be readily identified. This will reduce the amount of experimental effort required. Knowledge of phases precipitated and their amounts will explain the microstructural evolution of alloys, and thus will be helpful in explaining the mechanical properties of alloys. As the present obtained results are better than the previous optimizations, they will provide a better solution to the existing problems in the evolution of magnesium as a light-weight construction material.

In short, the use of the Modified Quasichemical Model (MQM) for the liquid phase has permitted short-range ordering to be taken into account. The inclusion of recent experimental data has improved the results obtained, and the thermodynamic properties obtained are more physically reasonable. The use of the MQM generally also results in better estimations of the properties of ternary and higher-order liquid alloys. These estimations of phase equilibria in magnesium alloys will aid in the design of novel magnesium alloys.

The following recommendations are made for the experimental data which would make the database more exhaustive and accurate.

Mg-Ce-Si (Chapter 4)

1. The thermodynamic properties of the reported ternary compounds in the system Mg-Ce-Si.

2. Ternary data, especially in the Mg-rich corner, of the Mg-Ce-Si system, such as the solubility of silicon in the liquid phase in order to fix the thermodynamic properties of the ternary liquid and to validate the predictions made for this system.

3. Data to establish the phase boundaries between the two compounds Ce_3Si_5 and $CeSi_2$ in the Ce-Si system so that these phases can be modeled as non-stoichiometric.

Mg-Y-Si (Chapter 4)

1. The melting behaviors of the silicides YSi and Y_5Si_4 in the binary Y-Si system.

2. Ternary data verifying the one available study in the ternary Mg-Y-Si system and also data in the Mg-rich corner of this ternary system to fix the thermodynamic properties of the ternary liquid and to validate the predictions made.

Mg-Mn-Si (Chapter 5)

1. The thermodynamic properties of the phases Mn_6Si or Mn_9Si_2 and also the phase boundaries between these two phases in order to model them as non-stoichiometric phases.

2. Data to verify the one available study of silicon solubility in the CUB phase.

3. Ternary data, especially in the Mg-rich corner in the Mg-Mn-Si system, to validate the predictions made in this system and also to fix the thermodynamic properties of the liquid phase.

Mg-Al-Mn (Chapter 6)

1. Solubility data in the Mg-rich corner of the Mg-Al-Mn system at high Al content (>7 wt. %) and at high temperature (>760 ^{0}C).

2. Solubility data in the liquid phase in the Al-rich corner of the Mg-Al-Mn system.

9. References

Abrikosov, N. Kh., Ivanova, L. D., & Muravev, V. G. (1972). Preparation and investigations of single crystals of solid solutions of manganic silicides with Ge and CrSi$_2$. *Izv. Akad. Nauk SSSR, Neorg. Mater.* 8(7), 1194-1200.

Ageev, N. V., Kornilov, I. I., & Khlapova, A. N. (1948). Magnesium-rich alloys of the system magnesium-aluminium-manganese. *Inst. Obshcheii Neorg. Khim., Akad. Nauk SSSR.* 14, 130-143.

Ahmad, N., & Pratt, J.N. (1978). Thermodynamic properties of liquid Mn-Si alloys. *Met. Trans. A,* 9, 1857-1863.

Andersson, J. O., Guillermet, A. F., Hillert, M., Jansson, B., & Sundman, B. (1986). A compound-energy model of ordering in a phase with sites of different coordination numbers. *Acta Metall.* 34(3), 437-445.

Bale, C. W., Chartrand, P., Degterov, S. A., Eriksson, G., Hack, K., Ben Mahfoud, R., Melançon, J., Pelton, A. D., & Petersen, S. (2002). FactSage thermochemical software and databases. *Calphad.* 26(2), 189-228.

Barlock J. G., & Mondolfo, L. F. (1975). Structure of some aluminum-iron-magnesium-manganese-silicon alloys. *Z. Metallkd.* 66 (10), 605-11.

Batalin, G. I., Beloborodova, E. A., Stukalo, V. A., & Chekhovskii, A. A. (1972). Thermodynamic properties of molten alloys of aluminum with manganese. *Ukr. Khim. Zh.* 38(8), 825-826.

Batalin. G. I., Bondarenko, T. P., & Sudavtsova, V. S. (1984). Heat formation of liquid alloys of the Si-Fe, Mn system. *Sov. Prog. Chem.* 50(2), 69-71.

Batalin, G. I., & Sudavtsova, V. S. (1974). Thermodynamic properities of molten Mn-Si alloys. *Sov. Prog. Chem.* 40(5), 88-89.

Beerwald, A. (1944). On the Solubility of iron and manganese in magnesium and in magnesium-aluminium alloys. *Metallwirtschaf.* 23, 404-407.

Benesovsky, F., Nowotny, H., Rieger, W., & Rassaerts, H. (1966). Investigation of the ternary system cerium-silicon-thorium. *Monatsh. Chem.* 97(1), 221-229.

Blouke, M. M., Holonyak, N., Streetman, B. G., & Zwicker, H. R. (1970). Solid solubility of Zn in Si. *J. Phys.Chem.Solids.* 31, (173-177).

Boren, B. (1933). X-ray investigations of alloys of silicon with Cr, Mn, Co and Ni. *Ark. Kem. Miner.Geol.* 11A (10), 1-28.

Bollenrath, F., & Grober, H. (1946). Aluminum alloys with Mg, Si, and Zn. *Metallfroschung.* 1, 116-122.

Bulanova, M.V., Zheltov, P.N., Meleshevich, K.A., Saltykov, P.A. & Effenberg, G. (2002). Cerium–Silicon system. *J. Alloys Comp.* 345, 110-115.

Butchers, E., & Hume-Rothery, W. (1945). The solubility of manganese in aluminum. *J. Inst. Met.* 71, 87-91.

Butchers, E., Raynor, G. V., & Hume-Rothery, W. (1943). The constitution of magnesium-manganese-zinc-aluminium alloys in the range 0-5 % magnesium, 0-2 % manganese, 0-8 % zinc, I-The liquidus. *J. Inst. Met.* 69, 209-228.

Button, T. W., McColm, I. J., & Ward, J. M. (1990). Preparation of yttrium silicides and oxide-silicides. *J. Less-Common Met.* 159, 205-222.

Carlson, R. O. (1957). Double-acceptor behavior of zinc in silicon. *Phys. Rev.* 108, 1390-1393.

Chakraborti, N., & Lukas, H. L. (1989). Calculation and optimization of the Mn-Si phase diagram. *Calphad.* 13(3), 293-300.

Chartrand, P., & Pelton, A.D. (2001). Thermodynamic evaluation and optimization of the $LiCl-NaCl-KCl-RbCl-CsCl-MgCl_2-CaCl_2$ system using the modified quasi-chemical model. *Metall. Mater. Trans. A.* 32, 1361-1383.

Chartrand, P., & Pelton, A.D. (2001). Thermodynamic evaluation and optimization of the $LiF-NaF-KF-MgF_2-CaF_2$ system using the modified quasi-chemical Model. *Metall. Mater. Trans. A.* 32, 1385-1396.

Chartrand, P., & Pelton, A.D. (2001). Thermodynamic evaluation and optimization of the Li, Na, K, Mg, Ca//F, Cl reciprocal system using the modified quasichemical model. *Metall. Mater. Trans. A.* 32, 1417-1430.

Chastel, R., Saito, M., & Bergman, C. (1994). Thermodynamic investigation on $Al_{1-x}Mn_x$ melts by Knudsen cell mass spectrometry. *J. Alloys and Comp.* 205, 39.

Chevalier, P. -Y., Fischer, E., & Rivet, A. (1995). A thermodynamic evaluation of the Mn-Si system. *Calphad.* 19(1), 57-68.

Decterov, S. A., Jung, I.-H., Jak, E., Kang, Y.-B., Hayes, P., & Pelton, A.D., (2004). Thermodynamic modelling of the Al_2O_3-CaO-CoO-CrO-Cr_2O_3-FeO-Fe_2O_3-MgO-MnO-NiO-SiO_2-S system and application in ferrous process metallurgy. Proceedings of the *VII International Conference on Molten Slags, Fluxes and Salts, Johannesburg, South Africa* (pp 839-850). Johannesburg, South Africa: Pistorius, C.

Dhar, S. K., Manfrinetti, P., & Palenzona, A. (1997). Magnetic ordering in $CeMg_2Si_2$ and Ce_2MgSi_2. *J. Alloys Comp.* 252, 24-27.

Dinsdale, A.T., (1991). SGTE data for pure Elements. *Calphad.* 15(4), 317-425.

Dix, E. H., Fink, W.L., & Willey, L. A. (1933). Equilibrium relations in Al-Mn alloys of high purity II. *Trans. AIME* 104, 335-352.

Doerinckel, F. (1906). On the compounds of manganese with silicon. *Z. Anorg. Chem.* 50, 117-132.

Drits, M. E., Kadaner, E.S., Padzhnova, E.M., & Bochvar, N.R. (1964). Determination of the boundaries of common solubility of Mn and Cd in solid aluminum. *Zh. Neorg. Khim.* 9(6), 1397.

Du, Y., Wang, J., Zhao, J., Schuster, J. C., Weitzer, F., Schmid-Fetzer, R., Ohno, M., Xu, H., Liu, Z., Shang S., & Zhang, W. (2007). Reassessment of the Al–Mn system and a thermodynamic description of the Al–Mg–Mn system. *Int. J. Mat. Res.* 98, 855-871.

Dudkin, L. D., & Kuznetsova, E. A. (1961). An investigation of the system Mn-Si in the silicon-rich region. *Dokl. Akad. Nauk SSSR.* 141(1) 94-97.

Dudkin, L. D., & Kuznetsova, E. A. (1962). Investigation of the electrophysical properties of alloys based on semiconductor disilicides of Cr and Mn. *Poroshk. Metall.* 12(6). 20-31.

Elchardus, & E., Laffitte, P. (1933). The constitution of Mg-Zn-Si alloys rich in Mg-rich corner. *C. R. Acad. Sci. Paris.* 197, 1125-1127.

Ellner, M., (1990). The stucture of the high-temperature phase MnAl (h) and the displacive transformation from MnAl (h) into Mn_5Al_8. *Metall. Mater. Trans. A.* 21, 1669-1672.

Eriksson, G., & Hack, K. (1990). ChemSage- a computer program for the calculation of complex chemical equilibria. *Metall. Trans. B.* 21, 1013-23.

Esin, Y. O., Bobrov, N. T., Petrushevskii, M.S., & Geld, P.V. (1973). Concentration variation of the enthalpies of formation of Mn-Al melts at 1626 K. *Russ. J. Phys. Chem.* 47, 1103.

Esin, Yu. O., Gorbunov, Yu., Petrushevskii, M.S., & Geld, P.V. (1975). Enthalpies of formation of molten Mn-Si alloys. *Chernaya Metallurgiya.* 2, 8-11.

Esin, Yu. O., Valeshev, M. G., Geld, P. V., & Tushkova, L. M., (1976). Partial and Intergral Enthalpies of Foramation of Liquid Y-Si Alloys. *Russ. Metall.* 1, 19-20.

FactSage (2008). *www.factsage.com*, Montreal, Quebec, Canada.

Fahrenhorst, E., & Hoffman, W. (1940). The solubility of manganese in aluminum containing up to 2 Percent of magnesium. *Metallwirtschaft.* 19, 891-893.

Fujino, Y., Shinoda, D., Asanabe, S., Sasaki, Y. (1961). Phase diagram of the partial system MnSi-Si. *Jpn. J. Appl. Phys.* 3, 431-435.

Fuller, C. S., & Morin, F. J. (1957). Diffusion and electrical behavior of zinc in silicon. *Phys. Rev.* 105, 379-384.

Fun, H. -K., Lin, H.-C., Lee T. -J, & Yipp B.-C. (1994). T-Phase $Al_{18}Mg_3Mn_2$. *Acta Crystallogr.* C50, 661-663.

Geld, P. V., Petrushevskii, M.S., Esin, Yu.O., & Gorbunov, Yu.V. (1974). Enthalpy of formation and short-range structure of liquid alloys of Mn with Si, Ge and Sn. *Doklady Akademii Nauk SSSR.* 217(5), 1114-1117.

Girault, B., (1977). Liquidus curves of various silicon-metal Systems. *C. R. Acad. Sci. Paris B.* 284, 1-4.

Godecke, T., & Koster, W., (1971). A supplement to the Constitution of the Al-Mn system. *Z. Metallkd.* 62(10), 727-32.

Gokhale, A.B., & Abbaschian, R. (1986). The Y-Si system. *Bull. Alloy Phase Dia.* 7(5), 485-489.

Gokhale, A.B., & Abbaschian, R., (1990). The Mn-Si system. *Bull. Alloy Phase Diagrams.* 11(5), 468-474.

Gorbunov, Yu. V., Esin, Yu. O., & Geld, P. V. (1974). Enthalpies of mixing of liquid manganese and silicon at 1773 K. *Russ. J. Phys. Chem.* 48(8), 1244.

Gröbner, J., Mirkovic, D., Ohno, M., & Schmid-Fetzer, R. (2005). Experimental investigation and thermodynamic calculation of binary Mg-Mn phase equilibria *J. Phase Equilib. Diffus.* 26(3), 234-239.

Gröbner, J., Mirkovic, D., & Schmid-Fetzer, R. (2004). Thermodynamic aspects of the constitution, grain refining, and solidification snthalpies of Al-Ce-Si alloys. Met. and Mat. Trans. A. 35, 3359-3362.

Gröbner, J., & Schmid-Fetzer, R. (2001). Selection of promising quaternary candidates from Mg-Mn-(Sc, Gd, Y, Zr) for development of creep-resistant magnesium alloys. *J. Alloys Compounds.* 320(2), 296-301.

Gschneidner, K. A., (1961). Yttrium–Silicon system. *Rare Earth Alloys* (1st), New York: D. Van Nostrand.

Gupta, K. P., (1964). New phases in the Mn-Si and Fe-Mn-Si systems. *Trans. Metall. Soc. AIME.* 230, 253-254.

Hanawalt, J. D., Nelson, C. E., & Holdeman, G. E. (1941). Removal of Iron from Mg-base alloys. *US Patent No. 2267862.*

Hillert, M. (2000). The compound energy formalism. *J. Alloy. Compounds.* 320(2), 161-176.

Hillert, M., & Staffansson, L. -I., (1970). Regular solution model for stoichiometric phases and ionic melts. *Acta Chem. Scand.* 24(10), 3618-26.

Jacobs, M.H.G., & Spencer, P.J., (1996). A critical thermodynamic evaluation of the systems Si-Zn and Al-Si-Zn. *Calphad.* 20 (3). 307-320.

Jansson, A. (1992). Thermodynamic evaluation of the Al-Mn system *Metall. Mater. Trans.* A. 23, 2953-2958.

John, M., Hein, K., & Buhrig, E. (1979). Investigations of II-IV-V systems by the method of differential thermal analysis. *Cryst. Res. Technol.* 14, 841-84.

Jung, In-Ho, (2003). Critical evaluation and thermodynamic modeling of phase equilibria in multicomponent oxide systems. Ph.D. dissertation, Ecole Polytechnique, Montreal, Quebec, Canada.

Kang, Y.-B., Pelton, A. D., Chartrand, P., Spencer, P., & Fuerst, C.D. (2007). Critical evaluation and thermodynamic optimization of the binary systems in the Mg-Ce-Mn-Y system. *J. Phase Equilib. Diffus.* 28(4), 342-354.

Kanibolotskii, D. S., & Lesnyak, V.V. (2006). Thermodynamic properties of Mn-Si alloys. *Russ. Metall.* 3, 199-205.

Kattner, U.R. (1997). The thermodynamic modeling of multicomponent phase equilibria. *J. Metals.* 49(12), 14-19.

Kaufman, L., & Bernstein, H. (1970). *Computer Calculation of Phase Diagrams with Special Reference to Refractory Metals.* New York: Academic Press.

Kematick, R. J., & Myers, C. E., (1992). Thermodynamics and phase equilibria in the Al-Mn system. *J. Alloys and Comp.* 178, 343-349.

Kikuchi, R. (1951). A theory of cooperative phenomena. *Phys. Rev.* 81, 988-1003.

Koch, A. J. J., Hokkeling, P., Steeg, M.G.v.d., & Devos, K. J. (1960). New material for permanent magnets on a base of Mn and Al. *J.Appl. Phys.* 31(5), 75S-77S.

Kono, H. (1958). On the ferromagnetic phase in the Mn-Al system. *J. Phys. Soc. Jpn.* 13, 1444.

Korshunov, V. A., Sidorenko, F. A., Geld, P. V., & Davydov, K. N., (1961). Phase components of the partial system MnSi-Si. *Fiz. Met. Metalloved.* 12(2), 277-284.

Koster, W., & Wachtel, E. (1960). Magnetic investigation of Al-Mn Alloys containing more than 25 at. % Mn. *Z. Metallkd.* 51, 271-280.

Kreiner, G., & Franzen, H. F., (1997). The crystal structure of λ-Al₄Mn. *J. Alloys Compd.* 261, 83-104.

Kubaschewski, O., Heymer, G. (1960). Heats of formation of transition-metal aluminides. *Trans. Faraday Soc.* 56, 473-478.

Kuzma, Yu. B., Gladyshveskii, E. I. (1964). The Co-Mn-Si system. *Russ. J. Inorg. Chem.* 9(3), 373-377.

Kuznetsov, G.M., Barsukov, A.D. & Abas, M.I. (1983). Study of manganese, chromium, titanium, and zirconium solubility in solid aluminum. *Sov. Non Ferrous Met. Res.* 11, 783.

Leemann, W. G., & Hanemann, H. (1938). The ternary system aluminium-magnesium-manganese. *Aluminium Arch.* 9, 6-17.

Letun, S. M., Geld, P.V., & Serebrennikov, N. N. (1965). The thermochemistry of Mn$_3$Si. *Russ. Metall.* 6. 97-103.

Liang, P., Tarfa, T., Robinson, J. A., Wagner, S., Ochin, P., Harmelin, M. G., Seifert, H. J., Lukas, H. L., & Aldinger, F. (1998). Experimental investigation and thermodynamic calculation of the Al-Mg-Zn system. *Thermochim. Acta.* 314, 87-110.

Little, A.T., Raynor, G.V., & Hume-Rothery, W. (1943). The constitution of magnesium-manganese - zinc - aluminium alloys in the range 0-5 % magnesium, 0-2 % manganese and 0-8 % Zinc, III-The 500 ^{0}C and 400 ^{0}C isothermals. *J. Inst. Met.* 69, 423-440.

Liu, X. J., Ohnuma, I., Kalnuma, R., & Ishida, K. (1996). Phase equilibria in the Mn-rich portion of the binary system Mn-Al. *J. Alloys Compd.* 235, 256-261.

Liu, X. J., Ohnuma, I., Kalnuma, R., & Ishida, K. (1999). Thermodynamic assessment of the Al-Mn binary phase diagram. *J. Phase Equilib.* 20(1), 45.

Livanov, V.A., & Vozdvizhenskii, V.M. (1958). Recrystallization of aluminum alloys with manganese. *Trudy Moskov. Aviatsion, Tekhnol. Inst.* 31, 65-83.

Lukas, H.L. (1998). The Y-Si system. *COST 507 – Thermochemical Databases for Light Metal Alloys, Vol. 2,* Ansara, I., Dinsdale, A.T., Rand, M.H., (Eds.) 274-277.

Mager, T., & Wachtel, E. (1970). On the constitution of the partial system MnSi-Si. *Z. Metallkd.* 61(11), 853-856.

McAlister, A. J., & Murry, J. L. (1987). The Al-Mn system. *Bulletin of Alloy Phase Diagrams.* 8(5), 438-443.

Meschel, S. V., & Kleppa, O. J. (1994). The standard enthalpies of formation of some 3d transition metal aluminides by high-temperature direct synthesis calorimetery. *NATO ASI Series, Ser.E.* 256, 103-112.

Meschel, S. V., & Kleppa, O. J. (1995). Standard enthalpies of formation of some carbides, silicides and germanides of cerium and praseodymium. *J. Alloys Comp.* 220, 88-93.

Meschel, S. V., & Kleppa, O. J. (1996). Standard enthalpies of formation of some carbides, silicides, germanides and stannides of samarium by high temperature direct synthesis calorimetry. *J. Alloys Comp.* 243, 186-193.

Meschel, S. V., & Kleppa, O. J. (1998). Standard enthalpies of formation of some 3d transition metal silicides by high temperature direct synthesis calorimetry. *J. Alloys Compd.* 267(1-2), 128-135.

Meschel, S. V., & Kleppa, O. J. (1998). Standard enthalpies of formation of some 3d transition metal silicides by high temperature direct synthesis calorimetry. *J. Alloys Comp.* 274, 193-200.

Minamino, Y., Yamane, T., Araki, H., Takeuchi, N., Kang, Y.-S., Miyamoto, Y., & Okamoto, T., (1991). Solid solubilities of Mn and Ti in aluminum at 0.1 MPa and 2.1 GPa. *Metall. Mater. Trans. A.* 22, 783-785.

Mirgalovskaya, M.S., Matkova, L. N., & Komova, E. M. (1957). The system Mg-Al-Mn. *Trudy Inst. Met. Im. A.A. Baikova, Akad. Nauk.* 2, 139-148.

Moissan, H., & Siemens, F. (1904). On the solubility of silicon in Zinc and in lead. *C. R. Acad. Sci. Paris.* 138, 657-661.

Munitz, A., Gokhale, A.B., & Abbaschian, G.Y. (1989). The Ce-Si system. *Bull. Alloy Phase Dia.* 10(1), 73-78.

Murray, J. L., McAlister, A.J., Schaefer, R.J., Bendersky, L.A., Biancaniella, F. S., & Moffatt, D. L. (1987). Stable and metastable phase equilibria in the Al-Mn system. *Metall. Trans. A.* 18, 385-392.

Muller, C., Stadelmaier. H., Reinsch, B., & Petzow, G. (1996). Metallurgy of the magnetic τ-phase in Mn-Al and Mn-Al-C. *Zeitschrift fuer Metallkunde.* 87 (7), 594-597.

Nelson, B. J. (1951). Equilibrium relations in Mg-Al-Mn Alloys. *J. Metals.* 3, 797.

Obinata, I., Hata, E., & Yamaji, K. (1953). Chiefly on the sub-cooled Al-Mn Alloys. *J. Inst. Met.* 17, 496-501.

Ohnishi, T., Nakatani, Y., & Shimizu, K. (1973). Phase diagrams and ternary compounds of the Al-Mg-Cr and the Al-Mg-Mn systems in Al-Rich side. *Light Metals Toky.* 23, 202-209.

Ohnishi, T., Nakatani, Y., & Shimizu, K. (1973). Phase diagram in the Al-Rich side of the Al-Mg-Mn-Cr quaternary system. *Light Metals Toky.* 23, 437-443.

Ohno, M., & Schmid-Fetzer, R. (2005). Thermodynamic assessment of Mg-Al-Mn phase equilibira on Mg-Rich alloys. *Z. Metallkd.* 96(8), 857-864.

Pelton, A.D. (2001). A general "geometric" thermodynamic model for multicomonent solutions. *Calphad.* 25 (2), 319-328.

Pelton, A. D., & Chartrand, P. (2001). The modified quasichemical model: Part II. Multicomponent solutions. *Metall. Mater. Trans. A.* 32, 1355.

Pelton, A.D., Chartrand, P. (2007). Authors' reply to: "Shortcomings of the recent modifications of the quasichemical solution model" by Dmitry Saulov. *Calphad.* 31 (3), 396–398.

Pelton, A.D., Degterov, S.A., Eriksson, G., Robelin, C., & Dessureault, Y. (2000). The modified quasichemical model I – binary solutions. *Metall. Mater. Trans. B.* 31, 651-659.

Pelton, A.D., & Kang, Y., -B. (2007). Modeling short-range ordering in solutions. *Int. J. Mat. Res.* 10, 907-917.

Pelton, A. D., & Schmalzried, H. (1973). On the geometrical representation of phase equilibria. *Met. Trans.* 4(5), 1395-404.

Phillips, H.W.L. (1942). The constitution of alloys of aluminium with manganese, silicon and iron. *J. Inst. Met.* 69, 275-316.

Polotskaya, R. I., & Sidorko, V. R. (1997). Thermodynamic properties of yttrium silicides. *Powder Metall. Met. Ceram.* 36(5-6), 315-319.

Ran, Q., Lukas, H. L., Effenberg, G., & Petzow, G. (1989). A thermodynamic assessmet of the Y-Si system. *Z. Metallkd.* 80, 402-405.

Redlich, O., Kister, A. T. (1948). Algebraic representation of thermodynamic properties and the classification of solutions. *J. Ind. Eng. Chem.* 40, 345-348.

Ryss, G. M., Esin, Yu. O., Petrushevskii, M. S., Stroganov, A. I., & Geld P. V. (1979). Enthalpy of formation of melts of yttrium with silicon. *Russ. Metall.* 6, 57-58.

Ryss, G. M., Esin, Yu. O., Stroganov, A. I., & Gel'd, P.V. (1977). The enthalpies of formation of liquid silicon-cerium alloys. *Zh. Fiz. Khim.* 51, 232-233.

Saulov, D. (2007). Shortcomings of the recent modifications of the quasichemical solution model. *Calphad.* 31 (3), 390–395.

Schaefer, R.J., Biancaniello, F.S., & Cahn, J.W., (1986). Formation and stability range of the G phase in the Al-Mn system. *Scr. Metall.* 20(10), 1439-44.

Schmid-Fetzer, R., & Gröbner, J. (2001). Focused development of magnesium alloys using the CALPHAD approach. *Adv. Engg. Mat.* 3(12), 947.

Schneidner, M., & Krumnacker, M. (1972). Study of the Zinc-Silicon phase diagram. *Neue Hutte.* 17, 519-521.

Simensen, C. J., Oberländer, B. C., Svalestuen, J., & Thorvaldsen, A. (1988). Determination of the equilibrium phases in molten Mg - 4 wt. % Al-Mn Alloys. *Z. Metallkd.* 79, 537-540

Simensen, C. J., Oberländer, B. C., Svalestuen, J. & Thorvaldsen, A. (1988). The phase diagram for magnesium - aluminium - manganese above 650°C. *Z. Metallkd.* 79, 696-699.

Stukalo, V. A., Batalin, G. I., Neschbimenko, N. Ya., & Kurach, V. P. (1980). Enthalpy of formation of liquid alloys of yttrium with silicon. *Ukr. Khim. Zh.* 46 (1), 98-99.

Sudavtsova V. S., Gorobets, Yu. G., & Batalin, G. I. (1988). Heat of formation of cerium-(silicon, nickel, copper) liquid binary alloys. *Rasplavy* 2:6. 79-81.

Tanaka, A. (1977). The determination of the activites in Mn-C and Mn-Si melts by the vapor pressure measurement. *J. Jpn. Inst. Met.* 41(6), 601-607.

Taylor, M.A. (1960). Intermetallic phases in the Al-Mn binary system. *Acta. Metall.* 8, 256-262.

Thurmond, C.D., & Kowalchik, M. (1960). Germanium and silicon liquidus curves. *Bell Syst. Tech. J.* 39, 169-204.

Tibbals, J. (1998). Mg-Mn system. *COST 507 – Thermochemical Databases for Light Metal Alloys*, I. Ansara, A.T. Dinsdale, M.H. Rand (Eds.), Vol 2. EUR 18499. 215-217.

Tibbals, J. (1998). Mn-Si system *COST 507 – Thermochemical Databases for Light Metal Alloys*, Ansara, I., Dinsdale, A.T., Rand, M.H., (Eds.), Vol 2. EUR 18499. 236-238.

Topor, L., Kleppa, O. J. (1990). Standard enthalpies of formation of Me, Si, (Me = Y, Lu, Zr) and of Hf_3Si_2. *J. Less-Common Metals.* 167, 91-99.

Wakeman, D. W., & Raynor, G. V. (1948). The constitution of aluminium-manganese-magnesium and aluminium-manganese-silver alloys, with special reference to ternary compound formation. *J. Inst. Met.* 75, 131-150.

Waldner, P., & Pelton, A.D. (2004). Thermodynamic modeling of the Ni-S system. *Z. Metallkunde.* 95, 672-681

Waldner, P., & Pelton, A.D. (2004). Critical thermodynamic assessment and modeling of the Fe-Ni-S System. *Metall. Mater. Trans. B.* 35, 897-907.

Waldner, P., & Pelton, A.D. (2005). Thermodynamic modeling of the Fe-S system. *J. Phase Equilib. Diffus.* 26(1), 23-38.

Wieser, P. F., & Forgeng, W. D. (1964). Phase relationships in Mn-Si Alloys containing from 2 to 24 at. % Si. *Trans.Metall.Soc. AIME.* 230, 1675-1681.

Van Laar, J.J. (1908). Melting-point and freezing-point curves in binary systems, when the solid phase is a mixture (amorphous solid solution or mixed crystals) of both components. First part. *Z. phys. Chem.* 63, 216-253.

Van Laar, J.J. (1908). Melting-point and freezing-point curves in binary systems, when the solid phase is a mixture (amorphous solid solution or mixed crystals) of both components. Second part. *Z. phys. Chem.* 64. 257-297.

Villars, P., Calvert, L.D. (1991). *Pearson's Handbook of Crystallographic Data for Intermetallic phases* (2nd). Ohio, USA: ASM, Materials Park.

Vogel, R., & Bedarff, H. (1933). The state diagram of Mn-Si. *Arch. Eisenhuttenwes.* 7, 423-425.

Zaitsev, A. I., Zemchenko, M. A., & Mogutnov, B. M. (1989). Thermodynamic properties of manganese silicides. *Russ. J. Phys. Chem.* 63(6), 806-810.

Zaitsev, A. I., Zemchenko, M. A., & Mogutnov, B. M. (1989). Thermodynamic properties of manganese-silicon melts. *Melts.* 3(2), 86-95.

Zaitsev, A. I., Zemchenko, M. A., & Mogutnov, B. M. (1990). Phase equilibria in the system MnSi-Si. *Russ. Metall.* 1, 208-213.

Zaitsev, A. I., Zemchenko, M. A., & Mogutnov, B. M. (1990). Phase equilibria in the Mn_9Si_2-MnSi system. *Russ. Metall.* 2, 188-192.